Final Report for the Low-level Radioactive Waste Disposal Authority: Preliminary Geologic and Hydrologic Studies of Selected Areas in Culberson and Hudspeth Counties, Texas

by

C. W. Kreitler, J. A. Raney, R. Nativ, E. W. Collins, W. F. Mullican, T. C. Gustavson, and C. D. Henry

Bureau of Economic Geology
W. L. Fisher, Director
The University of Texas at Austin
Austin, Texas 78713

Final report prepared for the
Low-level Radioactive Waste Disposal Authority
under contract no. IAC(86-87)-0828

July 1986

CONTENTS

Figures

Table

Plates (in pocket)

1. Geologic Map of State Land S-15, Culberson County
2. Geologic Map of University Lands Block 46
3. Geologic Map of study area in Hudspeth County
4. Flood-prone areas in Hudspeth County

EXECUTIVE SUMMARY

The Bureau of Economic Geology, The University of Texas at Austin, conducted preliminary investigations of the geology and hydrology of areas in Culberson and Hudspeth Counties, Texas, selected by the Texas Low-level Radioactive Waste Disposal Authority as potential sites for a low-level radioactive waste repository. This report discusses the results of those studies.

Two areas in Culberson County, Texas, Site S-15 and Block 46, and adjacent regions were investigated. The Permian Castile Formation underlies all of Site S-15 and the eastern half of Block 46. The Castile Formation displays evidence of extensive solution and local collapse and appears to contain a complex system of karst features and underground solution channels. The western half of Block 46 is underlain by the Permian Bell Canyon Formation, consisting of interbeds of sandstone and limestone. Both the Castile and the subjacent Bell Canyon Formation contain prominent joint systems and local areas of normal faults. Surficial deposits are commonly composed of detritus derived from local formations and appear to be both porous and permeable.

The ground-water flow in both areas is governed by karst dissolution and collapse features. The chemical and isotopic composition of ground water indicates active recharge through the thin unsaturated zone combined with older water flowing from the west. Residence time of ground water in the aquifers is relatively short, and numerous springs discharge from the shallow ground-water table.

Hudspeth County, Texas, includes a large area of State-owned lands to the north and east of the town of Fort Hancock. The Authority selected the area on which to focus the investigations based on the area's low relief and surface drainage

into Alamo Arroyo, which does not pass through any populated areas. The region has an arid climate and receives less than 10 inches of rainfall a year. Drill testing of the primary study area indicates that about 40 ft (13 m) of alluvial sands and gravels with near-surface calcrete horizons overlie a thick sequence of silty and clayey older bolson-fill deposits. The older bolson-fill deposits, as shown by both drilling and surface exposures, are an interbedded sequence of clay, silt, and fine sand. The clays are expansive, and local selenite crystals are present at the surface. The depth to Mesozoic bedrock is variable, but drilling at the primary study area encountered bedrock at approximately 400 to 500 ft (122 to 152 m). The primary study area lies about 4 mi (6 km) northeast of a northwest-striking fault that cuts the bolson-fill deposits and at least the base of the overlying alluvial deposits. The age of most recent faulting has not been determined.

Three regional aquifers, located in the Cretaceous rocks, the bolson fill, and the Rio Grande alluvium, are present near the site. In the site area proper, no water was encountered in the bolson fill, and in the Cretaceous aquifer the water level is 478 ft (145.7 m) below land surface. Water in the Cretaceous aquifer is old, suggesting either very slow movement of water in the aquifer or hydraulic disconnection of the aquifer in the site area from the recharge zone at the Cretaceous plateau due to faulting. There are, however, indications of current recharge into the Cretaceous. Water in the bolson fill occurs 2 to 6 mi (3 to 9 km) southwest of the site, where the thickness of the unsaturated zone varies from 90 to 360 ft (27 to 110 m). Water in the bolson fill is old and may be recharged by water moving upward from the Cretaceous aquifer. In the Rio Grande valley, water in the bolson fill is modern and is mainly recharged by the Rio Grande alluvium aquifer. Average annual recharge rate into the gravel cover that overlies the bolson fill is estimated to be 0.003 to 0.02 inch/yr (0.07 to

0.5 mm/yr). Ground-water flow in both the Cretaceous and bolson-fill aquifers is to the southwest toward the Rio Grande valley. The Rio Grande alluvium in the valley contains an aquifer that is fed by the Rio Grande and that probably discharges into the bolson fill in the valley.

INTRODUCTION

In December 1985 the Bureau of Economic Geology (BEG) was asked by the Texas Low-level Radioactive Waste Disposal Authority to conduct a preliminary study of the geology and hydrology of sites being considered for construction of a low-level radioactive waste repository. The sites are located in Culberson and Hudspeth Counties, Texas.

The potential host rocks being considered for the repository are the Permian evaporites in Culberson County and the Cenozoic gravels and silty clays of the Hueco Bolson in Hudspeth County. The repository is to be constructed within the unsaturated zone. The geologic investigations provide data for evaluation of the general geologic framework of the proposed sites and provide site-specific data for evaluation of the physical and structural character of the units as well as for active geomorphic processes.

The hydrologic investigations emphasize six major issues:

(1) Are there any regional aquifers below these sites that can be affected by radioactive waste disposal? Aquifers are defined as water-bearing formations capable of producing water from a well.

(2) What is the depth to the uppermost regional ground-water table at each site? Is the unsaturated zone sufficiently thick to prevent vertical migration of contaminants from the repository to the water table?

(3) What are the flow directions of ground water in this aquifer?

(4) What is the residence time of water in the regional aquifers? Are flow rates sufficiently low such that radionuclides would not spread contaminants away from the site in case of an accidental spill?

(5) What are the methods and rates of recharge to these aquifers? How much of the recharge comes from direct precipitation and surface flooding on the sites' land surface? How much recharge water could percolate through the layers being considered as host rocks for the repository?

(6) Where are the discharge points (natural and wells) of these aquifers and what is their distance from the site? In the case of an accidental spill, is the distance large enough to allow complete radioactive decay before water reaches the biosphere?

Hydrogeologic study of both the unsaturated and saturated zones at each site was conducted to provide an initial assessment of these concerns.

The report is organized so that topics of regional scope that apply to both of the Trans-Pecos counties are discussed first, and then the results of the geologic and hydrologic investigations that are more specific to the areas of investigation are presented.

J. A. Raney and C. W. Kreitler are co-principal investigators for the geologic and hydrologic studies. E. W. Collins, T. C. Gustavson, and C. D. Henry conducted much of the work on the geologic aspects of the sites, and R. Nativ, W. F. Mullican, and D. A. Smith investigated the hydrology of the sites. C. S. Caran provided information on the present climatic conditions of the areas. We are appreciative of the cooperation of the local landowners during our investigations.

REGIONAL SETTING: CULBERSON AND HUDSPETH COUNTIES, TEXAS

Regional Geologic Setting

Culberson and Hudspeth Counties lie in Trans-Pecos Texas in the southeastern part of the Basin and Range structural province. This province consists of topographically high ranges separated by major normal faults from adjacent topographically low basins. Structural development of the province began about 24 million years ago (mya) during east-northeast-oriented extension. Faulting and associated relative subsidence of the basins began at that time and continues to the present. The basins were progressively filled by detritus eroded from the adjacent ranges.

Only the northern and western parts of Trans-Pecos Texas have well-developed northwest-trending basins and ranges, having as much as 5,000 ft (1,500 m) of relief. The two Culberson County study areas are in the easternmost part of the province at its transition to the Great Plains. Basin and Range faults are present but they are of small displacement, and the study region lies outside the area of distinct Basin and Range topography. The site in Hudspeth County is along the margin of Hueco Bolson, a major Basin and Range graben. Hueco Bolson is bordered on the west by the Chihuahua Tectonic Belt, a part of the Laramide fold belt.

Regional Seismicity

No detailed studies of seismicity are available for either the Culberson County or the Hudspeth County areas. Information on possible seismic activity in these areas is based on a consideration of the tectonic setting of Trans-Pecos Texas, including the presence of Quaternary fault scarps, and on recent seismicity in adjacent areas and in the Basin and Range structural province. Quaternary fault

scarps occur throughout much of Trans-Pecos Texas (Muehlberger and others, 1978; Henry and Price, 1985). Quaternary scarps are abundant in the Salt Basin, a large Basin and Range graben at the western edge of Culberson County, approximately 12 mi (20 km) west of Block 46. Quaternary scarps have not been found near either Block 46 or Site S-15, but recognition of scarps is hindered by the paucity of outcrop of Quaternary deposits.

Quaternary scarps are abundant in the northern part of Hueco Bolson 30 mi (50 km) northwest of the Hudspeth County study area (S-34). A distinct Quaternary scarp lies 3 mi (5 km) southwest of the initial drillhole in Site S-34. This scarp and related structures are discussed more thoroughly below.

Recent compilations of regional seismicity data include (1) the entire Basin and Range province (Askew and Algermissen, 1983), (2) southeastern New Mexico (Sanford and Toppozada, 1974), and (3) southern Culberson County and adjacent areas (Dumas, 1980). Askew and Algermissen (1983) show six epicenters in the Trans-Pecos region between 1803 and 1977, two with Richter magnitudes (surface waves) 5 and 6. Both of these latter earthquakes occurred near Valentine, 50 mi (80 km) south of the Culberson County sites; one, the 1931 Valentine earthquake, had a modified mercalli intensity of VIII and was the strongest reported earthquake in Texas. The 1955 earthquake near Valentine had a modified mercalli intensity of IV (Reagor and others, 1982). Dumas (1980) detected about 300 earthquakes, all with magnitudes less than 3.7, between 1976 and 1980 near the site of the Valentine earthquake. Dumas (1980) also identified a seismically active area along the eastern margin of the Salt Basin in the area of abundant Quaternary fault scarps. However, this area could not be located precisely because it was outside the seismic network. Sanford and Toppozada (1974) listed 11 felt earthquakes prior

to 1961 and 6 instrumentally detected quakes between 1961 and 1972 in southeastern New Mexico and West Texas. Askew and Algermissen (1983) identified a swarm of earthquakes, all having magnitudes less than 4, centered near Juarez, Chihuahua, Mexico, about 45 mi (70 km) northwest of the Hudspeth County site.

Climate

The Hudspeth and Culberson study areas lie within the northern Chihuahuan Desert, south and southwest of the southern Guadalupe Mountains (King, 1948, his fig. 2; Miller, 1977, his fig. 1). The region has a subtropical arid climate (classification of Thornthwaite, 1931, as modified by Larkin and Bomar, 1983). Such climates are characterized by (1) high mean temperatures with marked fluctuations over broad diurnal and annual ranges and (2) low mean precipitation with widely separated annual extremes (Orton, 1964). For example, total annual precipitation at Carlsbad, New Mexico, just north of the study areas, ranges from 2.95 to 33.94 inches (7.5 to 86.2 cm) (Orton, 1964). Winds generally are from the north and west during fall and winter and from the south and west during spring (Bomar, 1983b). None of these winds carry significant moisture (Carr, 1967), except under unusual circumstances such as the intrusion of Pacific Hurricane Paul in September 1982, which introduced enormous quantities of moisture over the highlands of Mexico and into the West Texas region (Bomar, 1983a). Precipitation normally is dominated by late summer and early autumn rainfall from thundershowers. These storms occur when moist air from the Gulf of Mexico penetrates northwestward and rises to higher elevations as it approaches the mountains (Carr, 1967). Rainfall events are locally intense but short-lived, and surface water is ephemeral because of consistently high evaporative rates. Mean annual lake-surface evaporation in the study areas is approximately 83 inches

(211 cm) (Larkin and Bomar, 1983). Evaporation is aided by strong winds that also produce conditions of blowing dust several days each year, primarily during early spring (Bomar, 1983b). High evaporation and low, highly localized rainfall combine to form drought conditions during all or part of most years. During the period 1951 to 1981, Hudspeth, Culberson, and adjacent counties recorded the lowest annual precipitation of any reporting stations in Texas in 19 of those 31 years (Bomar, 1983a). Climatic data from stations of long record near the study areas are summarized in table 1.

CULBERSON COUNTY INVESTIGATIONS

Location

The Texas Low-level Radioactive Waste Disposal Authority selected two areas in Culberson County, Texas, for evaluation as possible sites for a low-level radioactive waste repository. The two areas are shown in figure 1 and are referred to as Site S-15 and Block 46.

Site S-15 consists of Sections 16 and 21 in PSL Block 114, which is administered by the General Land Office. Block 46 is owned and administered by The University of Texas System. Site S-15 is located on the Gypsum Plain west of the Rustler Hills. It lies on the Seven L Peak NE 7 1/2' Quadrangle approximately 8 mi (13 km) west-northwest of the Pennzoil Sulphur Mine. Access to Site S-15 and adjacent areas was obtained from property owners J. Covington, R. L. Harrison, and H. M. Phillips, Jr., and from lessee F. Armstrong. Block 46 is located about 8 mi (13 km) west of Site S-15 and lies mostly on the Seven L Peak and Chico Draw East 7 1/2' Quadrangles. Block 46 straddles the boundary between the western edge of the Gypsum Plain and the eastern margin of the

Table 1. Summary of climatic data.

	Hudspeth Co. Cornudas Service Station*	El Paso Co. El Paso**
Temperature		
Maximum (1960)		109°F (43°C)
Minimum (1962)		-8°F (-22°C)
Mean (1951-80)		63.4°F (17°C)
Precipitation		
Mean (1951-80)	8.85 (22.5 cm)	7.82 inches (20 cm)
Wind		
Mean velocity (1931-60)		10.0 (mph)
Mean direction		N

*National Climatic Data Center (1985, p. 15)

**Orton, (1969, p. 33, 39); National Climatic Data Center (1985, p. 15)

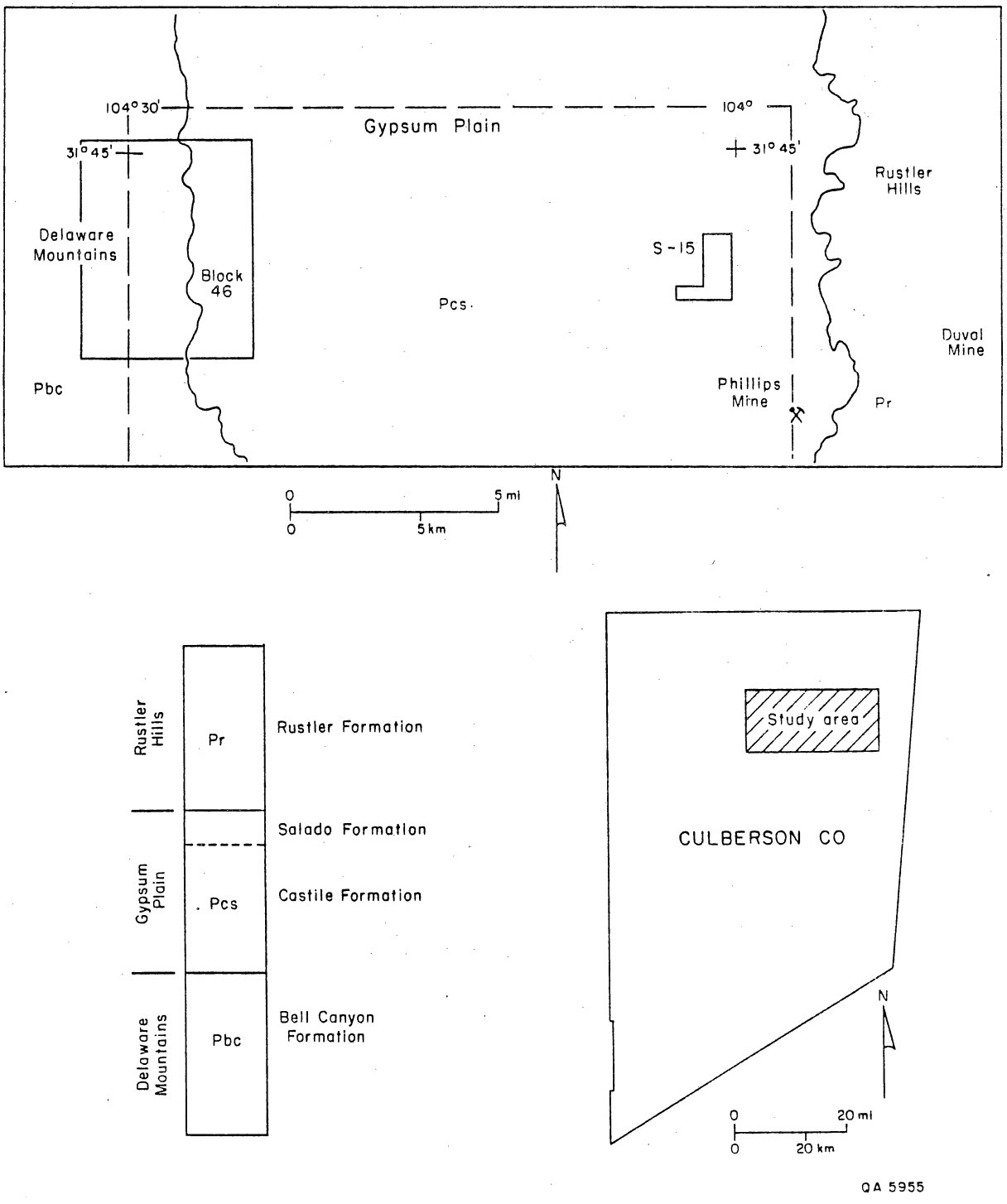

Figure 1. Location and stratigraphy of Block 46 and S-15 study areas, Culberson County. Stratigraphy from Barnes (1983). Dashed lines locate figure 4.

Delaware Mountains. Access to Block 46 was obtained from the Rounsavill family, owners of the KC Ranch and lessees of surface grazing rights in Block 46.

Methods

The general proximity and geologic similarity of Site S-15 and Block 46 required that a somewhat larger region encompassing both areas be considered in our current investigations. Low sun-angle aerial photographs of the region, printed at a scale of 1:12,000 (1 inch = 1,000 ft), were acquired. The area flown includes part of the Rustler Hills east of S-15 and a portion of the Delaware Mountains west of Block 46. Particular attention was focused on those features, such as faults, fractures, and evidence of solution or collapse, that are pertinent in evaluating the viability of the areas to host a low-level radioactive waste repository.

The surface geologic investigations attempted to document geologic features identified on the aerial photographs and to refine our understanding of the structural geology, geomorphology, and near-surface lithologic units present in the two areas. Six man-days were spent in the field in S-15, and 12 man-days were spent in Block 46. Access to the areas is restricted by the local landowners, and no drilling or excavations were done in either S-15 or Block 46. Engineers from the Civil Engineering Department of The University of Texas at Austin collected surface samples from S-15.

Water levels were available only for wells east of the S-15 site in the area of the Pennzoil Sulphur Mine. No water levels from wells were available within S-15 or in the neighboring areas to the north, west, or south borders. However, many springs are present in this area and their altitudes were used as water-level altitude markers (fig. 2). Information about water levels in Block 46 was very scarce (two wells and two springs, fig. 3) and did not allow the production of a potentiometric

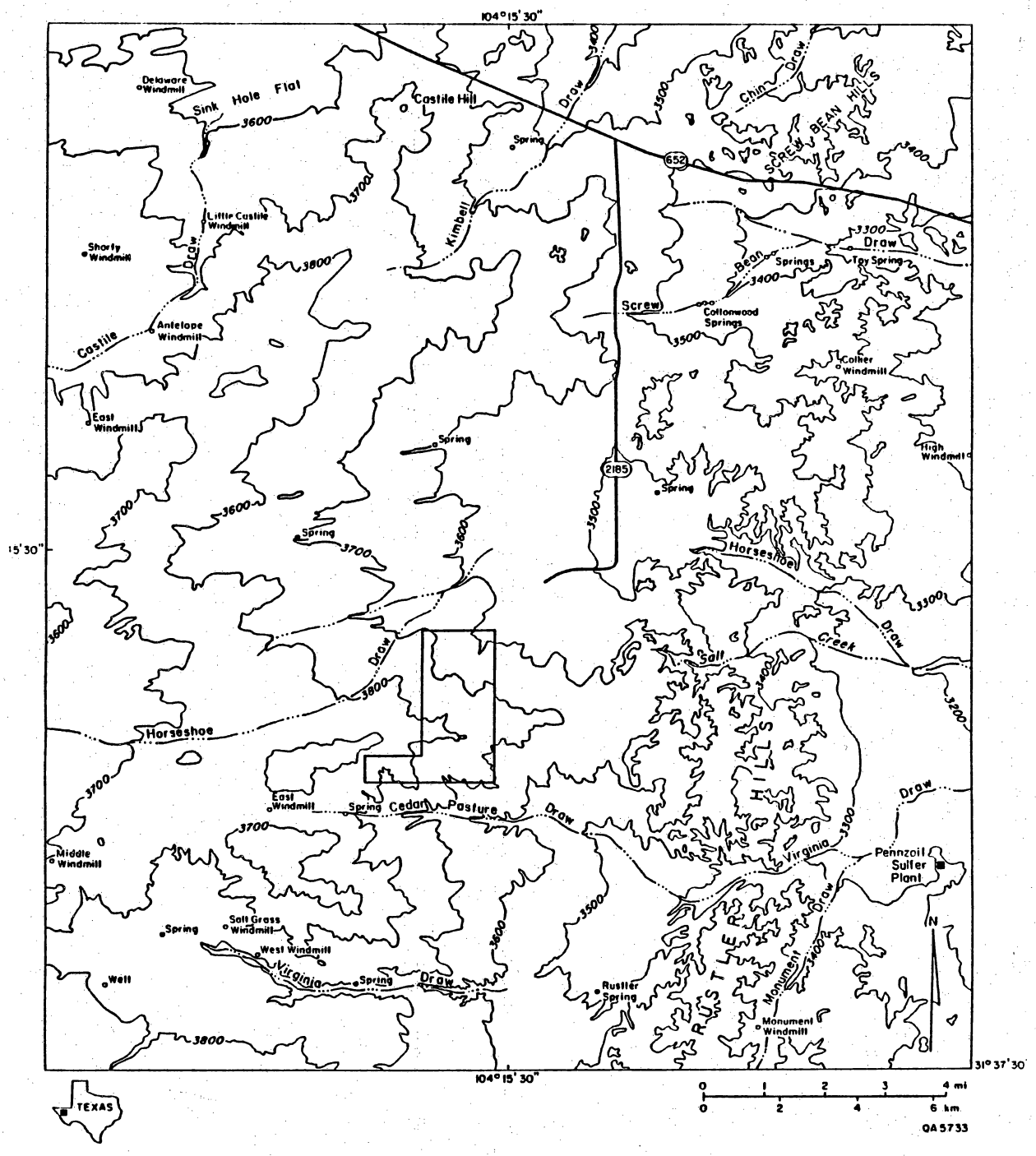

Figure 2. Base map and location of springs in the vicinity of S-15 study area in Culberson County. Bold line approximately locates the site area.

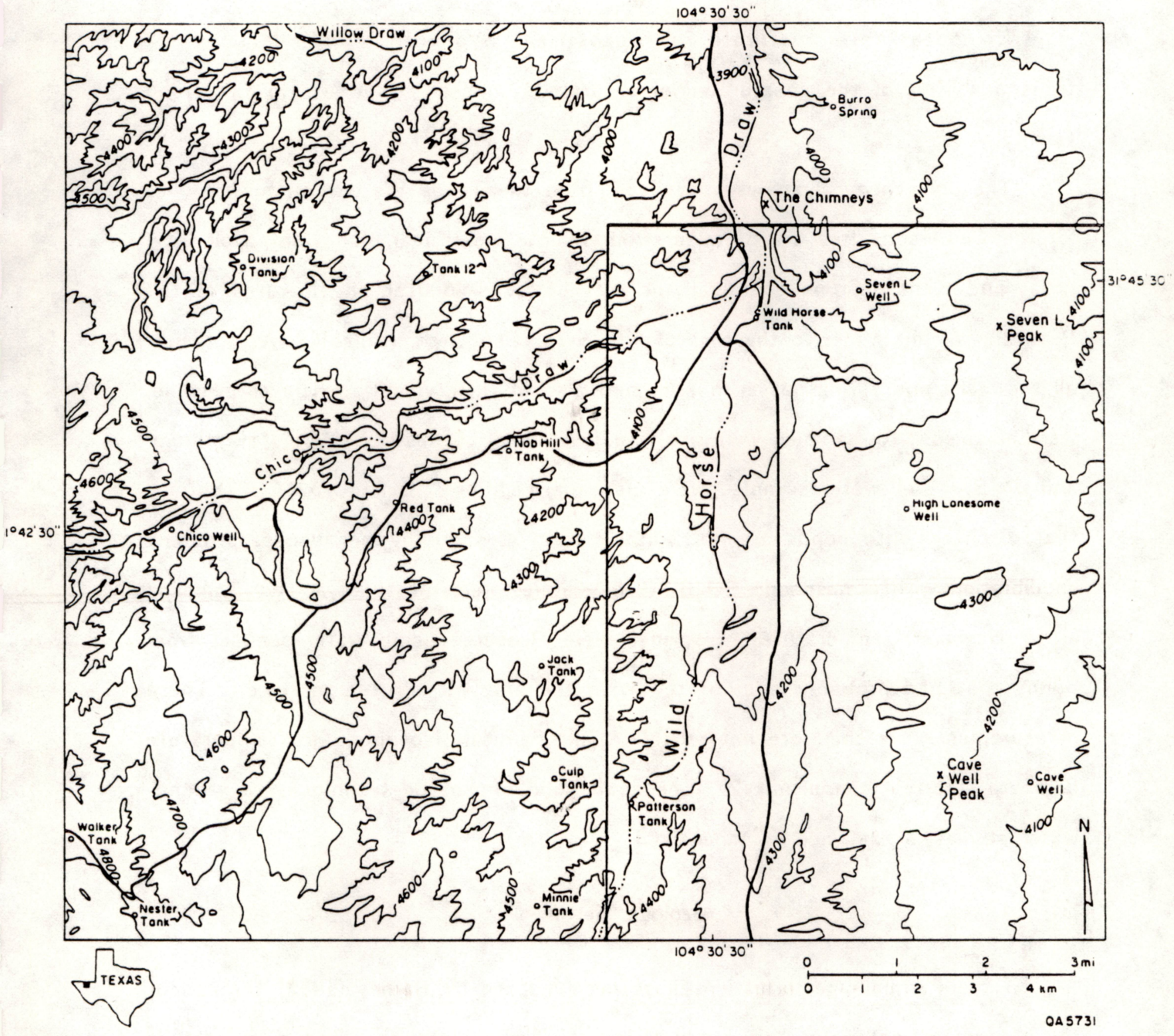

Figure 3. Base map and location of springs and wells in the vicinity of Block 46 study area in Culberson County. Bold line approximately locates the site area.

surface map of the site. All information about water levels is presented in appendix 1.

No data were available for porosities, hydraulic conductivities, or transmissivities of the unsaturated or saturated zones of either site in Culberson County.

The only chemical analyses available from the Texas Water Commission files for the Culberson sites are of water from remote wells near Van Horn, Dell City, Orla, and Kent. Some chemical analyses of wells located in the area of the Pennzoil Sulphur Mine, to the east of site S-15, also were available. As a result, all the wells and springs at each site, and also in their vicinity wherever possible, were sampled. All samples were analyzed for general chemistry, $\delta^{18}O$, $\delta^{2}H$, tritium, and $\delta^{34}S$. Well-water samples were also analyzed for ^{14}C and $\delta^{13}C$. (Springs that discharge into ponds are not suitable for ^{14}C sampling because of probable equilibration with atmospheric CO_2.) Temperatures were measured at each sampling site. However, temperatures of springs were measured using water samples from ponds that had probably equilibrated with the ambient air temperature. These measurements are therefore not reliable. All chemical, isotopic, and temperature data are reported in appendix 2. The application of isotope techniques to ground-water studies is explained in appendix 3.

Geologic Setting

Three Permian-age formations have been mapped by Barnes (1983) throughout the area investigated for this study (fig. 1). These units are, from youngest to oldest, the Rustler, Castile, and Bell Canyon Formations (fig. 1). The Rustler Formation consists of limestone, siltstone, sandstone, gypsum, and clay up to 140 ft (45 m) thick (Barnes, 1983). The Castile Formation (Anderson and others, 1972) consists of gypsum, anhydrite, and limestone up to 2,000 ft (610 m) thick;

halite (salt) occurs in the subsurface (eastward) but does not crop out. Limestone lenses occur within the bedded gypsum of the Castile Formation. At the surface these resistant limestone bodies appear as castlelike hills and are named castiles (Adams, 1944; Motsch, 1951). Strata of the Salado Formation may crop out between the Castile and Rustler Formations. Barnes (1983) did not differentiate the upper Castile and Salado Formations, probably because of their similar lithologies and poor exposures. The Bell Canyon Formation is 700 to 1,000 ft (215 to 305 m) thick and consists of fine-grained sandstone and interbedded thin limestone lenses. The formations dip 1° to 2° toward the east. The three formations have distinctive physical and weathering properties such that the outcrop areas are physiographically distinct. The Rustler Formation forms irregular low hills (the Rustler Hills) with up to 330 ft (100 m) of relief. The nonresistant evaporite beds of the Castile Formation form gently rolling topography called the Gypsum Plain. More resistant beds in the Bell Canyon Formation form hills of greater relief in the eastern part of the Delaware Mountains.

Karst Topography of the Gypsum Plain

Karst landforms and landforms possibly indicative of ancient karst processes are common throughout both of the potential low-level radioactive waste sites in Culberson County. These features include, from smallest to largest, karren, swallow holes, collapse sinks, dolines, blind valleys, and subsidence basins (fig. 4). Castiles are landforms that are not true karst features but that perhaps result in part from karst processes. Troughlike features in the western part of the study area also have been attributed to solution and subsidence (Olive, 1957). Karst landforms are discussed in detail in appendix 4.

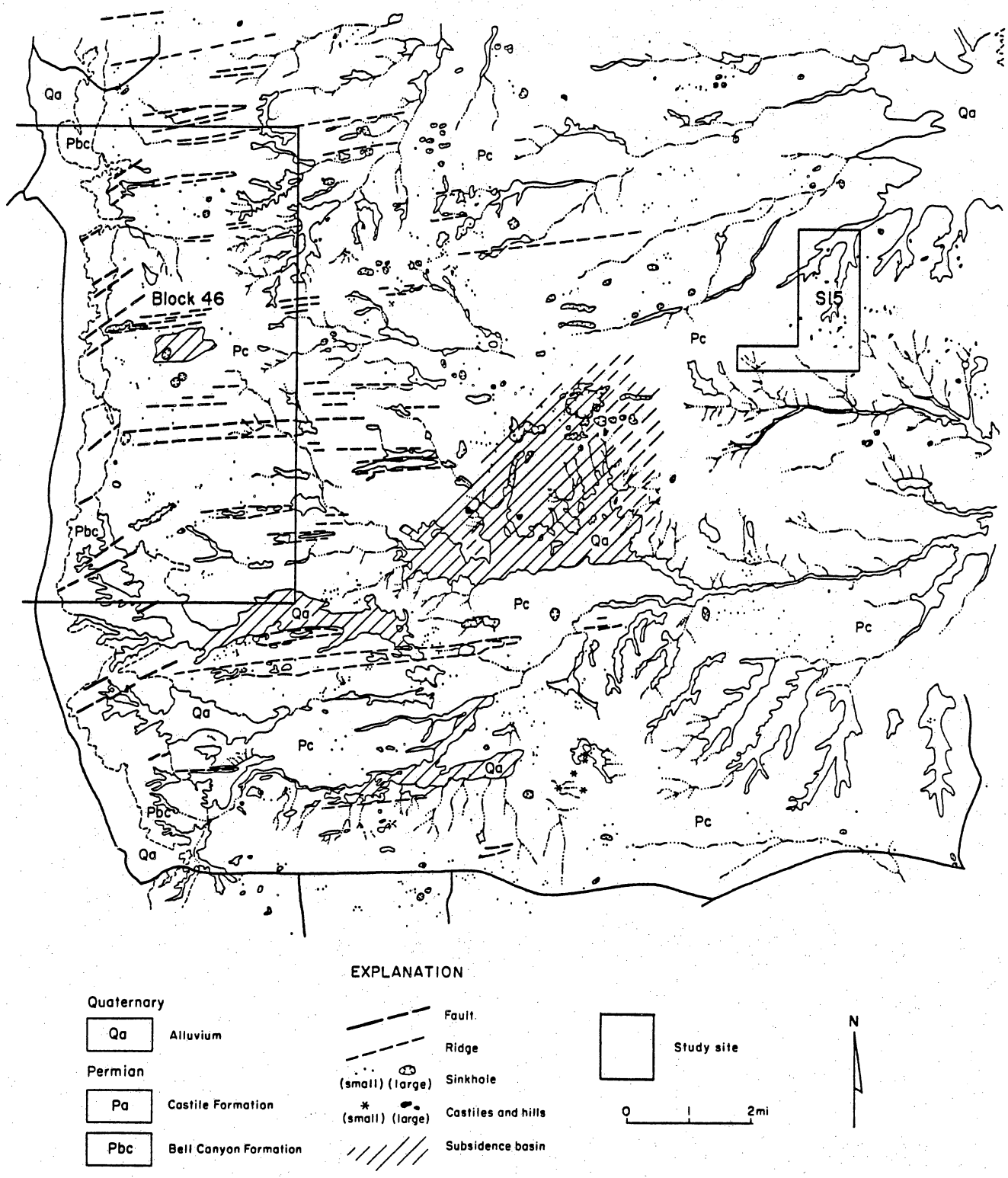

Figure 4. Geomorphic map of Culberson County study region. See figure 1 for location of figure 4.

The widespread distribution of karst landforms and related features is strong evidence that the study area, including both potential low-level radioactive waste repository sites, is underlain by a system or systems of caverns. The complexity and openness of the karst drainage system underlying the proposed low-level waste isolation sites in Culberson County are difficult to characterize. For example, the cavern system extends to the surface, but the depth of cavern development is unknown. Although the general direction of ground-water movement can be determined from potentiometric head maps, the actual paths and velocities of ground-water movement through cavern systems have not been determined. Furthermore, because the distribution of caverns is not known, the potential for developing new sinkholes or other subsidence features anywhere in the study area cannot be determined, nor can the potential location of these features be predicted.

Parallelism between cavern segments and joints is a common relationship in areas of karst drainage. Field and aerial photographic evidence suggests that aspects of the surface drainage of the study area are influenced by joint systems. These observations, in conjunction with the interpretation that several groups of sinkholes, castiles, and subsidence basins parallel northeasterly striking joints and faults, suggest that subsurface drainage also has been influenced by joint systems.

Geology of Site S-15

The S-15 site is an area of about 3 mi^2 (5 km^2) (fig. 5, pl. 1). The topography is rolling and includes several small hills with 35 to 65 ft (10 to 20 m) of relief that project above the surface of the Gypsum Plain. The hills contain outcrops and surface rubble of a massive to platy dolomite and a siliceous sandstone and conglomerate. Cobbles in the conglomerate consist of chert,

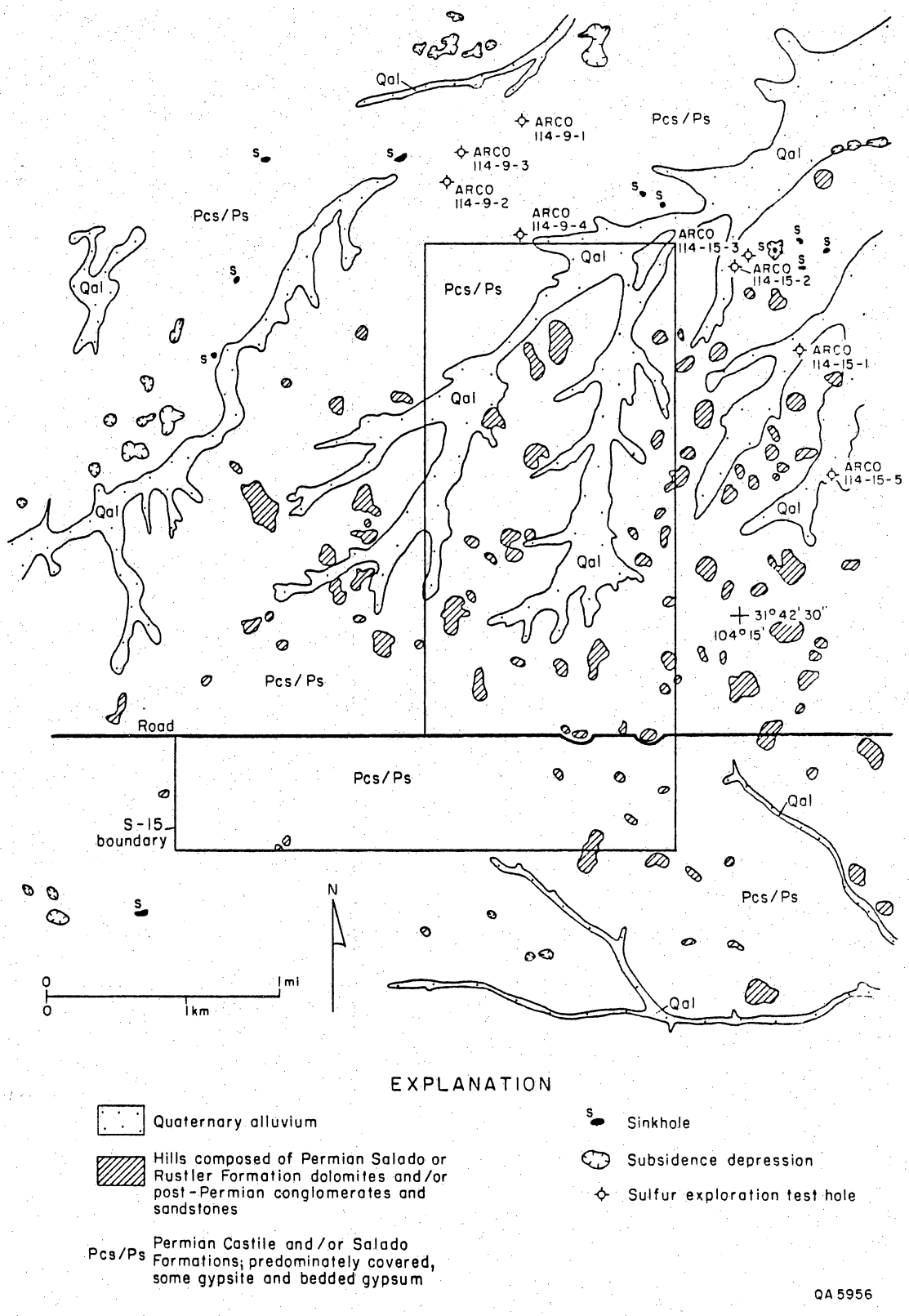

Figure 5. Geologic map of S-15 study area. Location in Culberson County is shown in figure 1.

quartzite, and siliceous volcanic clasts. A lithologically similar conglomerate, which contains fossils probably reworked from Cretaceous marine sedimentary rocks, occurs on hills located about 6 mi (10 km) to the southwest of S-15 near Virginia Draw.

Outcrops are not common on the hills at S-15, but the sandstone tends to occur as steeply inclined blocks that appear to dip toward the core of the hills. The dolomite, sandstone, and conglomerates are interpreted to be collapsed remnants of overlying units that fill relic sinkholes in the Castile Formation. The dolomite is interpreted to be either from the Salado or Rustler Formations, and the sandstones and conglomerates are probably post-Cretaceous in age. A clay-rich soil that may be a residue from solution of more soluble units is locally present on the hills.

Strata at the S-15 site are generally poorly exposed. Either sediments comprising the upper section of the Castile Formation or sediments of the Salado Formation crop out around the hills (fig. 5, pl. 1). Near-surface gypsum exposures have decomposed to gypsite, although some bedded gypsum is also exposed. Driller's logs of several sulfur exploration wells near the site suggest that 20 to 60 ft (6 to 18 m) of interlayered clay, sand, and gypsum may overlie thicker sequences of gypsum. Although no recently formed karst landforms are present in S-15, they do occur in the immediate vicinity of the site. The relic sinkhole fillings in the hills of S-15, coupled with the proximity of karst landforms of more recent origin, imply that a system of subsurface solution channels may be present near or within the study area. Some of the intense deformation in the Rustler Formation, 2.5 mi (4 km) east of S-15, was probably caused by evaporite dissolution and subsidence.

Geology of Block 46

The Permian Bell Canyon and Castile Formations crop out in Block 46 (fig. 1, pl. 2). The contact between the formations runs roughly north-south through the middle of the block; the Bell Canyon Formation crops out in the western part and the Castile Formation in the eastern part. In general, the Bell Canyon Formation consists of fine-grained sandstones and numerous thin limestone lenses. The Castile Formation consists of a distinctively banded rock composed of alternating layers of calcite and anhydrite. This rock does not commonly crop out. Instead a weathered residuum of gypsite and clay mantles the bedrock to variable depths.

The stratigraphic section at the contact between the two formations was examined in detail to define the contact and to interpret structure. The section is:

Castile Formation	
Massive banded limestone; typical rhythmic Castile bedding but contains little if any anhydrite	
Bell Canyon Formation	
Platy, dark-brown limestone, laminated at a scale of a few mm, petroliferous; forms bench	1.64 ft (0.5 m)
Finely laminated, thin-bedded sandstone, a few 5- to 10-cm-thick beds of sandstone; forms slope	9.84 ft (3 m)
Platy, gray limestone, petroliferous, nonlaminated; forms bench	1.64 to 3.28 ft (0.5 to 1 m)
Finely laminated, thin-bedded sandstone	6.56 ft (2 m)
Massive, crossbedded sandstone	2.62 ft (0.8 m)
Finely laminated, thin-bedded sandstone	6.56 ft (2 m)
Massive, crossbedded sandstone with laminated, thin-bedded sandstone	9.84 ft (3 m)

Structures in Block 46

Significant structures in Block 46 (King, 1949) include a major set of northeast-striking normal faults, a lesser set of north-striking faults, and several prominent joint sets that are in part parallel to the fault trends (pl. 2).

Northeast-striking faults, oriented between N 45 and 65 E, are the most prominent structures in Block 46, although they generally have less than 35 ft (10 m) of displacement. These faults are easily observable on aerial photographs, both within the Bell Canyon Formation and where the contact between the Bell Canyon and Castile Formations is displaced. Northeast alignment of sinkholes, castiles, and sulfur deposits in the Castile Formation indicates continuation of these faults at least as far east as the Rustler Hills.

Faults in the Bell Canyon Formation

Northeast-striking faults (N 45-65 E) cutting the Bell Canyon Formation are common throughout Block 46. Several northerly striking faults (N 0-10 E) also occur in the western part of the site. Fault traces up to 1.2 mi (2 km) long were observed on aerial photographs and throws up to 25 ft (7 m) were estimated from outcrop exposures. Some of the northeast-striking fault traces exhibit an en echelon pattern, indicating that these faults are part of a 1,300-ft- (400-m-) wide zone that crosses Block 46 and cuts Bell Canyon and older strata at least 5 mi (8 km) to the southwest. Many of the northeast-striking faults that occur at the Bell Canyon-Castile contact appear to die out southwestward; however, they project into zones of closely spaced joints.

The fault traces are usually poorly exposed in outcrop. Where strata are exposed, closely spaced joints striking parallel to the fault traces are abundant. A few small-scale normal faults dipping between 65° and 90° also were identified along the major fault traces, suggesting that the major faults are high-angle normal faults.

Fault planes were observed at two locations: near hill 4144 at the eastern edge of the Chico Draw East Quadrangle and west of hill 4295 just east of the main road on the Seven L Peak Quadrangle. Near hill 4144, two small faults (N 61 E, 68 SE, ~3 ft [~1 m] of displacement; N 52 E, 76 SE, ~1 ft [~30 cm] of displacement) occur in massive sandstones. Observed displacement of beds and slickensides on the fault planes indicates normal displacement down to the southeast. These small faults parallel a prominent topographic escarpment immediately to the north, which probably marks a fault of greater displacement.

West of hill 4295, a fault striking N 57 E and dipping 68 NW displaces massive and laminated sandstones in the upper part of the Bell Canyon Formation just below its contact with the Castile Formation. Displacement of beds and slickensides in the fault plane shows that displacement is normal down to the northwest. Total displacement is approximately 10 ft (3 m). The northeastward continuation of the fault toward the contact with the Castile Formation is poorly exposed. However, the fault is adjacent to one of the northeast-striking fault/flexure grabens that occur along the contact and that are described below.

Fault/Flexure Grabens at the Bell Canyon - Castile Contact

At least seven fault/flexure grabens occur along the Bell Canyon - Castile contact within or immediately adjacent to Block 46. These structures are the continuation of northeast-striking faults from the Bell Canyon Formation; however,

their style of displacement is considerably more complex than the simple normal motion observed in the Bell Canyon. All are marked by linear topographic depressions resulting from erosion of the Castile Formation within the graben. The margins consist of the resistant banded carbonate rock that is considered to be the lowest part of the Castile Formation.

Structures at the margins of the grabens are faults, flexures, or both. Actual fault displacement at the margins is indicated by apparent abrupt termination of some rock units but is difficult to demonstrate due to poor exposure. Exposed flexures consist of the banded carbonate rock that forms resistant northeast-trending ridges. The beds generally dip into the graben as much as 65^{o}. Several flexures appear to be monoclines having no fault displacement. Some flexures are asymmetric anticlines: beds dip gently away from the grabens on the outer limb and more steeply into the graben on the interior limb.

The floors of the grabens are commonly slightly asymmetric with the structurally lowest part near one margin. Beds on the higher side dip gently toward the structurally lower side.

Total displacement across these grabens includes both the displacement from the structural margin into the graben and the displacement across the faulted margin. Displacement in the grabens ranges from as much as 100 ft (30 m) on one of the structures at the south end of the Seven L Peak Quadrangle south of Block 46, to about 10 to 15 ft (3 to 5 m) on structures within Block 46. Net displacement across the grabens is small and cannot be determined precisely; displacement is apparently almost canceled out by nearly equal but opposite senses of motion on the paired graben faults. This net displacement may be comparable to that shown by the faults in the Bell Canyon Formation. Although dominant motion appears to be normal, microfaults, shear zones, and tension gashes in the

banded carbonate at the base of the Castile Formation indicate at least some component of right-lateral strike-slip motion.

A similar grabenlike structure, discussed below, has been mapped in the subsurface about 9 mi (15 km) to the east, where it localizes sulfur mineralization at the Phillips Ranch deposit. Several small sulfur prospects occur along the structures in Block 46; all were in the laminated sandstone between the two petroliferous limestones at the top of the Bell Canyon Formation.

Origin of the grabens is not clear. Certainly they are continuations of the northeast-striking faults. The restriction of the grabens to the basal Castile Formation indicates that their complex geometry is a result of the contrast in mechanical properties of the Bell Canyon and Castile Formations.

Northeast-striking Faults in the Castile Formation

Continuations of northeast-striking faults and the fault/flexure structures into the Castile are indicated by photo lineations and alignment of castiles and sinkholes. Most notably, several castiles, including Cave Well Peak, and several large sinkholes occur along a photo lineation that extends from the northern limb of a prominent graben near the southern boundary of Block 46 (fig. 2). Two castiles just north of High Lonesome Well lie on the continuations of each limb of a graben.

Northeast-striking Faults in the Rustler Hills

Test drilling for sulfur has delineated several northeast-striking faults in the vicinity of the Rustler Hills (Smith, 1980). These faults trend about N 65 E and have 25 to 80 ft (8 to 25 m) of displacement. They commonly localize sulfur deposits, including the major Culberson Mine and Phillips Ranch deposits. Smith (1980) shows isopach and structure-contour maps that demonstrate the faults. The

Phillips Ranch deposit occurs at the base of the Castile Formation in a narrow graben about 985 ft (300 m) wide and possibly 1.2 mi (2 km) long. The structure-contour map of the deposit (Smith, 1980, his fig. 5) shows a feature remarkably similar to the fault/flexure grabens mapped by us at the same contact.

Timing of Northeast-striking Faults

The time of displacement along the northeast-striking faults is not well constrained by available data. The northeast-striking faults are most likely related to Basin and Range extension, which began about 24 mya but occurred in two different episodes of different stress orientations. East-northeast-oriented extension during the earlier episode produced the characteristic northwest-striking faults that dominate the Basin and Range province of Trans-Pecos Texas. During the younger episode, possibly from 15 or 10 mya to the present, extension was oriented northwest, which would have produced northeast-striking faults. The northeast strikes of the faults and of the slickensides within them indicate northwest extension and suggest that the faults formed during the younger episode of late Basin and Range extension.

Joints

Four joint sets occur in Bell Canyon and Castile strata. Orthogonal sets are comprised of joints striking N 40-70 E and N 20-30 W, and joints striking N 80-100 E and N 10 W-N 10 E. Northeast-striking joints (N 40-70 E) are the most common (fig. 6, pl. 2). Zones of closely spaced joints exist throughout the area for all four joint sets; however, most of the zones strike northeast (N 40-70 E). Some of the closely spaced joint zones are related to the fault traces that cross the area. Joint zones may be as wide as 130 ft (40 m), and the joint spacing within

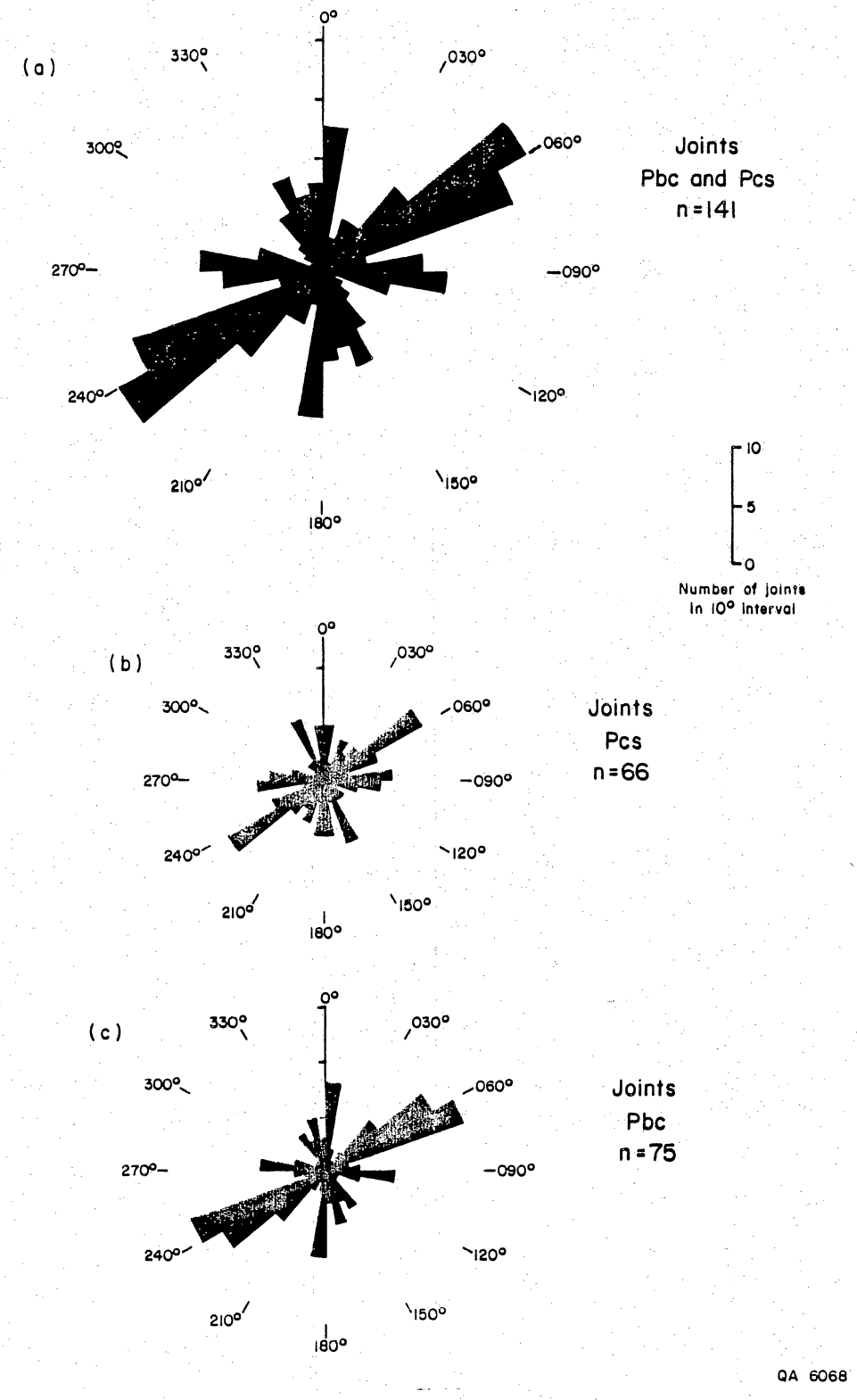

Figure 6. Rose diagram plots for joints measured in strata of (a) Bell Canyon (Pbc) and Castile (Pcs) Formations, (b) Castile Formation (Pcs) and (c) Bell Canyon Formation (Pbc). n = number of joint measurements.

the joint zones is as great as 12 joints/6 ft (2 m) in beds that are 5 to 6 ft (1.5 to 2 m) thick. Dissolution and erosion along joints have developed caverns in the gypsum strata of the Castile Formation. Joints also locally control the direction of surface drainage in Bell Canyon and Castile strata.

Sulfur Mining in the Rustler Hills Region

The Rustler Hills region of Culberson County contains substantial sulfur deposits that have been mined at two locations by means of the Frasch process. Future sulfur mining in close proximity to site S-15 could alter the geology of the site. In the Frasch process, sulfur is mined by injecting very hot waters, melting the sulfur, and pumping the liquid sulfur to land surface. Land subsidence results from the sulfur extraction.

The Pennzoil Sulphur Company Culberson Mine (formerly Duval Sulphur Mine), located 6.5 mi (10.5 km) east of site S-15 and 39 mi (63 km) west of Pecos, Texas, on FM 2119, is the only operating Frasch sulfur mine. Production of sulfur began September 30, 1969, with cumulative production of 28,703,157 long tons (LT) and estimated recoverable resources of 31,524,000 LT. The Culberson Mine is the largest producing sulfur mine in the western hemisphere. Currently, sulfur is being produced from the Permian Salado Formation at depths of approximately 300 to 600 ft (90 to 180 m) below land surface. The total interval of sulfur occurrence in the area ranges from the top of the Permian Bell Canyon Formation to ground surface (see stratigraphic column, this report) (Joseph W. Mussey, Chief Geologist, Pennzoil Sulphur Company Culberson Mine, personal communication, 1986). Production also occurred at the Phillips Mine, 1.5 mi (2.4 km) southeast of site S-15; the mine is now inactive.

Land-surface subsidence and collapse are common natural features around the Culberson Mine, resulting from the dissolution and removal of Permian-age evaporites by ground water in the subsurface (Snyder and Gard, 1982). Subsidence at the Culberson Mine, however, is man-induced, resulting from the removal of sulfur by Frasch mining. This type of subsidence is generally a slow, controlled occurrence and is classified as trough subsidence (Obert and Duvall, 1967). As of December 31, 1985, maximum vertical subsidence was 60 ft (18 m). Subsidence is contained within the mine area (~4 mi^2 [~10.4 km^2]) and is not expected to affect site S-15, which is 6.5 mi (10.5 km) away.

Future mining in areas that are closer, if not directly adjacent, to S-15 could result in subsidence at the site. Porsch (1917) identified sulfur deposits throughout the Rustler Hills area as potential or active areas of sulfur mining. Field investigations conducted in the vicinity of site S-15 found several localities of sulfur at the surface and of springs that contain sulfur-bearing water, indicating sulfur mineralization in the subsurface.

Surface Flow

Both sites are dissected by narrow valleys that contain ephemeral streams (figs. 2 and 3). The direction of the surface flow is locally affected by dissolution features. Dissolution arches made of gypsum that represent formerly breached land surface can be observed hanging above current, lower surface drainage systems.

Close relationships exist between the surface drainage system and ground water at both sites. The presence of many springs in the draws indicates that the draws serve as a discharge zone for the shallow aquifer. Some ground water discharges into the draws by direct evaporation, which is indicated by large moist

areas covered with salt crust (e.g., Virginia Draw west of Rustler Spring, fig. 2). Prolonged periods of drought during which no surface-flow runoff is observed are common in this area (Olive, 1957).

Hydrologic Setting

Water-bearing Characteristics

The Castile Formation at sites S-15 and Block 46 contains aquifers. Porosity and permeability distributions in these aquifers are dominated by dissolution processes. The limestone and evaporite beds have vugular porosity and in some cases form caverns (e.g., Cave Well, Block 46 site). Hollow spaces that underlie a thin crust of soil are common at both sites, possibly suggesting soil piping. No data on transmissivity and storativity coefficients were available for this region. Large declines of water levels, to the extent that wells may run dry after several years of pumpage (Seven L Well, Block 46 site) or even after one year of drought (Cave Well, Block 46 site) (K. Moore, University Land Office, personal communication, 1986), indicate that the values of transmissivity and storativity are probably small (also Brown and others, 1973). Aquifer thicknesses at the sites are unknown.

Recharge

Recharge into the Castile aquifers results from direct precipitation on outcrops and from flash floods in permeable riverbed clastics at the washes. Olive (1957) suggests that most of the water that flows through underground channels in the Castile Formation is derived from the underlying Delaware Mountains Group (whose upper formation is the Bell Canyon) and that only a minor amount comes from surface runoff.

Ground-water samples were collected and analyzed for tritium and ^{14}C. Tritium and ^{14}C are radioactive isotopes used to estimate the age of water. Tritium may be used to qualitatively identify waters less than 40 yr old, and ^{14}C can be used for water less than 30,000 yr old (see app. 5 for method of calculation of ^{14}C ages). Ground-water analyses from both sites show high tritium activities (6.7 to 28 TU) in combination with high to moderate values of ^{14}C (modern to 5,900 yr old) (figs. 7 and 8, app. 2). This observation supports Olive's suggestion of ground water "base flow" coming from the west (fig. 9), parallel to the regional dip (characterized by lower ^{14}C values), that is supplemented by recent recharge sources (with high tritium activities) from local rains and surface water.

Discharge

Many springs occur in the S-15 site and in its vicinity. Some of them issue directly from the Castile Formation, whereas others discharge from the contact between the Castile Formation and the overlying permeable alluvial deposits. The annual discharge of these springs is relatively small and varies from seeps to 111 gpm (7.0 lps) (Brune, 1981). In topographically low areas, discharge may also take place through direct evaporation from an extremely shallow water table, resulting in the formation of gypsum crusts and increased salinity of the ground water (this is the case in Virginia Draw, south of the S-15 site, fig. 2). Changes in vegetation types were observed in many of the low areas, which may indicate a shallow water table and discharge via evapotranspiration.

Potentiometric Surface

Based on the shallow depth to water that ranges from 0 to 150 ft (0 to 46 m) (app. 1) it is assumed that water in the Castile Formation flows under

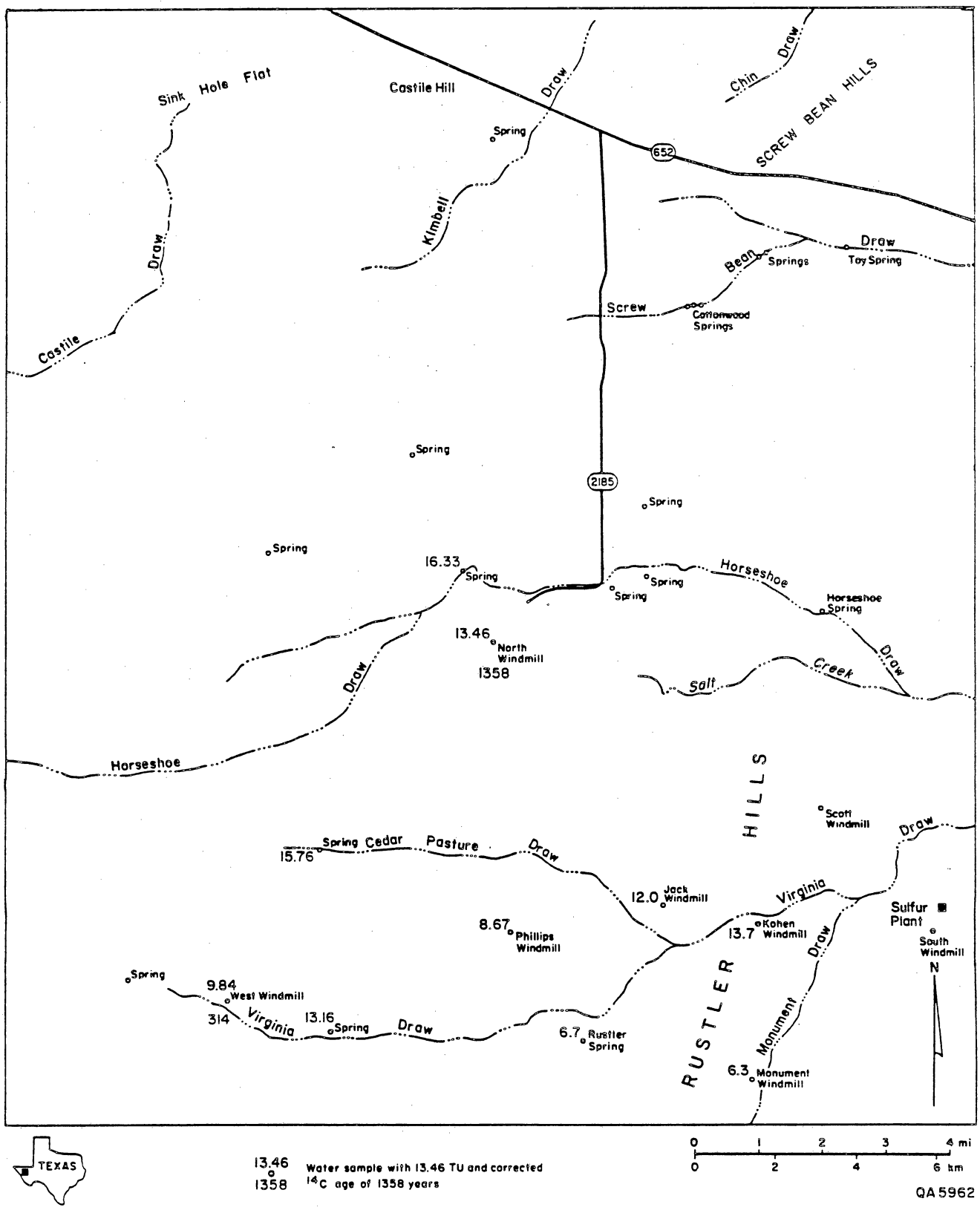

Figure 7. Tritium activity and ^{14}C corrected ages distribution in ground water of S-15 study area, Culberson County.

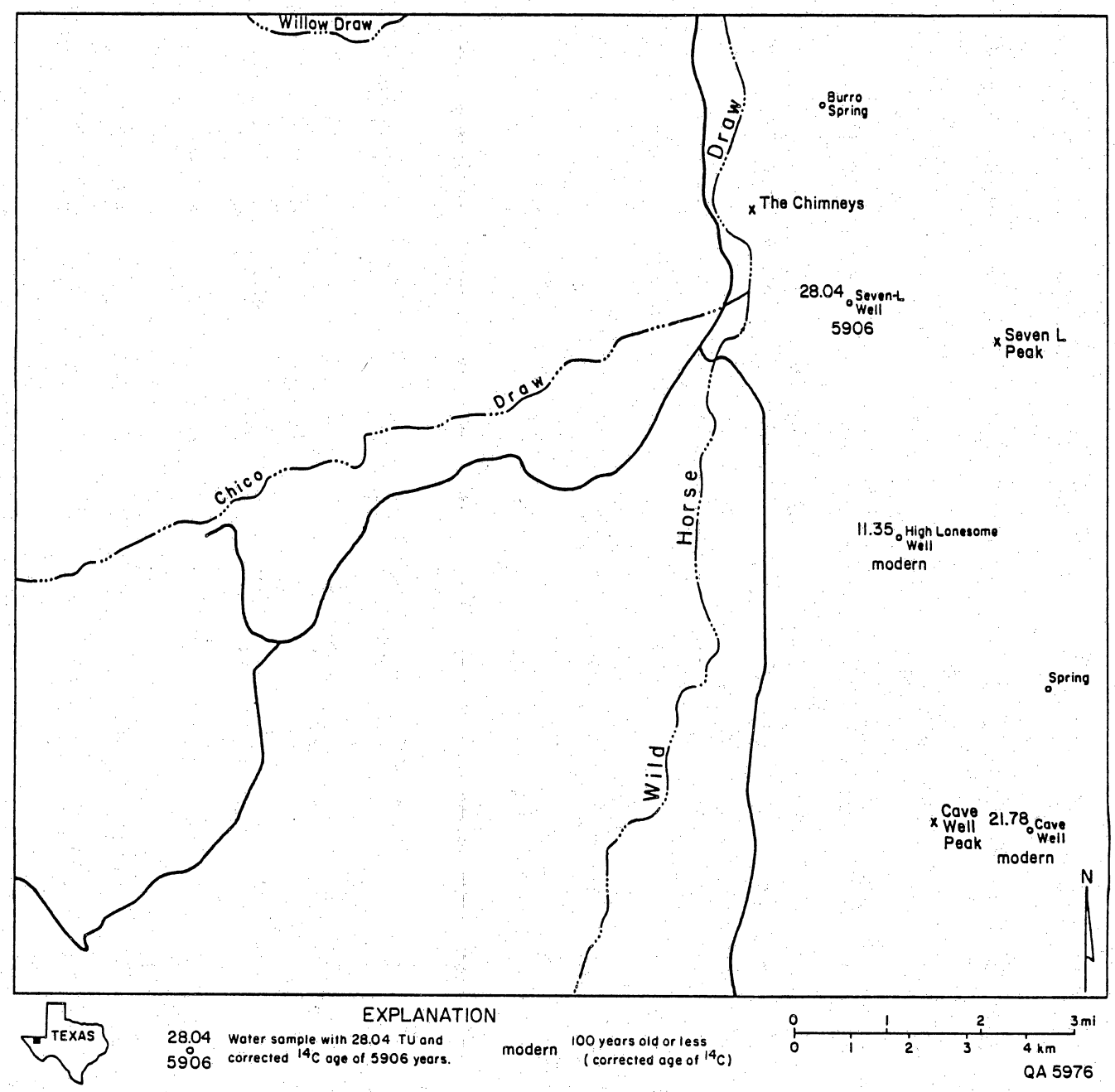

Figure 8. Tritium activity and ^{14}C corrected ages distribution in ground water of Block 46 study area, Culberson County.

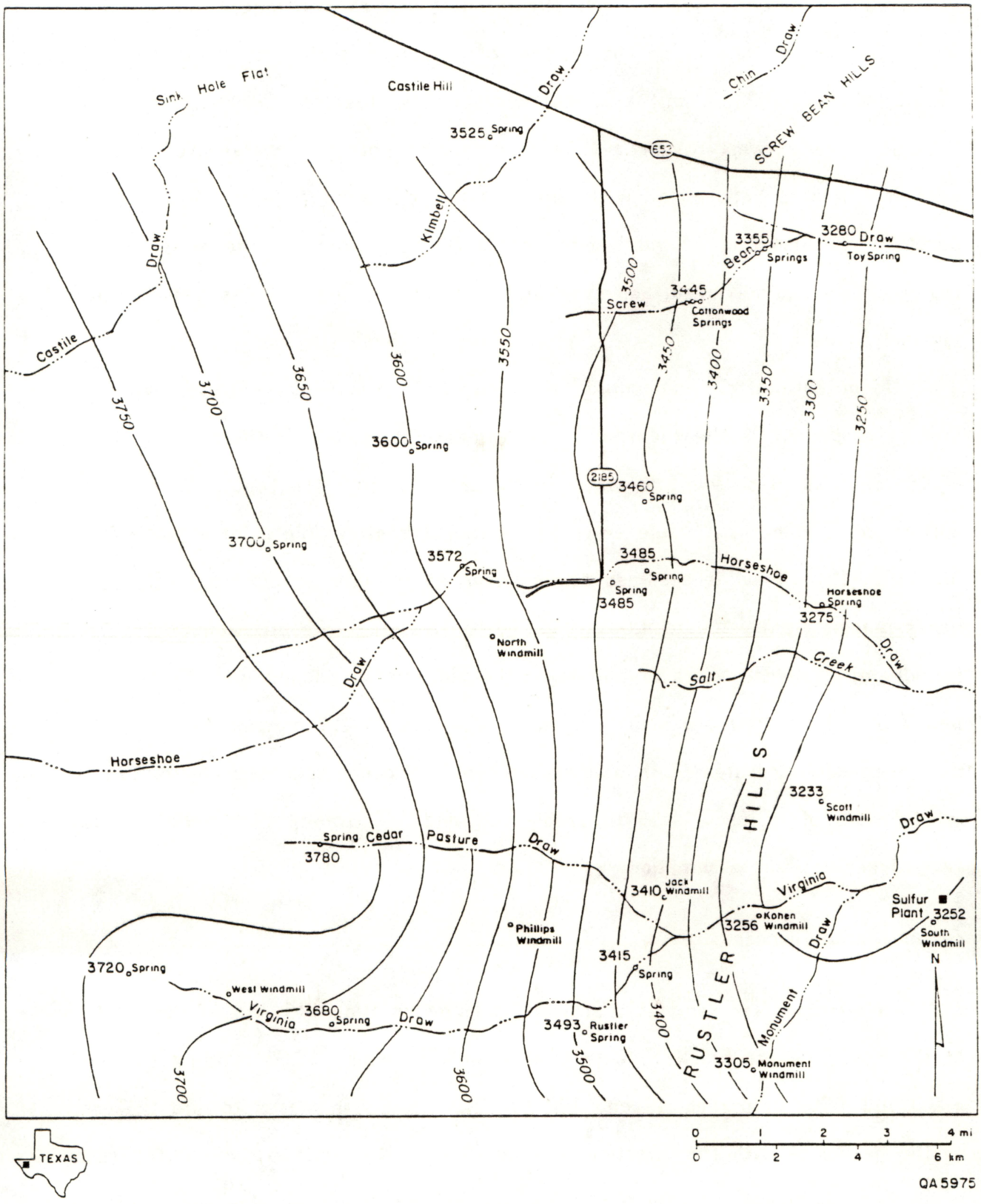

Figure 9. Ground water level distribution (ft) of S-15 study area in Culberson County.

water-table conditions. Water levels (fig. 9) at the S-15 site range from 3,700 to 3,250 ft (1,130 to 990 m) . The gradient of water-level surface ranges from 13 to 120 ft/mi (2.5 to 23 m/km). Ground water follows the regional topographic and geologic dip from west to east. It is important to note that water-level contours were interpolated between all wells and springs, regardless of which aquifers they penetrate, because that information was not available. However, the presence of a regional potentiometric surface suggests some interconnectedness between the regional aquifers.

No potentiometric map could be produced for the Block 46 site, owing to scarcity of data. Despite the shallow water table, indicated by the minimal depth of 20 to 30 ft (6 to 9 m) to water in the wells of the site (app. 1), only two springs were found that could serve as additional control points for a water-table map (fig. 10). Flow is assumed to be under water-table conditions, with water heads ranging from 4,130 to 4,006 ft (1,260 to 1,221 m). Reports about wells that run dry after several years of pumpage (the old and abandoned well next to the new 7-L well) or after one year with little rain (Cave Well) may indicate a poorly developed karstic system with a low degree of interconnectedness. Water having large ranges of tritium (11.35 to 28.04 TU) and ^{14}C (modern to 5,900 yr old) (fig. 8) support this assumption.

Ground-water Geochemistry

All ground-water samples that were collected in Block 46 and in the vicinity of the S-15 site are brackish, with total dissolved solids (TDS) ranging between 1,200 and 4,000 ppm (figs. 11 and 12, app. 2). Salinity increases toward the east of the S-15 site with the direction of flow (figs. 9, 11, and 13) and indicates a longer time of interaction with the host rocks. Ground water in the area is of the

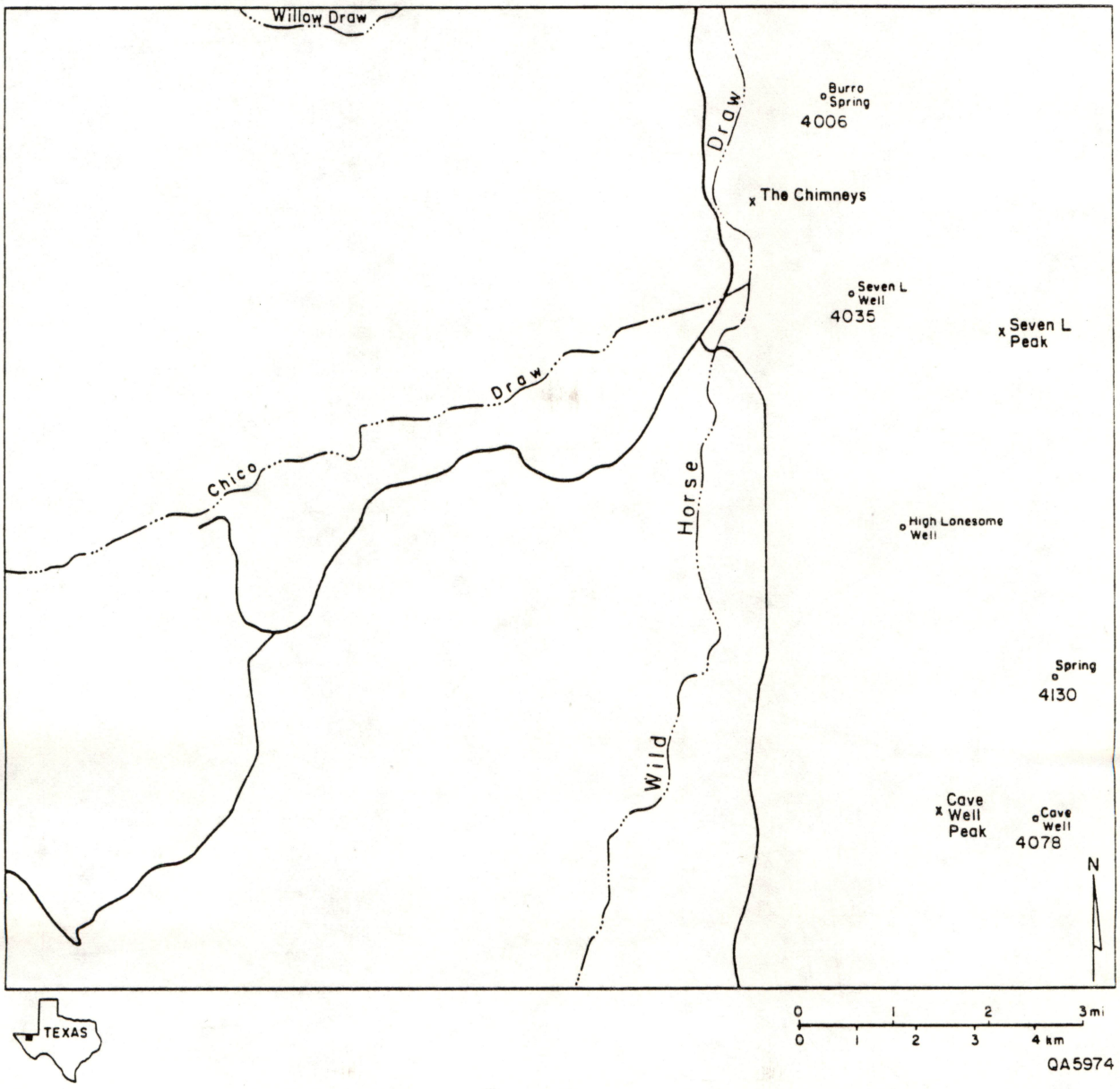

Figure 10. Ground water level distribution (ft) of Block 46 study area in Culberson County.

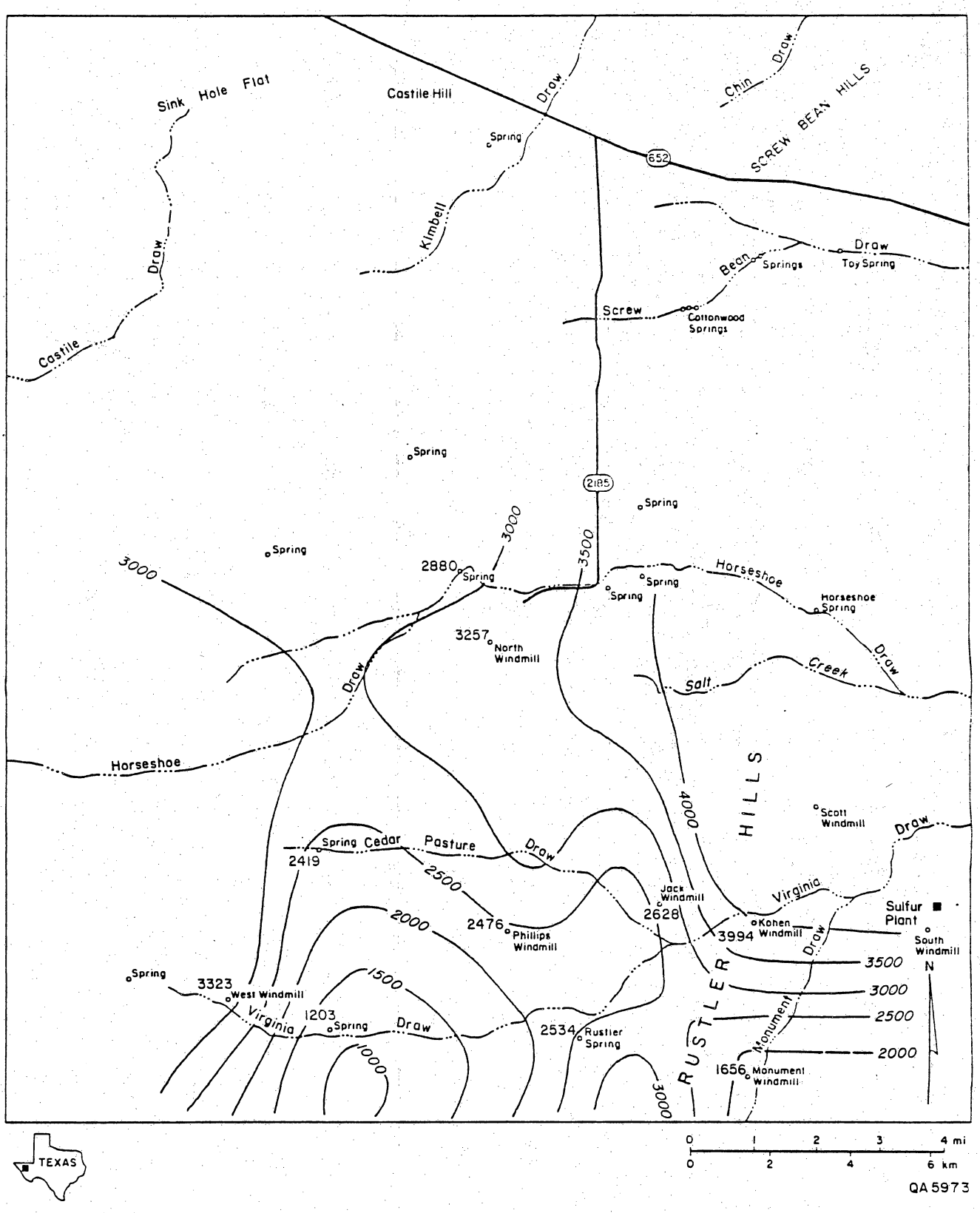

Figure 11. Contour map of total dissolved solids (TDS) (mg/l) distribution in ground water of S-15 study area, Culberson County.

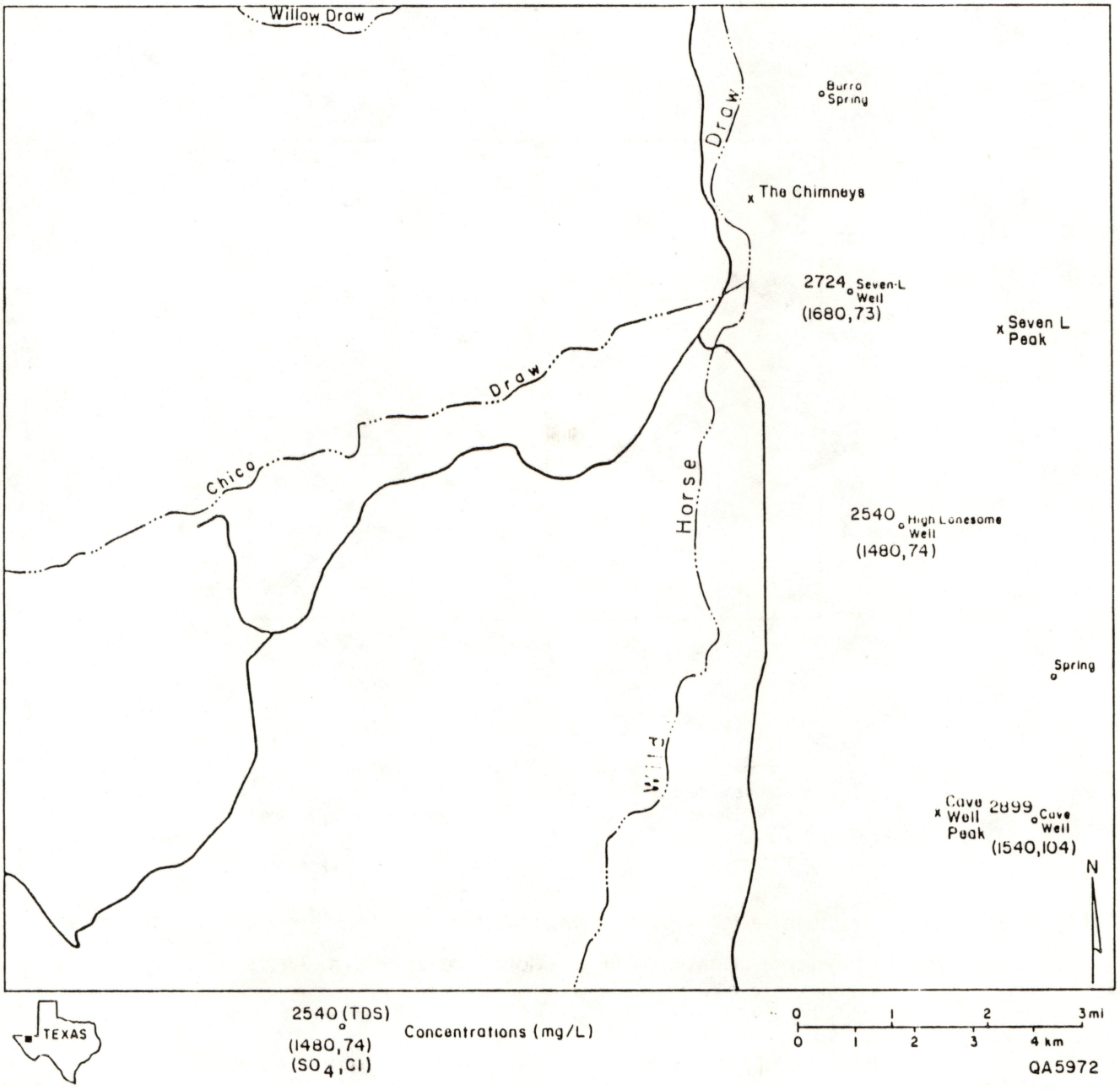

Figure 12. Total dissolved solids (TDS). SO_4^{2-}. and Cl^- (all in mg/l) distribution in ground water of Block 46 study area. Culberson County.

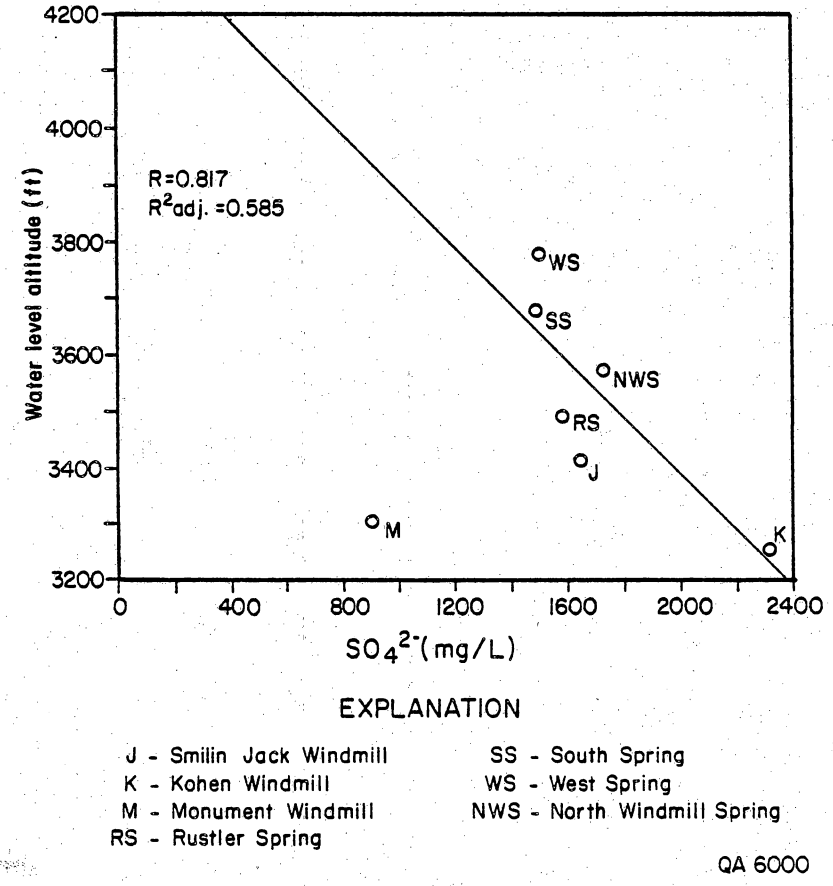

Figure 13. SO_4^{2-} concentration (mg/l) versus altitudes (ft) of ground-water samples in S-15 study area, Culberson County. Well locations are shown in figure 11.

Ca-SO_4 facies, as was expected based on the gypsiferous nature of the host formations. In addition, sulfate correlates well with Na^+, Mg^{2+}, and with TDS (figs. 14 and 15), suggesting other salts are dissolving.

$\delta^{34}S$ values (figs. 16 and 17) indicate that the dissolved SO_4^{2-} in ground water is from dissolution of the gypsum in the host rock. These $\delta^{34}S$ values of dissolved sulfate are typical of Permian sulfate minerals (12 °/oo) (Hoefs, 1973), as shown by a range of +9.3 to +11.3 °/oo. Samples from Monument Windmill and the South Spring near the S-15 site had $\delta^{34}S$ values of +5.8 and +17 °/oo, respectively, which differ from the normal range. In the case of Monument Windmill, the value can be attributed to the dissolution of the native sulfur (which has lighter $\delta^{34}S$ values than those of SO_4^{2-} in the gypsum because of isotopic fractionation [Hoefs, 1973]) that is mined in the immediate vicinity. The high values of $\delta^{34}S$ in South Spring may be attributed to local bacterial reduction of the Permian sulfate, which results in higher $\delta^{34}S$ values in the gypsum host rocks.

Some of the ground water at both sites has been recharged recently (indicated by tritium values ranging from 6.3 to 28 TU) and mixed with an older component of ground-water flow (indicated by ^{14}C ages of up to 5,900 yr). An alternate explanation is that the apparent old ^{14}C ages of some of the water samples result from calcite precipitation. This is suggested by the negative correlation between Ca^{2+} and SO_4^{2-} (fig. 15) in ground water at these sites. The solution of gypsum causes increased concentrations of Ca^{2+} and SO_4^{2-} and the subsequent precipitation of less soluble calcite that contains ^{14}C. The residual ground water becomes depleted in ^{14}C and therefore appears older than it really is. It is

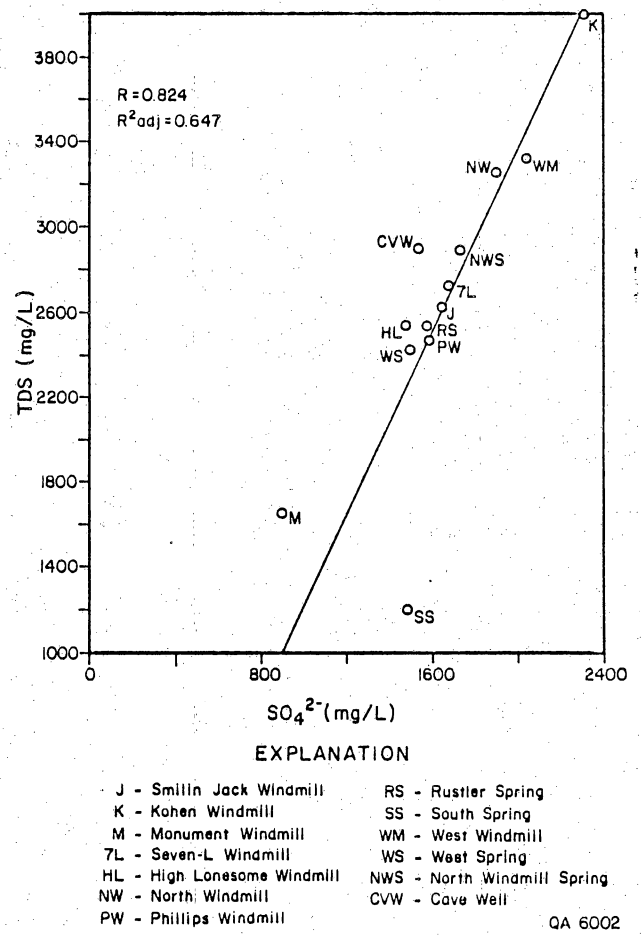

Figure 14. SO_4^{2-} concentration versus TDS concentration in ground water of Culberson County study areas. Well locations are shown in figures 11 and 12.

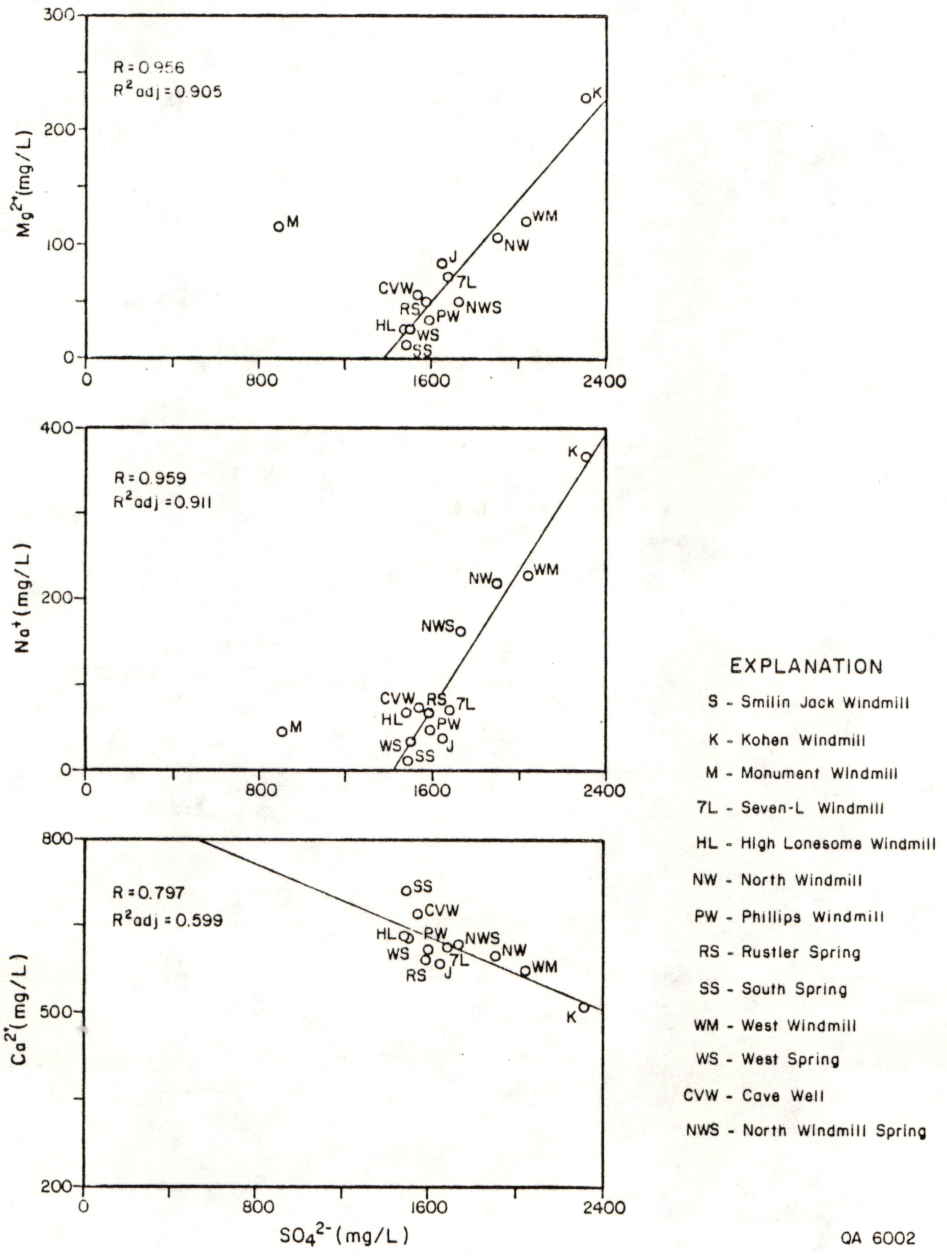

Figure 15. SO_4^{2-} concentration versus Ca^{2+}, Mg^{2+}, and Na^{+} concentrations (all in mg/l) in ground water of Culberson County study areas. Well locations are shown in figures 11 and 12.

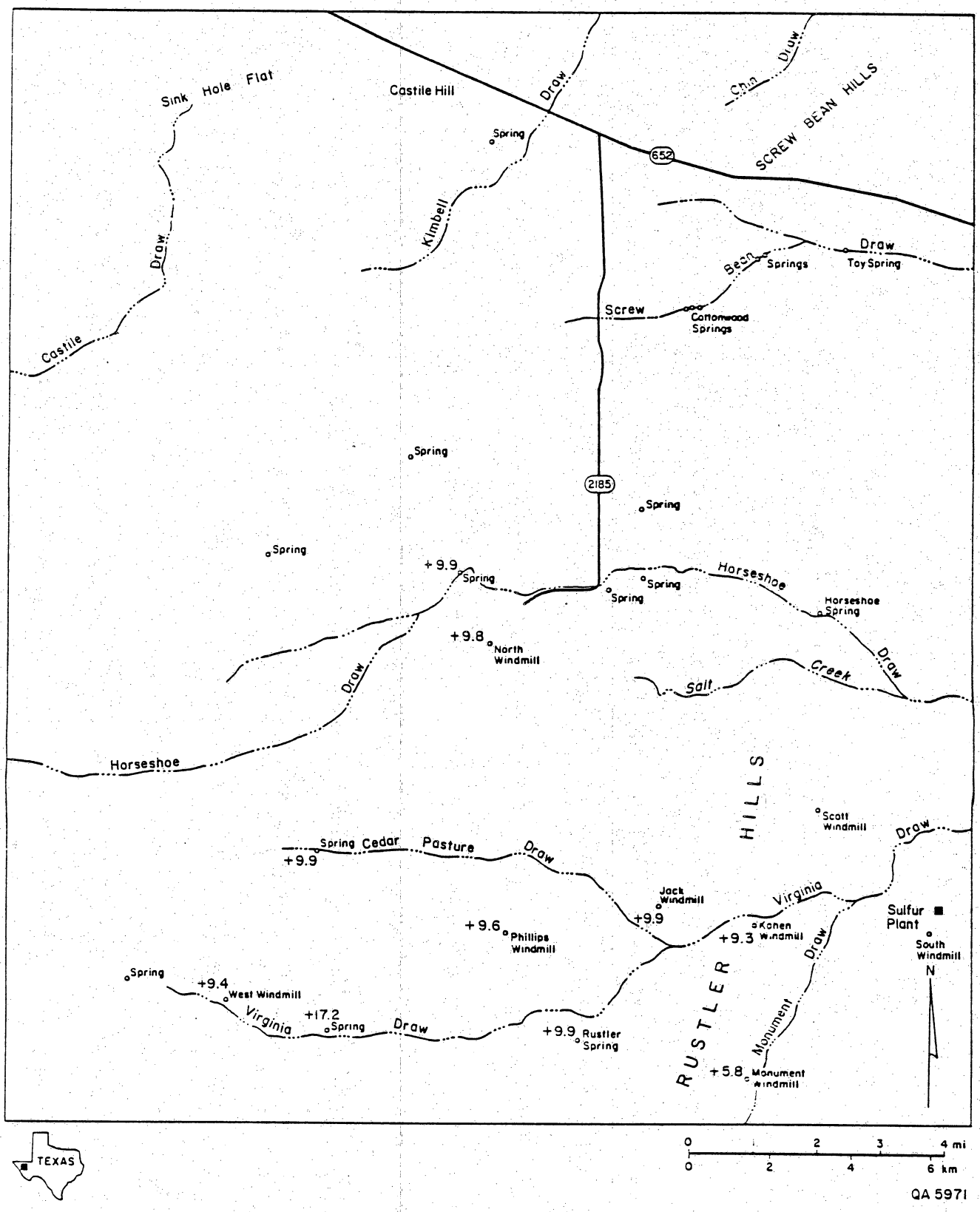

Figure 16. $\delta^{34}S$ distribution in ground-water samples of S-15 study area, Culberson County (in $^{o}/oo$ deviation from the Canyon Diablo Troilite).

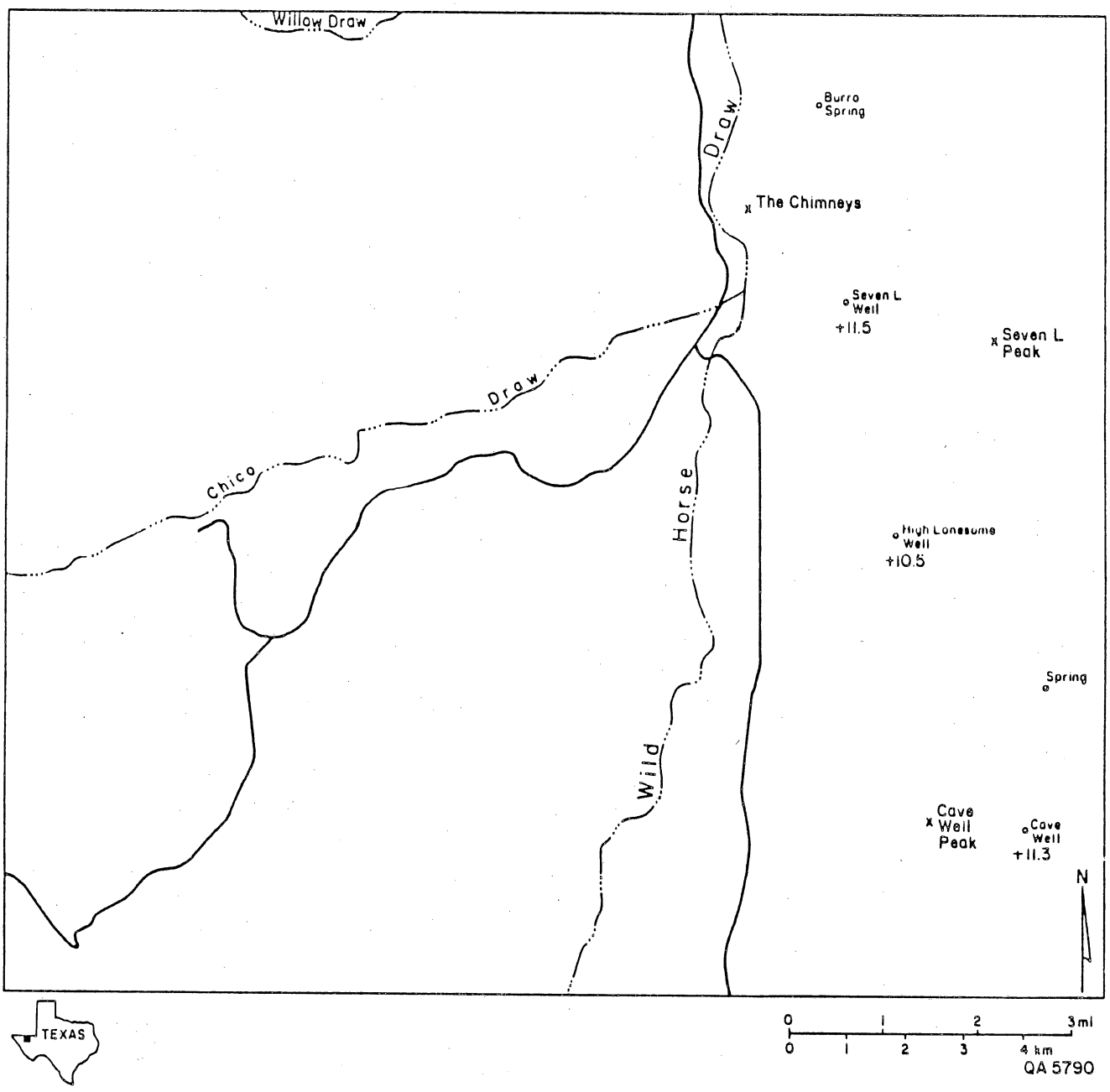

Figure 17. $\delta^{34}S$ distribution in ground-water samples of Block 46 study area, Culberson County (in $^{o}/oo$ deviation from the Canyon Diablo Troilite).

therefore possible that there is no older component of ground water and that all the ground water is young, as suggested by the tritium activities. Variations in tritium and ^{14}C activities over short distances (e.g., High Lonesome Well and Cave Well, Block 46 site) that are typical of karstic systems and that probably reflect hydraulic discontinuity and independent pathways of recharge are observed. However, some degree of connectedness in the S-15 site is indicated by the good correlation between decreasing tritium activities and lower water-level altitudes (fig. 18). Based on figure 18, water that flows into the site from the west at higher water-level elevations has higher tritium activities and perhaps a shorter residence time in the aquifer. $\delta^{18}O$ and $\delta^{2}H$ values indicate recharge from current precipitation (figs. 19, 20, and 21). Their narrow range (-7.4 to -6.1 °/oo for $\delta^{18}O$ and -56 to -40 °/oo for $\delta^{2}H$) does not support the concept of ground-water base flow coming from higher elevations in the west; perhaps it indicates a well-mixed ground water system.

The chemical and isotopic characteristics of the water at both Culberson sites reflect relatively fast moving flow systems (high tritium and ^{14}C activities) in karstic channels and other dissolution features, but with a high degree of interaction with the evaporitic host rocks (high values of TDS, SO_4^{2-}, and $\delta^{4}S$).

CULBERSON COUNTY--CONCLUSIONS

Geologic investigations in the Culberson County area produced the following preliminary conclusions that should be considered in the evaluation of Site S-15 and Block 46 as potential sites for a low-level radioactive waste repository. The region of Culberson County that is underlain by the Castile Formation includes all of S-15 and the eastern portion of Block 46. This part of the Gypsum Plain has been

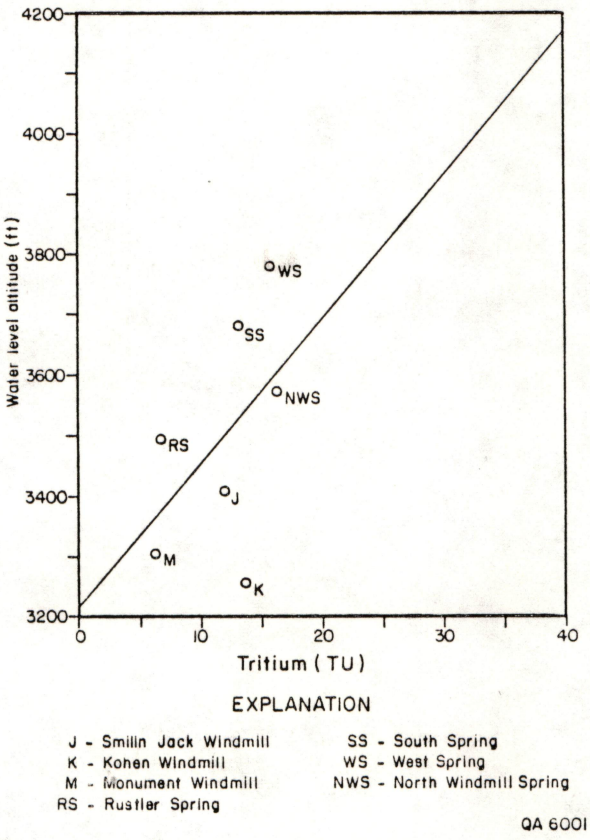

Figure 18. Tritium activity (TU) versus altitude (ft) of ground-water samples from S-15 study area, Culberson County. Well location is shown in figure 7.

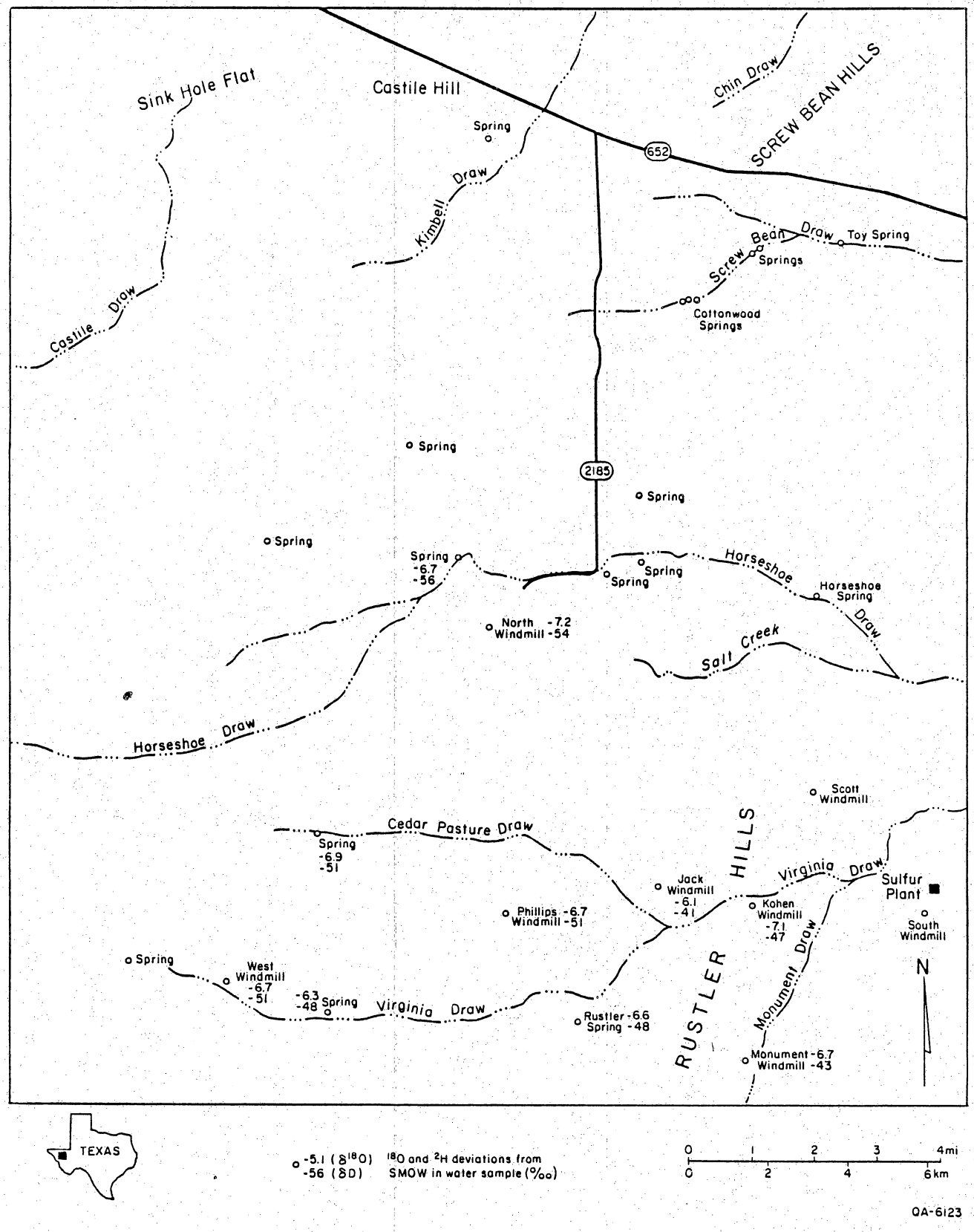

Figure 19. $\delta^{18}O$ and $\delta^{2}H$ distribution in ground water of S-15 study area, Culberson County (in $^{o}/oo$ deviation from SMOW).

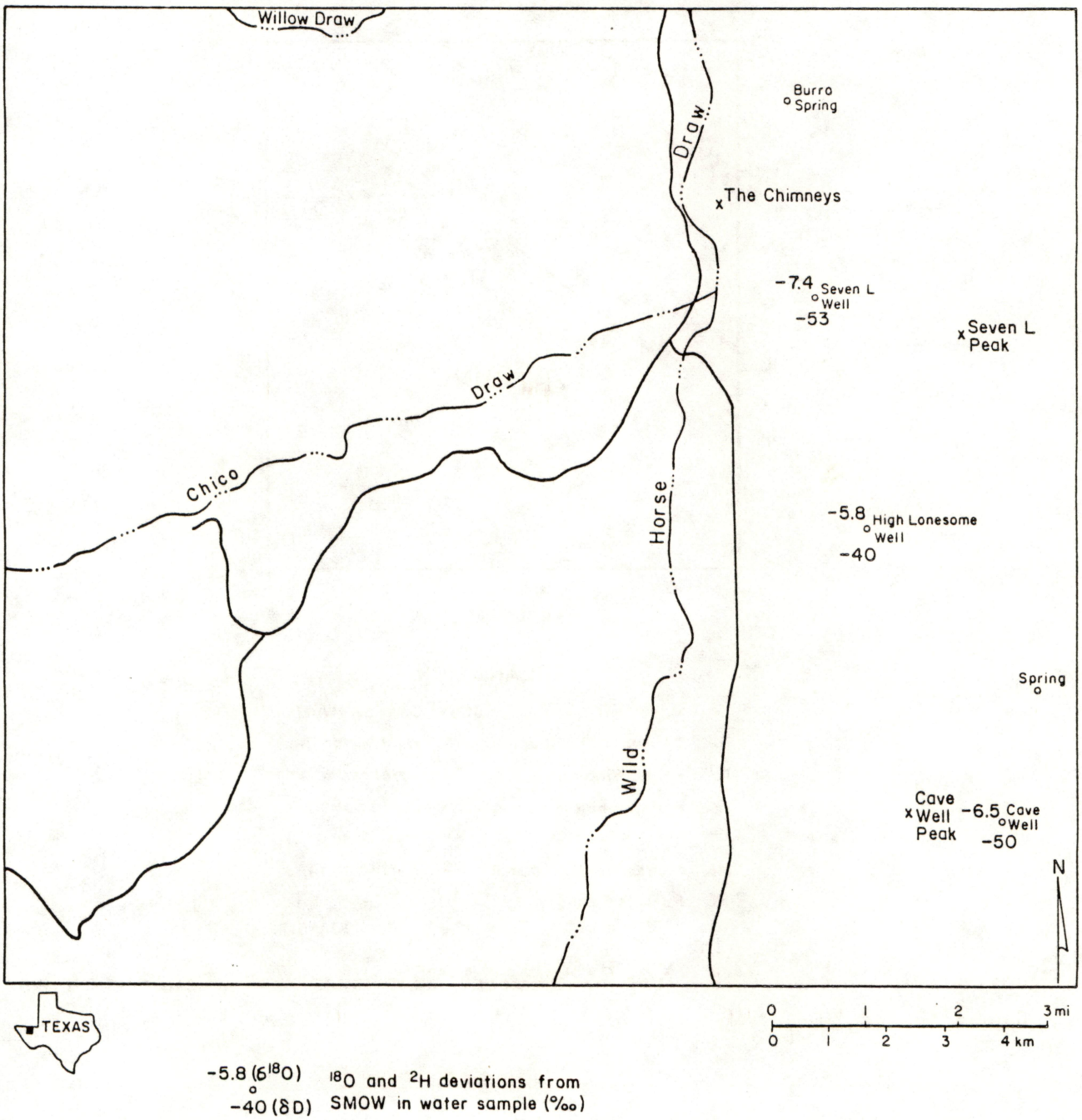

Figure 20. $\delta^{18}O$ and $\delta^{2}H$ distribution in ground water of Block 46 study area, Culberson County (in $^{o}/oo$ deviation from SMOW).

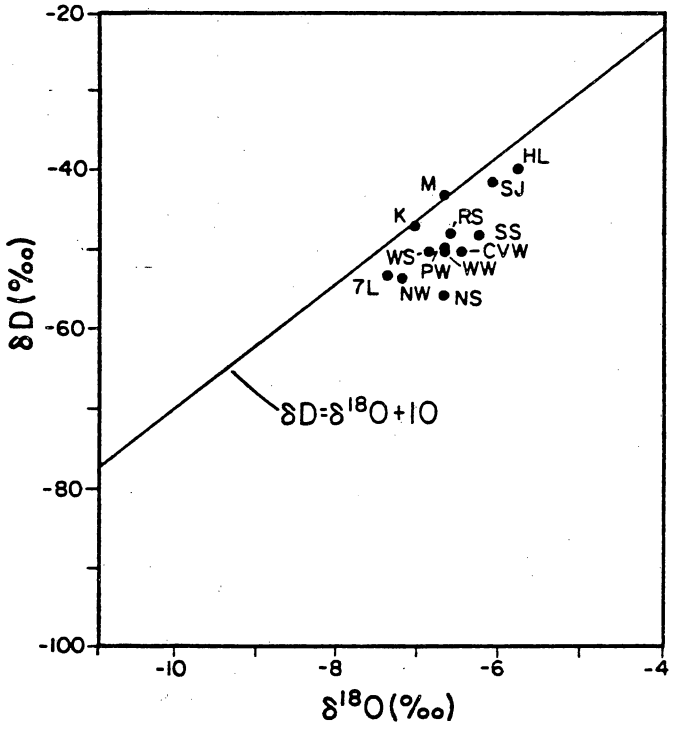

EXPLANATION

M	Monument Windmill	CVW	Cave-well Windmill
SJ	Smilin Jack Windmill	WW	West Windmill
KW	Kohen Windmill	7L	Seven-L Windmill
P	Phillips Windmill	SS	South Spring
NW	North Windmill	WW	West Spring
HL	High Lonesome Windmill	NS	North Spring
RS	Rustler Spring		

QA-6120

Figure 21. $\delta^{18}O$ versus $\delta^{2}H$ ($^{o}/oo$) in Culberson County sites. Well location is shown in figures 19 and 20.

repeatedly subjected to processes of dissolution and collapse. These processes have resulted in both modern features with sharply defined geomorphic expression and in paleofeatures having a more or less subtle expression. The density of these features suggests that most of the area is underlain by a very complex system of dissolution channels whose geometry and precise distribution cannot be described with any certainty.

Lack of exposure of the Castile Formation over much of the Gypsum Plain, except for deeply incised drainages and in castiles, makes structural interpretations difficult. However, many of the surface drainages are controlled by a system of joints, and local areas of faulting are present. The faults are commonly inferred by projection from exposures in the Delaware Mountains. In the Gypsum Plain, the faults are expressed as linear northeast-trending drainages and aligned zones of sinkholes and castiles, but the displacement on these faults, although believed to be small, cannot be demonstrated.

Surficial materials in the Gypsum Plain consist mostly of gypsite, a granular product formed by the breakdown of bedded gypsum, and other locally derived alluvium. These materials could be easily excavated, but they appear to be highly porous. The gypsite and other alluvial sediments mantle much of the surface and fill valleys and depressions. Some of these features appear to have been formed by dissolution and collapse of the underlying Castile Formation.

The western portion of Block 46 is underlain by the Bell Canyon Formation. Most of the Bell Canyon Formation is a weakly cemented sandstone that appears to be highly porous and permeable. It is well jointed and is locally faulted by small displacement normal faults. Northeast-striking faults are the most prominent, especially in the vicinity of the contact between the Bell Canyon and Castile

Formations. Locally drainages are joint controlled.

Surficial materials in Block 46 consist of recent and older alluvium derived from erosion of the Bell Canyon Formation. The alluvium could be easily excavated, but it appears to be very porous. The alluvium occurs in small alluvial fans and as valley-fill deposits.

Six hydrologic issues relevant to the evaluation of the two sites in Culberson County were presented at the beginning of this report. Based on our findings the following preliminary conclusions can be stated:

(1) Karstic aquifers underlie both study areas in Culberson County. The aquifer underlying the S-15 area seems to have a regional distribution and to have more connectedness than the aquifer underlying the Block 46 area.

(2) The water table is shallow in both areas, ranging from 0 to 150 ft (0 to 46 m).

(3) Ground-water flow at the S-15 study area is from west to east, following the topographic and geologic dip. At the Block 46 study area, flow direction in the aquifer could not be determined because of a scarcity of data.

(4) The residence time of the water in the aquifer varies from a few tens of years to possibly several thousands of years. The oldest water sampled (5,906 yr old) is a mixture of younger and older water. Calculated ^{14}C ages may be too old because of possible calcite precipitation in the site area. Therefore, the high tritium activities in ground water sampled in the sites may be a better indicator of short residence time of recently recharged ground water. Because of the karstic nature of the system, residence time of the ground water may be highly variable.

(5) Recharge to the aquifers of both areas seems to combine water coming from a remote distance (perhaps the Delaware Mountains) with water from local

precipitation that percolates through the relatively thin unsaturated zone.

(6) Natural discharge points are scattered all over the S-15 study area as springs that issue water from the shallow aquifer. In some locations, the water table is close enough to land surface to permit large areas of seepage and direct evaporation. Both sites have pumping wells within or adjacent to the area that provide water mainly for grazing cattle. Future mining activies closer to the S-15 site may result in man-induced dissolution features and unpredicted flow directions and discharge points.

HUDSPETH COUNTY INVESTIGATIONS

Location

The Texas Low-level Radioactive Waste Disposal Authority selected an area in Hudspeth County, Texas, for consideration as a site for the location of a low-level radioactive waste repository. The site is on State-owned lands lying between the Rio Grande to the south and the Diablo Plateau to the north (fig. 22). The Finlay Mountains lie about 4 mi (6.5 km) east of the primary study site.

The primary study area (fig. 22) is located in the Diablo Canyon West 7 1/2' Quadrangle. It is accessed by a well-maintained gravel road that leads from Fort Hancock, about 9 mi (15 km) to the southwest, to the Lee Moore Ranch. The site is an area of low relief, having surface drainage to the west and south into Alamo Arroyo. Alluvial sands with some pebbles and cobbles occur at the surface, locally overlain by windblown sands. Camp Rice Arroyo lies south of the primary study area. The primary study area lies close to the northern border of the lands owned by the State of Texas.

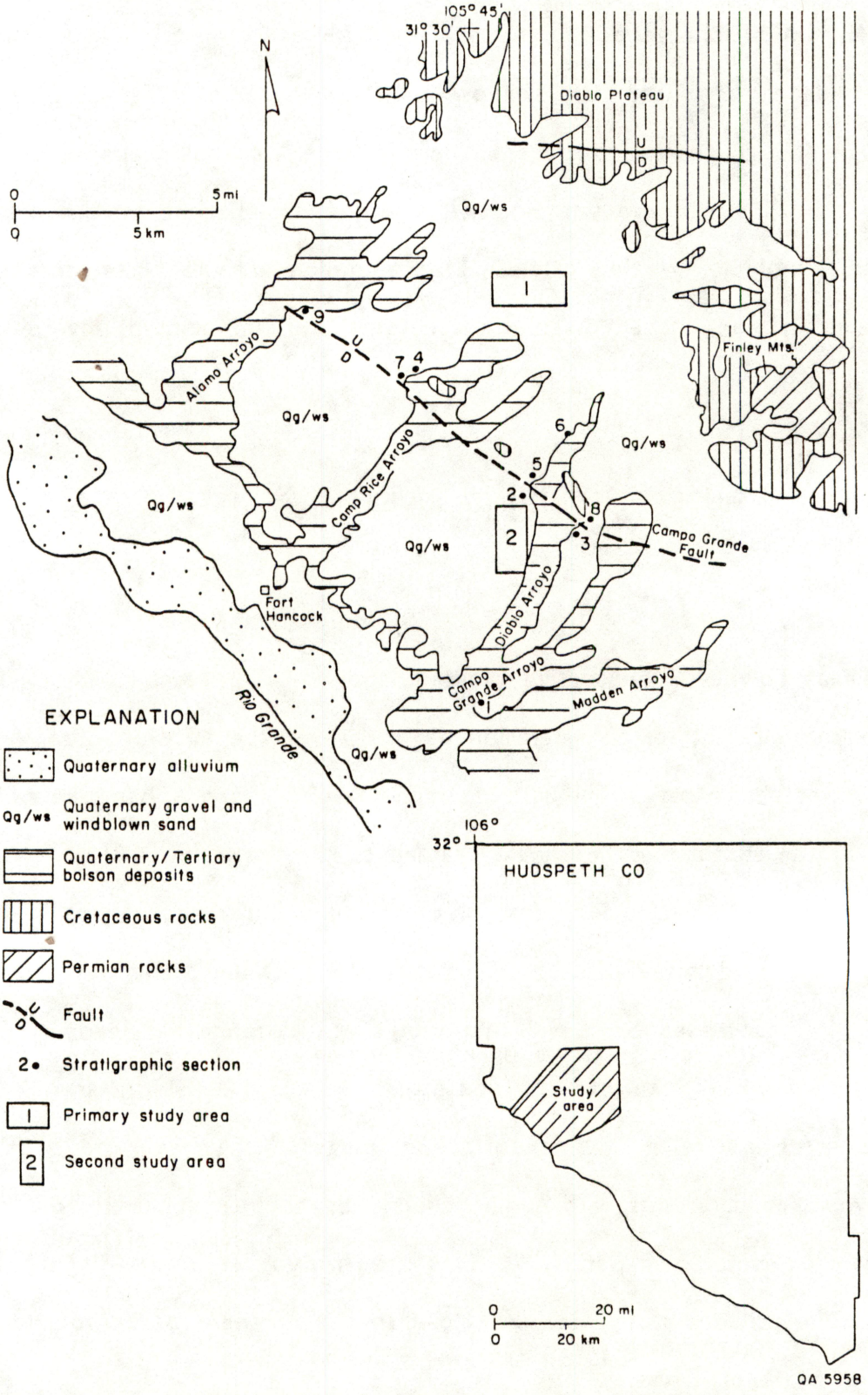

Figure 22. Map of geologic setting and location of (1) primary and (2) alternate study areas in Hudspeth County. Geology after Barnes (1983). Described stratigraphic sections are in appendix 8.

A second study area also was selected for preliminary drill testing by BEG. The second study site lies in an area of low relief on the west side of Diablo Arroyo about 2 mi (3 km) southwest of Campo Grande Mountain (fig. 22). The area is overlain by a surface veneer of windblown sand.

Methods

Aerial photographs at a scale of 1:12,000 (1 inch = 1,000 ft) were acquired for a large area in the vicinity of the proposed site. The area includes the drainages of most of the major arroyos from near their headwaters at the rim of the Diablo Plateau to their mouths on the Rio Grande. Approximately 30 man-days were spent examining the aerial photographs. Particular attention was placed on identification of fault traces and the location of well-exposed stratigraphic sections. Local areas were interpreted in detail, and the results were compared with published maps of the region. Aerial photographs were also used to extend the published mapping into previously unmapped areas to the west.

Approximately 40 man-days were spent doing geologic field work in the vicinity of the proposed site. Interpretations made from aerial photographs were verified, sections were measured, landforms were studied, and areas of faulting were investigated. Five shallow holes were drilled by BEG personnel to assist in the location of deeper holes subsequently drilled by Underground Resource Management, Inc. (URM). URM drilled four holes to define the local stratigraphy of the primary site in addition to five holes for hydrologic testing. Geophysical logs were run in five holes. BEG personnel were on site during all drilling operations and supervised sample collection.

Water-level data for the Rio Grande alluvium aquifer in Hudspeth County near the proposed site were obtained from the Texas Natural Resources Information

System (TNRIS) computerized data base and from open-file reports of the Texas Water Commission. Water levels in the Hueco Bolson and the Cretaceous aquifers in the vicinity of the site were reported by the well owners and may be considered as approximations only. All information about water levels is presented in appendix 1.

No data were available for porosities, hydraulic conductivities, or transmissivities of the unsaturated or saturated zones of this site. Two permeability tests were performed during this study in the unsaturated zone of the bolson fill at the site. The tests were performed in gravels and in the entire lithologic sequence beneath the gravels to a depth of 150 ft (48 m). Six additional permeability tests and 12 grain-size analyses on core samples from the unsaturated zone of this formation at this site were carried out by URM labs. A pumping test in the saturated zone of the Cretaceous aquifer was part of the completion program of the water well drilled at this site. Data from the core analyses and the pumping test are presented in appendices 6 and 7, respectively.

Chemical analyses of water from wells that penetrate the Rio Grande alluvium near the site in Hudspeth County were obtained from the Texas Water Commission files. No data were available for wells that penetrate the bolson sediments or the Cretaceous rocks in the vicinity of this site. Therefore, all bolson and Cretaceous wells adjacent to the site were sampled. All samples were analyzed for general chemistry, $\delta^{18}O$, $\delta^{2}H$, tritium, and $\delta^{34}S$. Well-water samples were also analyzed for ^{14}C and $\delta^{13}C$. Temperatures were measured at the sampling sites. All chemical and isotopic data are reported in appendix 2.

Chloride and water content analyses were done on cores that were collected from shallow boreholes by BEG personnel. These boreholes were augered into

gravels to a total depth of 40 to 50 ft (12 to 15 m) at the two Hudspeth sites.

The well numbering method used for some of the wells in Hudspeth County follows the system adopted by the Texas Water Commission (Alvarez and Buckner, 1980).

Geologic Setting

The Hudspeth County site lies at the eastern edge of the Hueco Bolson, a major Basin and Range graben. Rocks in the area range in age from Permian to Recent; the strata most important to this investigation are late Tertiary to Recent sediments that fill the Hueco Bolson. They were deposited on a surface of considerable relief developed largely on Cretaceous sedimentary rocks, including massive, indurated Lower Cretaceous sandstones and limestones, and Upper Cretaceous marly limestones and shales. These Cretaceous rocks were folded and faulted during early Tertiary Laramide deformation. During this deformation, the rocks were folded and thrust northeastward toward the relatively undeformed Diablo Plateau. The boundary between highly deformed rocks to the west and relatively undeformed rocks to the east approximately underlies the primary study area. Deformed rocks are exposed at Campo Grande Mountain about 5 mi (8 km) south of the site; relatively undeformed rocks occur along the Diablo Rim less than 3 mi (5 km) to the northeast. Plate 3 displays the geology of the Hudspeth County site.

Stratigraphy of Hueco Bolson Deposits

Tertiary deposits that fill the Hueco Bolson are being considered as potential host sediments for a low-level radioactive waste repository. These strata include the informally named older basin deposits described by Albritton and Smith (1965). The same strata, but named the Fort Hancock Formation, are described by Strain

(1966). Relatively coarse bolson deposits unconformably overlie the Fort Hancock Formation and have been called the Camp Rice Formation by Strain (1966). This unit is apparently equivalent to the younger basin deposits as well as to the Miser, Madden, Gills, Ramey, and Balluco Gravels of Albritton and Smith (1965). Very similar sequences of sediments also have been described for the Presidio Bolson, the next basin to the southeast along the Rio Grande (Groat, 1972).

For the purposes of this study the term "bolson deposits" means all bolson deposits; the term "older bolson deposits" is equivalent to both the older bolson deposits of Albritton and Smith (1965) and the Fort Hancock Formation of Strain (1966). The term "younger bolson deposits" is equivalent to younger bolson deposits of Albritton and Smith (1965), but it also includes some near-surface gravels that may be equivalent to the Miser, Madden, Gills, Ramey, or Balluco Gravels of Albritton and Smith (1965). In this usage, younger bolson deposits are probably equivalent to the Camp Rice Formation of Strain (1966).

The base of the bolson deposits is not exposed in the study area. Locally, small erosional outliers of Cretaceous sediments crop out within exposures of bolson deposits. The upper part of the bolson deposit sequence has been eroded to form a pediment surface such that progressively older bolson deposit sediments are exposed toward the Rio Grande. Bolson sediments are overlain by thin fluvial gravels, and both the modern surface and the erosional surface that are cut into bolson deposits slope toward the Rio Grande at about 30 to 50 ft/mi (6 to 9 m/km).

Age of Bolson Sediments

On the basis of a vertebrate fauna identified from Madden Arroyo, the arroyo southeast of the area investigated, Strain (1966) interpreted the age of the

Hudspeth local fauna, which is preserved in the Fort Hancock Formation, to be Blancan. In its present usage the Blancan Age is late Pliocene.

On the basis of volcanic ash beds identified as the Pearlette Ash and vertebrate remains, Strain (1966) considers the Camp Rice Formation to be middle Pleistocene. Izett and Wilcox (1982) have recently shown that volcanic sediments identified as the Pearlette Ash by Strain (1966) are actually part of the Huckleberry Ridge ash bed of the Pearlette family of ash beds, which has a fission-track zircon age of 2.02 million yr. Therefore, the lower part of the Camp Rice Formation and presumably the lower part of the younger bolson deposits are late Pliocene. The age of the upper part of the younger bolson deposits or of the upper part of the Camp Rice Formation is not known but is presumed to be Pliocene (Gile and others, 1981).

Stratigraphy

Eleven stratigraphic sections through bolson deposits and younger fluvial sediments in Hudspeth County are described from outcrops along Alamo, Camp Rice, and Diablo Arroyos and unnamed tributaries to these arroyos (app. 8). Collectively, these sections include ~720 ft (~220 m) of strata, but no single section includes more than ~ 100 ft (~30 m) of strata. In many places parts of the valley walls leading into the arroyos are covered with colluvium or terrace deposits, and correlation from upstream sections to downstream sections is not possible. For these reasons the described sections represent only increments of the entire stratigraphic thickness of the bolson deposits. The sections that are described were chosen to characterize bolson deposits in specific geographic areas rather than to define or to fully describe the formation.

A single section is described to characterize coarse-grained facies of the younger bolson deposits exposed in the downstream part of Diablo Arroyo southeast

of Fort Hancock. Most of the remaining sections described are to either side of the Campo Grande fault, which strikes northwest-southeast across the study area. In these sections, relatively coarse, younger bolson deposits composed of fluvial sand and gravel are exposed in downthrown blocks southwest of the fault, and fine silty clay and clayey silt of the older bolson deposits are exposed in the upthrown block northeast of the fault. Additional observations indicate that surface exposures of bolson deposits become progressively coarser northeast of the fault. Albritton and Smith (1965) and Groat (1972) recognized similar lithologic variations in areas to the south of this study area.

Stratigraphic Sections

Stratigraphic sections that form the basis for the following descriptions of facies of the bolson deposits are in appendix 8. Generalized descriptions of surface outcrops are given for four representative areas: (1) an outcrop near the Rio Grande River, (2) outcrops in the downthrown block and within a few hundred meters of the fault, (3) outcrops in the upthrown block within a few hundred meters of the fault, and (4) an outcrop to the far northeast of the fault.

Section Near the Rio Grande River.--Nearly 23 ft (8 m) of younger bolson deposits are exposed on the southeast valley wall of Diablo Arroyo, approximately 0.5 mi (0.8 km) northeast of the Diablo Reservoir No. 2 (app. 8). These sediments consist of approximately 20 ft (6.3 m) of fluvial sands and gravels interbedded with bioturbated clayey silt. This section is apparently equivalent to part of the Camp Rice Formation of Strain (1966).

Composite Section, Downthrown Side of Campo Grande Fault.--Coarse-grained sediments of the younger bolson deposits crop out in stream cuts southwest of the Campo Grande fault (fig. 22). Sections described in these sediments occur in Diablo Arroyo and Alamo Arroyo, and both occur within 100 ft (30 m) of the Campo Grande fault (app. 8). Older bolson deposits consisting of pale-red-brown silty clay and pale-brown laminated clayey silt occur at the base of the section. Preserved primary sedimentary structures are very rare in the silty clay unit. Where primary structures were seen, they consist of very fine graded laminae of silty clay and clay. The silty clay lithology makes up approximately 78 percent of the section. Desiccation cracks, slickensides on fracture surfaces, and a surface popcornlike texture indicate that the red-brown clays contain a high proportion of expansive clay minerals, most likely montmorillonite.

Younger bolson deposits composed of sand and gravel overlie an erosion surface cut into the older bolson deposits. Typically these sands and gravels are a series of upward-fining sequences and are up to 90 ft (27.5 m) thick. Sequences commonly overlie an erosion surface and consist of basal, horizontally bedded, clast-supported limestone pebble to cobble gravel overlain by horizontally to crossbedded coarse to medium sand. Pedogenic calcrete nodules occur throughout the sandy sections, and $CaCO_3$ films cover the lower part of gravel clasts. As many as three pedogenic calcretes may be preserved in the lower part of this unit. These calcretes are composed of nodules of $CaCO_3$ and are Stage III calcretes in the classification of Bachman and Machette (1977). The younger bolson deposits are capped by a massive pedogenic calcrete that is locally up to 6 ft (2 m) thick. At least one cycle of brecciation has resulted in a polygonal fracture system in which carbonate laminae are deposited. The upper part of the calcic horizon is well

indurated and weathers to a platy structure. This calcrete is probably a Stage IV to V calcrete in the Bachman and Machette (1977) classification.

Composite Section, Upthrown Side of Campo Grande Fault.--Sections on the upthrown side of the Campo Grande fault were described from Alamo, Camp Rice, and Diablo Arroyos. Fine-grained older bolson deposits are exposed in the upthrown block northeast of the Campo Grande fault in each of these areas. Because there are no distinctive lithologic units nor any datable material in these sections, it is not possible to correlate them with sections of older bolson deposits exposed south of the Campo Grande fault.

Older bolson deposits in sections within the upthrown block and within a few hundred meters of the Campo Grande fault are up to 90 ft (27.5 m) thick and consist of interbedded pale-red-brown silty clay and pale-brown clayey silt. The silty clay is devoid of preserved sedimentary structures and the clayey silt is commonly laminated. In these sections silty clay makes up from 48 to 78 % of the older bolson deposits. In the section northwest of Diablo Reservoir, a 6-ft (2-m) thick sequence of deltaic topset, foreset, and bottomset beds is preserved. These strata are primarily clayey silt and very fine sand.

As much as 43 ft (13 m) of younger bolson deposits overlie an erosion surface developed on the older bolson deposits. The younger bolson deposits in these sections consist of thin units of silty clay and clayey silt and thick units of flat-bedded to trough and planar crossbedded and ripple cross-laminated sand. Mud drapes with desiccation cracks are preserved within the sequence. Pedogenic calcrete nodules are dispersed throughout the younger bolson deposits. Thin ground-water calcretes cement some very thin sandstones. Layers of ground-water calcrete nodules are locally preserved above mud drapes.

Locally, the younger bolson deposits are overlain by Recent eolian sand or by a thin layer of gravel that underlies the regional pediment surface. The gravel contains a pedogenic calcrete that appears to have been partly stripped away in the areas where these sections were described. The calcrete is massive to platy in outcrop and up to 5 ft (1.5 m) thick. At least one cycle of fracturing has occurred, and fractures, which are up to 0.4 inches (1 cm) wide, are filled with laminated $CaCO_3$. These are Stage IV calcretes in the classification of Bachman and Machette (1977) and may actually be Stage V calcretes.

Section Near Bolson Margin.--A section of sediment was examined at Alamo Tank in the headwaters of Alamo Arroyo. This outcrop occurs only about 0.6 mi (1 km) downslope from the projected margin of the Hueco Bolson (the contact between bolson deposit sediments and Cretaceous rocks) and thus may expose coarse proximal bolson deposit facies. This section consists of approximately 15 ft (5 m) of sand and gravel. The sediments are flat bedded and contain pedogenic calcrete nodules. Three pedogenic calcrete horizons are preserved. The Alamo Tank section appears to be representative of proximal coarse-grained younger bolson deposits but, unfortunately, the correlation of this section to bolson deposits farther south is not clear because no datable material has been found and outcrops are not continuous.

Discussion

Bolson deposits consist of a lower sequence of silty clays and clayey silts that are apparently equivalent to the older bolson deposits of Albritton and Smith (1965) and to the Fort Hancock Formation of Strain (1966). Unconformably above these fine-grained sediments lies a sequence of mostly sands and gravels that are equivalent to the younger bolson deposits of Albritton and Smith (1965) and the Camp Rice Formation of Strain (1966). These strata become progressively coarser to the northeast toward the margin of the Hueco Bolson. The silty clay content

decreases from nearly 80 percent to the southwest to only 32 percent near the Campo Grande fault. Thick sands and gravels overlie older bolson deposits in the hanging wall south of the fault. Fine-grained older bolson deposits are exposed in the foot wall north of the Campo Grande fault and contain from 48 to 78% silty clay. The percentage of silty clay in this sequence decreases to the northeast toward the basin margin. As much as 43 ft (13 m) of younger bolson deposits, sands, and gravels occur above the silt and clay beds of the older bolson deposits north of the Campo Grande fault. Younger bolson deposits and surface gravels also appear to coarsen toward the margin of the basin.

Within the study area, fine-grained and presumably low-permeability rocks crop out in arroyos near the Rio Grande valley and short distances northeast of the Campo Grande fault. At equivalent stratigraphic horizons these fine-grained sediments become progressively coarser toward the northeast.

Relatively thin sections of younger bolson deposits, consisting of sand and gravel, overlie silt and clay units of the older bolson deposits in the southern part of the study area. North of the Campo Grande fault as much as 43 ft (13 m) of sand and gravel overlie fine-grained sediments of the older bolson deposits.

Structure

Quaternary Faults

A fault system cutting the Quaternary and late Tertiary alluvial and basin-fill deposits in the vicinity of the study area was mapped by Albritton and Smith (1965). The main fault is well exposed in several branches of Diablo Arroyo near Campo Grande Mountain and is informally referred to as the Campo Grande fault.

The fault is also exposed in Alamo Arroyo. The trace of the Campo Grande fault is shown in figure 22 and plate 3. It lies about 4 mi (6 km) southwest of the primary study area and about 2 mi (3 km) northeast of the alternate study area (fig. 22). No evidence of faulting was observed in other outcrops closer to the main areas of detailed investigation.

The Campo Grande fault can be traced as a nearly continuous scarp of slightly higher slope than the pediment surface and is cut only by incised arroyos from the eastern edge of the Campo Grande Mountain Quadrangle northwest onto the southern edge of the Cavett Lake Quadrangle, a distance of about 7.5 mi (12 km). A topographic scarp, locally covered by windblown sand, probably marks the continuation of the fault another 9 mi (15 km) to the northwest, giving an inferred total length of about 17 mi (27 km). The apparent Quaternary displacement becomes imperceptible to the southeast and increases to a maximum of about 15 ft (5 m) just west of Campo Grande Mountain. The amount of displacement may be greater to the northwest because the size of the sand-veneered scarp increases; however, the displacement cannot be determined precisely.

The Quaternary scarp probably marks a major fault, having much greater displacement in the subsurface, that makes up part of the eastern boundary of the Hueco Bolson. Well and geophysical data collected by the U.S. Geological Survey for ground-water exploration (Gates and Stanley, 1976; Alvarez and Buckner, 1980) indicate that basin fill thickens significantly toward the southwest near the Quaternary scarp. The geophysical data are not sufficiently detailed to locate the area of thickening more precisely. Nevertheless, the Quaternary scarp probably marks the location of most recent movement on a fault or fault zone that forms the eastern boundary of the Hueco Bolson. Net displacement on this fault may be as much as 3,300 ft (1 km).

Where seen in outcrop, the main strand of the Campo Grande fault strikes about N 50 to 55 W and dips approximately 65° to 85° southwest. It commonly consists of several fault strands, each of which has up to 10 ft (3 m) of normal displacement. Stratigraphic studies of the older bolson fill suggest that as much as 100 ft (30 m) of displacement may be the aggregate displacement across the zone in some localities. The total width of the zone of demonstrable faulting seldom exceeds 165 ft (50 m). The one exception to this occurs in outcrops exposed in a major tributary to Diablo Arroyo south-southeast of Campo Grande Mountain. At this locality there is a second zone of faulting about 3,300 ft (1 km) south of the main fault trace. The faults are presumed to be related to the same period of activity that formed the main Campo Grande fault, but fault strikes are both northwesterly and almost due north-south. The north-south faults are also normal faults, but some occur as an antithetic set dipping to the east in the hanging wall of a "typical" northwest-striking fault. Farther down the arroyo there is a large outcrop of highly disturbed sandstone that may result from soft-sediment deformation formed by liquefaction during earthquake activity.

The timing of the latest episode of movement along the Campo Grande fault has not been established with confidence. The fault cuts the Camp Rice Formation, which contains the 2.02 million-yr-old Huckleberry Ridge ash bed (Izett and Wilcox, 1982) and displaces the pediment surface developed on Camp Rice Formation sediments. Deposition of the Camp Rice Formation probably ceased between 300,000 and 400,000 yr ago (Gile and others, 1981), indicating that the most recent displacement on the fault is younger than about 300,000 to 400,000 yr. The relationship of the fault to the caliche horizons is unclear. Nowhere is there definitive evidence of the fault cutting the caliche. If it can be demonstrated that

the caliche caps the fault trace and is not offset by the fault, it may be possible to determine a minimum upper limit to the age of last fault movement.

East-West Fault along the Diablo Rim

An east-striking fault and monocline system displace Cretaceous rocks at the edge of the Diablo Plateau approximately 4 mi (7 m) north of the site (fig. 22). The maximum displacement on a single fault strand is about 20 to 30 ft (6 to 9 m) down to the south; the displacement generally increases from east to west. At the far east end the fault dies out into a monocline, which continues to decrease in displacement still farther east until there is no displacement. Along much of the fault trend at least part of the displacement is taken up by monoclinal warping.

An east-striking topographic escarpment about 2.5 mi (4 km) east of the primary study area may mark another east-striking fault. A ridge of Cretaceous rock, dominantly Cox Sandstone, is abruptly terminated on the south by a scarp with as much as 330 ft (100 m) of relief. Cretaceous rocks are covered by Quaternary deposits in the valley to the south and do not reappear for about 0.6 mi (1 km). East along the trend of the scarp, in an area we did not visit, the Cox Sandstone overlies the Campagrande Formation. Albritton and Smith (1965) show the contact as being depositional. The abruptness of the scarp suggests joint or fault control, but no offset can be demonstrated.

A similar but north-northwest-trending geomorphic escarpment connects the two east-trending zones. The northern end, north of the east-striking fault, consists of a zone of closely spaced joints having no discernible displacement. It forms the large indentation into the Diablo Rim where the county road crosses. This trend continues to the south where it forms a narrow valley, covered with alluvium,

between ridges of Cretaceous rock. Displacement across the valley is at most minor, but dips on the western side are greater than on the eastern side, suggesting at least some flexure. Also, north-northwest-striking joints are abundant in rocks on both sides of the valley. The trend must be either a major joint zone or a minor fault.

Seismic Survey

The final results of the seismic survey are not currently available, but BEG geologists have reviewed the preliminary results of the line along the main access road to the study area from Fort Hancock. The Campo Grande fault is clearly visible, as are nearly flat-lying bolson sediments above gently dipping Cretaceous rocks in the vicinity of the primary study area. The amount of displacement on the Campo Grande fault is not apparent on the currently available seismic section, but the Cretaceous rocks may be deeply buried by younger sediments in the hanging wall block.

An interesting feature seen in seismic data is a buried "basement" high of presumed Cretaceous rocks in the footwall block of the Campo Grande fault. The basement high appears to be a continuation of the deformed mass of Cretaceous rocks that occur on Campo Grande Mountain and in small isolated outcrops to the northwest. The northeast margin of the block has no evidence of a bounding fault in the available data, but regional relationships suggest that this area may contain a southwest-dipping reverse fault that separates strongly deformed Cretaceous rocks to the southwest from gently dipping but little deformed Cretaceous rocks to the northeast. The northeast margin of the structural block appears on the seismic section to locally constitute the southwestern boundary of the lower portion of the bolson sediments that underlie the proposed site. The deeper strata of the bolson sediments in the primary study area may have been deposited in a basinal area

that was locally topographically distinct from the nearly coeval sediments deposited closer to the present Rio Grande across the topographic divide formed by the structural block. The structural block may hydrologically isolate the deep bolson sediments along the Rio Grande from those in the footwall block of the Campo Grande fault. Additional definitiion of the topographic shape and continuity of the structural block is needed because the single seismic line does not provide sufficient data to define the extent to which the structural block serves to isolate the older updip bolson sediments from the downdip bolson sediments.

Drilling Program

The drilling program at the Hudspeth County site was designed to provide data on the detailed stratigraphy of the site, to drill wells for hydrologic tests, and to provide control for the seismic study. An initial program was carried out by BEG personnel using BEG drilling equipment, and subsequent deeper holes were drilled by Underground Resource Management, Inc. (URM) of Austin, Texas.

BEG Drilling

Lack of exposure of the silty and clayey older bolson fill deposits (Albritton and Smith, 1965) at the primary study area prompted an initial investigation to verify the depth of gravel overburden overlying the silty and clayey sediments. A second study area also was tested. The locations of the three holes drilled at the primary study area are shown in figures 23a and 23b; two holes drilled at the second area are displayed in figures 24a and 24b.

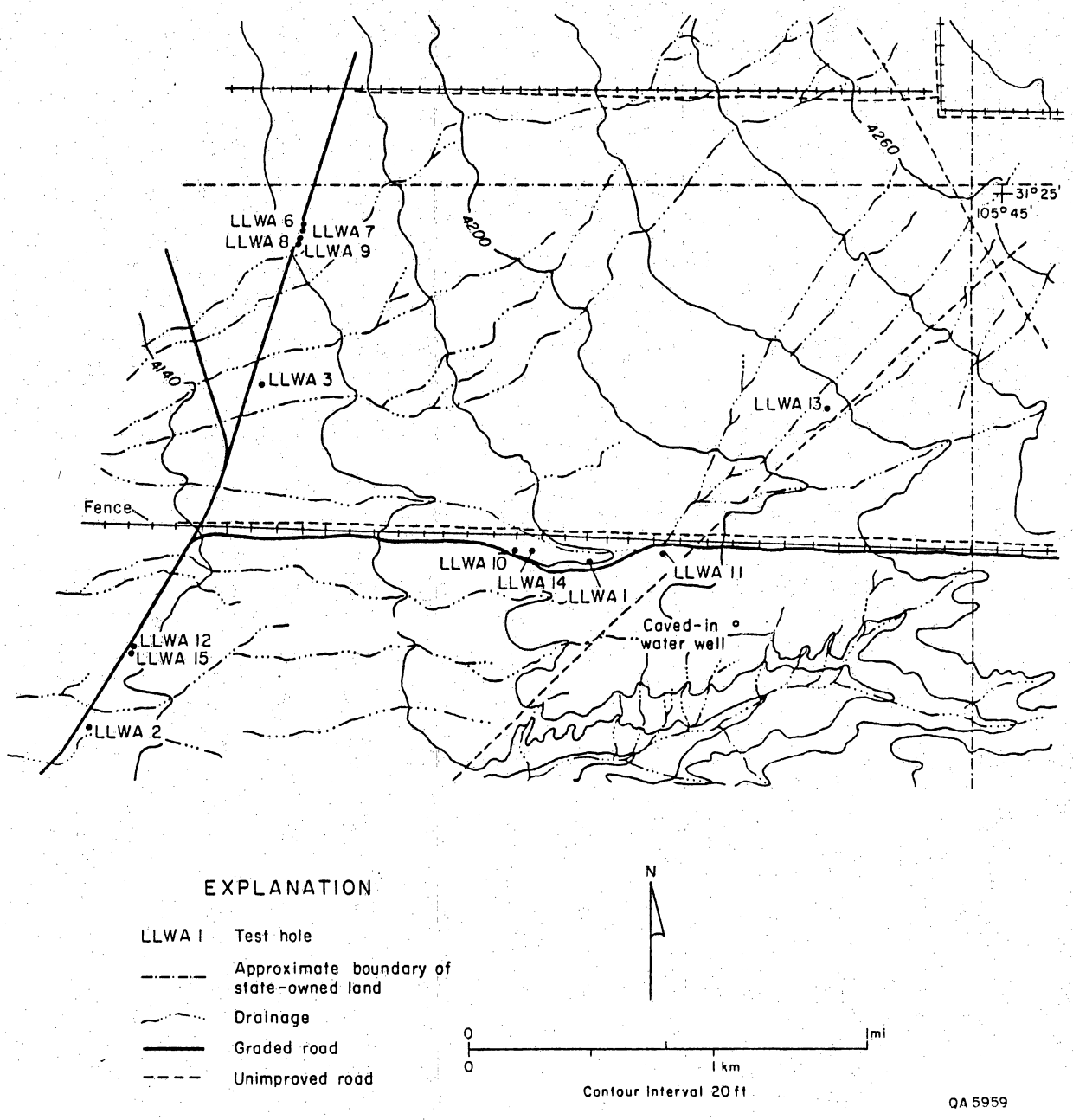

Figure 23. a) Map of topography, drainage, and test holes in primary study area in Hudspeth County. Location of area is shown in figure 22. Topography from U.S. Geological Survey Diablo Canyon West Quadrangle.

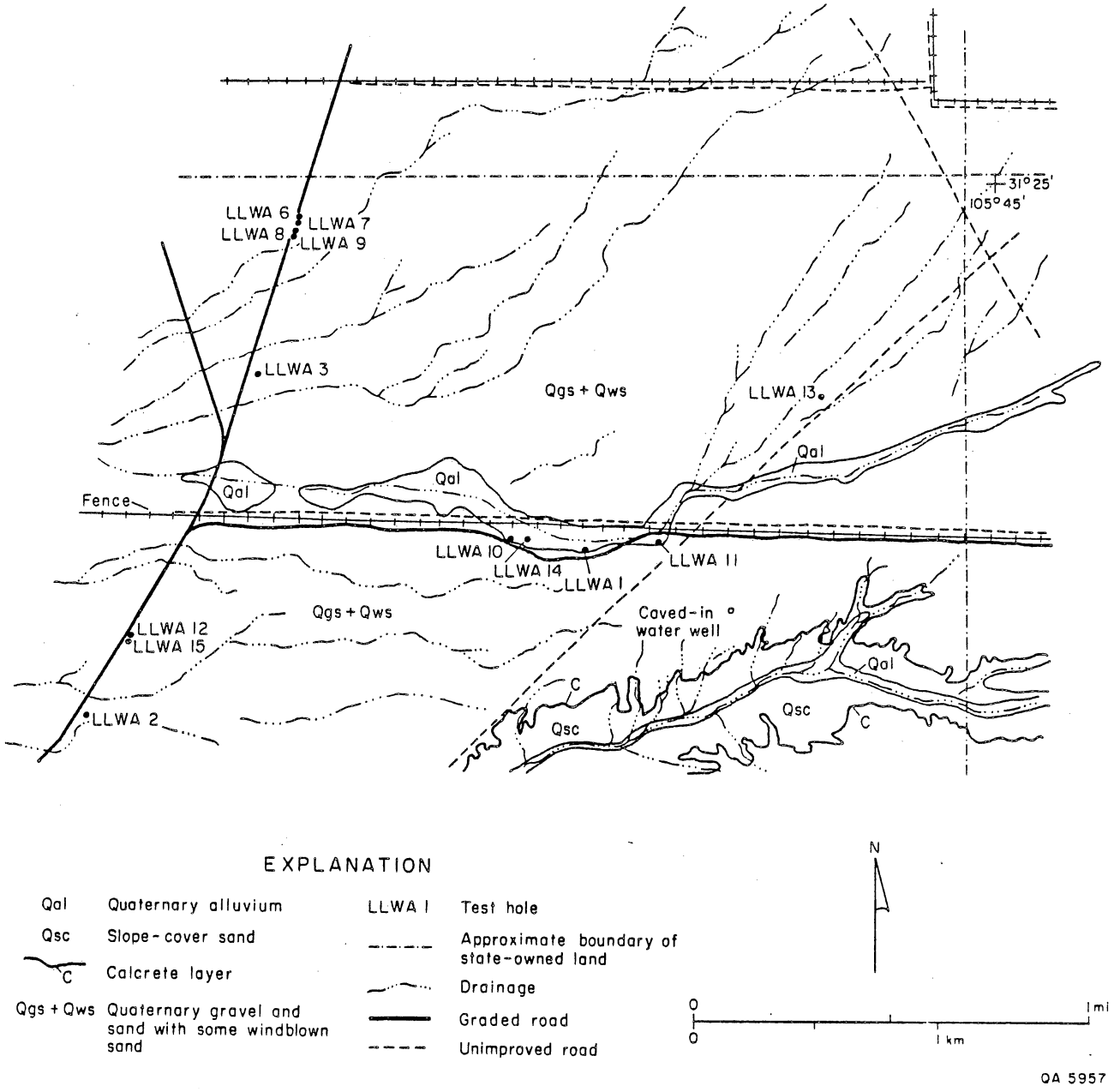

Figure 23. b) Geologic map of primary study area in Hudspeth County. Lithologic description of core and cuttings from test holes are in appendix 9.

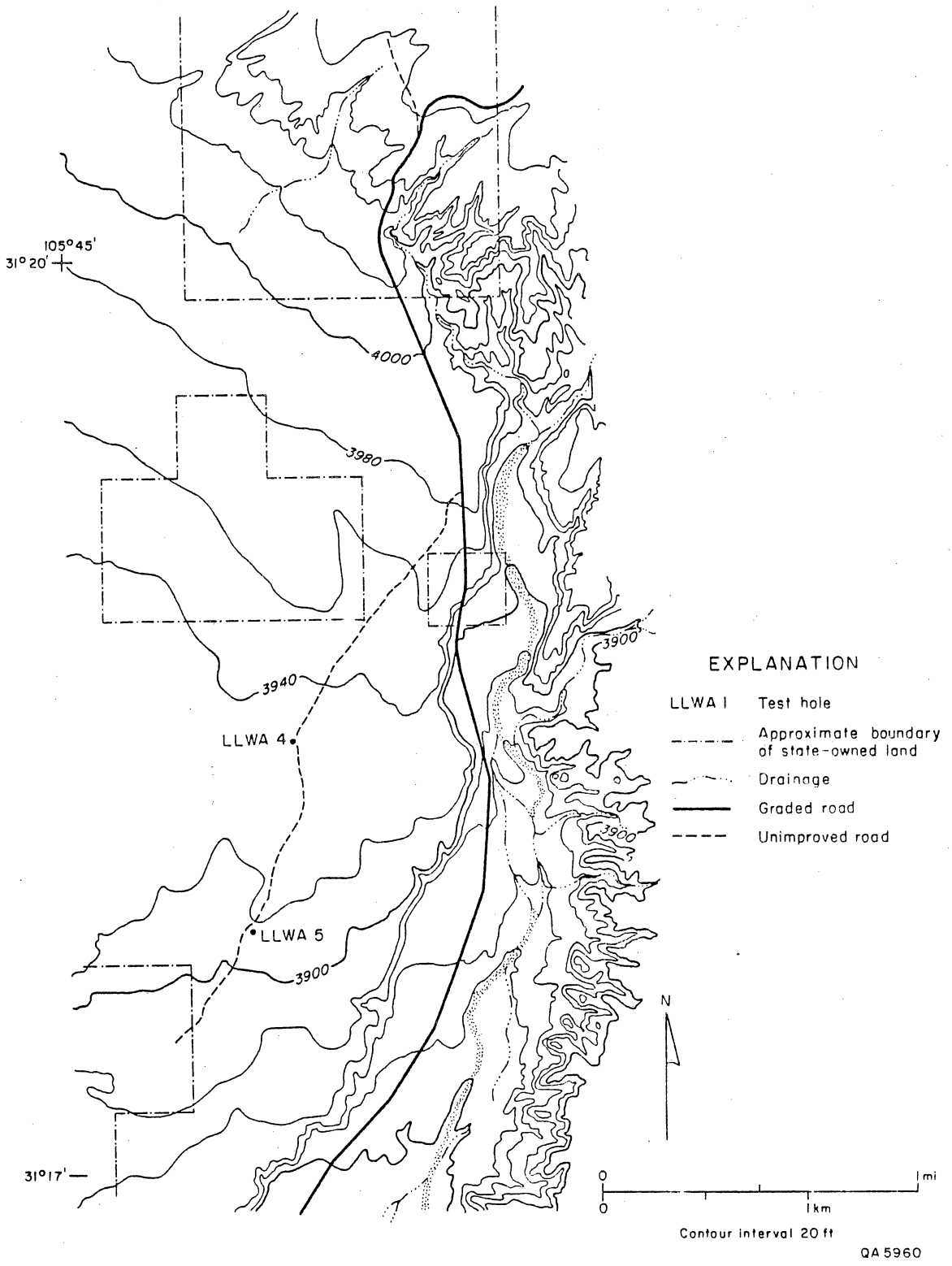

Figure 24. a) Map of topography and test holes at second study area in Hudspeth County. Location of area is shown in figure 22. Topography from U.S. Geological Survey Campo Grande Mountain Quadrangle.

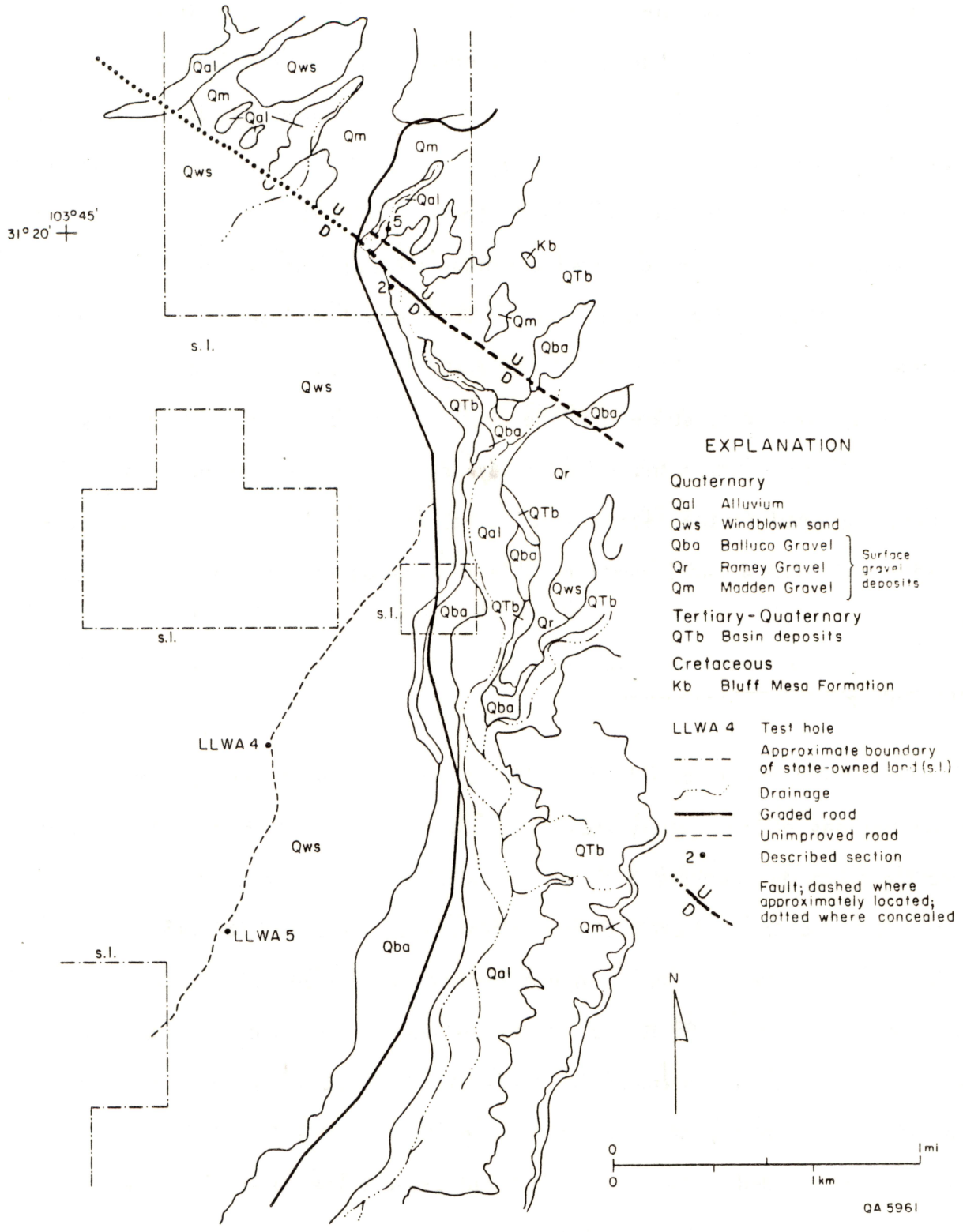

Figure 24. b) Geologic map of second study area in Hudspeth County. Lithologic description of cuttings from test holes are in appendix 9.

At the primary study area, three auger holes (LLWA 1, 2, and 3) were drilled to depths of about 44 ft (13 m). Dense, compact clays and silts prevented further penetration. The clays and silts are overlain by a sequence that is 30 to 40 ft (9 to 12 m) thick and composed of limestone gravel, sand, and silt. Calcrete, sand, and silt overlie the gravel sequence. The two holes (LLWA 4 and 5) augered at the second study site encountered a similar stratigraphic sequence. Drillhole LLWA 5 was abandoned at a total depth of 20 ft (6 m) because the small drill rig was unable to penetrate the cobble-sized gravel. Results of the drilling at the second study area demonstrate that the depth to the top of the silt and clay is similar at both the primary and second study areas. The gravel sequence may also be coarser grained at the second study area, although the larger sized gravel penetrated in LLWA 4 and 5 might be a local variation that occurs at both study areas.

URM Drilling

URM drilled four holes (LLWA 7, 11, 12, and 13) 150 ft (45 m) deep to test the stratigraphy of the primary area (figs. 23a and 23b). Additional holes were drilled for hydrologic purposes, although several of these holes also provide valuable stratigraphic control. LLWA 6 was intended to be a 150-ft- (45-m-) deep stratigraphic test hole; however, sampling methods were inadequate, and the auger pipe broke at a depth of 65 ft (20 m), so the hole was abandoned. LLWA 8, 9, and 15 were drilled for permeability tests; however, LLWA 15 was not tested because silty clay was penetrated rather than clay. LLWA 10, drilled to 465 ft (142 m), was intended to be a water well, but because the packer failed when the casing was being cemented, the test zone and screen were accidentally cemented as well. LLWA 14 was subsequently drilled to 500 ft (152 m) to replace the

abandoned LLWA 10. Lithologic logs composed from on-site sample descriptions for the test holes are displayed in appendix 9.

Geophysical Log Interpretation

Geophysical logging conducted in open boreholes 7, 11, 12, and 13 included the Spontaneous Potential curve (SP), Gamma-Ray log (GR), Dual Induction-Spherically Focused log (DIL-SFL), Compensated Neutron log (CNL), and the Litho-Density log (LDT). Depth of coverage for these four boreholes was 150 ft (46 m) to surface. This suite of logs was designed to support core analyses.

One cased hole, borehole 10 (a 470-ft cased water well), was also logged to provide information on the bolson intervals below 150 ft (46 m). Logging tools in cased holes were restricted to GR and CNL. Due to casing conditions in this hole, the section logged was restricted to 303 ft (92 m) to surface.

Composite logs for the five boreholes are reproduced in appendix 10. Basic features of these logs and analysis of quantitative data are also provided in appendix 10.

Lithologic determination was accomplished using LDT and GR logs. One component of the LDT, the photoelectric curve (P_e), was useful in supporting the presence of limestone gravels because it indicates the presence of calcite and clean sands. This is best illustrated by the confirmation of the presence of a limestone gravel sequence from 94 to 97 ft (29 to 30 m) in borehole 13. Failure of the P_e to detect any calcite in the limestone gravels in borehole 12 may be a result of higher clay content masking the calcite response or greater depths of borehole invasion as recorded on SFL logs throughout this interval.

The GR is beneficial in stratigraphic and structural correlations and in the quantification of clay content. GR logs indicate that 40% of the sequences contain 0 to 25% clay, 34% contain 26 to 50% clay, 17% contain 51 to 75% clay, and 8% contain 76 to 100% clay. Methods used to determine clay content are presented in appendix 10.

Porosity values were determined by crossplotting CNL values with LDT values. Porosity values from the four open boreholes range from a minimum of 19% in borehole 13 to a maximum of 54% in boreholes 7 and 12. Correction factors determined by crossplotting indicate that true porosity is 1 to 2 porosity units greater than the computer-derived average porosity curve (labeled PHIA) displayed in Track #3 of the geophysical logs (app. 10).

Quantification of formation water resistivity values from the DIL was not possible because of the unsaturated nature of the section logged. The DIL was useful as an indicator of units containing higher irreducible water content, intervals where drilling fluid invasion of the borehole had exceeded 16 inches (41 cm) (thus a more permeable interval), and in stratigraphic correlation. True resistivity in unsaturated intervals is best represented by the deep-induction log (ILd).

Discussion

The test holes indicate three distinct units based on lithology. The units are (1) limestone, (2) silt and clay, and (3) gravel. Limestone, which was penetrated in LLWA 10 and 14, is the deepest unit. It is approximately 390 ft (120 m) deep in the study area. The limestone cuttings are multicolored (tan, brown, gray, and black) and resemble a conglomerate unit within the Cretaceous Mesa Bluff Formation that is exposed in Camp Rice Arroyo about 3 mi (5 km) southwest of

the boreholes. The cuttings could also be interpreted as a Tertiary limestone gravel overlying bedded Cretaceous limestone.

Above the limestone unit is a dominantly silt and clay unit that includes some sand layers. This unit has been described by Albritton and Smith (1965) as older basin fill. Based on the test holes and geophysical logs, the individual sand layers do not seem to correlate from hole to hole, suggesting they are not continuous; however, a silt-sand-clay sequence, or package, appears to extend across the area. The sandier package of older basin sediments is thickest in the northeastern part of the study site and thins west-southwestward (figs. 25 and 26). The silt-sand-clay sequence comprises most of the older basin fill penetrated in test holes LLWA 11 and 13. LLWA 7 and 10 penetrated two sandier layers that are approximately 10 ft (3 m) and 30 ft (9 m) thick, respectively, whereas LLWA 12 penetrated only 10 ft (3 m) of the silt-sand-clay sequence.

The upper unit, overlying the silt and clay unit, is composed of limestone pebble- and cobble-sized gravel, sand, silt, and some clay. This unit comprises younger basin fill and surface gravel deposits, which have been discussed by Albritton and Smith (1965). The upper gravel unit appears to be consistently 40- to 50-ft- (12- to 15-m-) thick throughout the study area (figs. 25 and 26).

Surface Flow

The primary site is located on a sloping area that drains the Diablo Plateau and Finlay Mountains (Finlay Mountains, Smith Mesa in fig. 27) via narrow arroyos such as Diablo Arroyo, Camp Rice Arroyo, and Alamo Arroyo. These ephemeral washes extend from northeast to southwest toward the Rio Grande. The arroyos cut into the bolson fill, and near Campo Grande Mountain and the

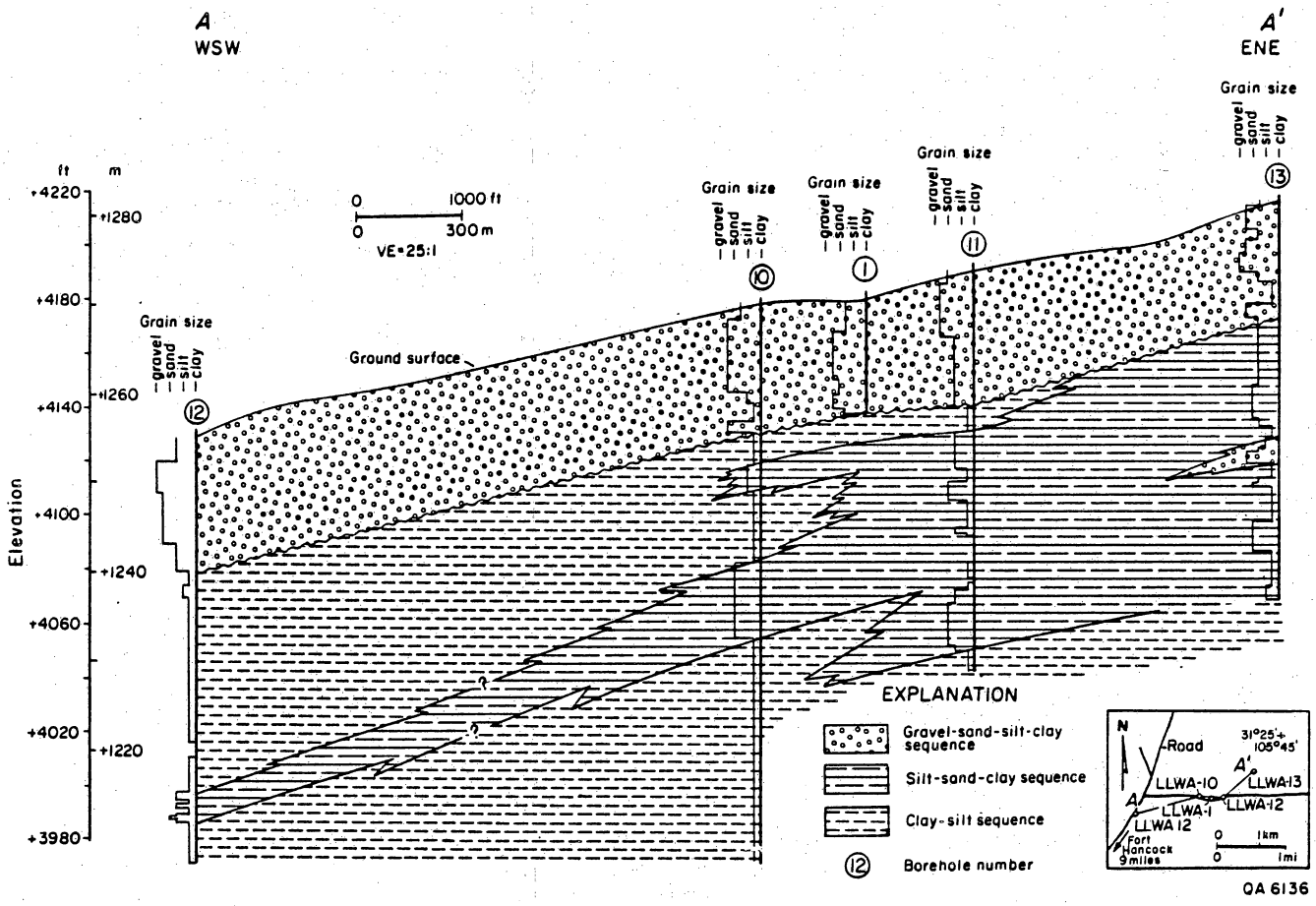

Figure 25. Cross section A-A' (west-southwest to east-northeast) across primary study site in Hudspeth County. Well locations are shown in figure 23.

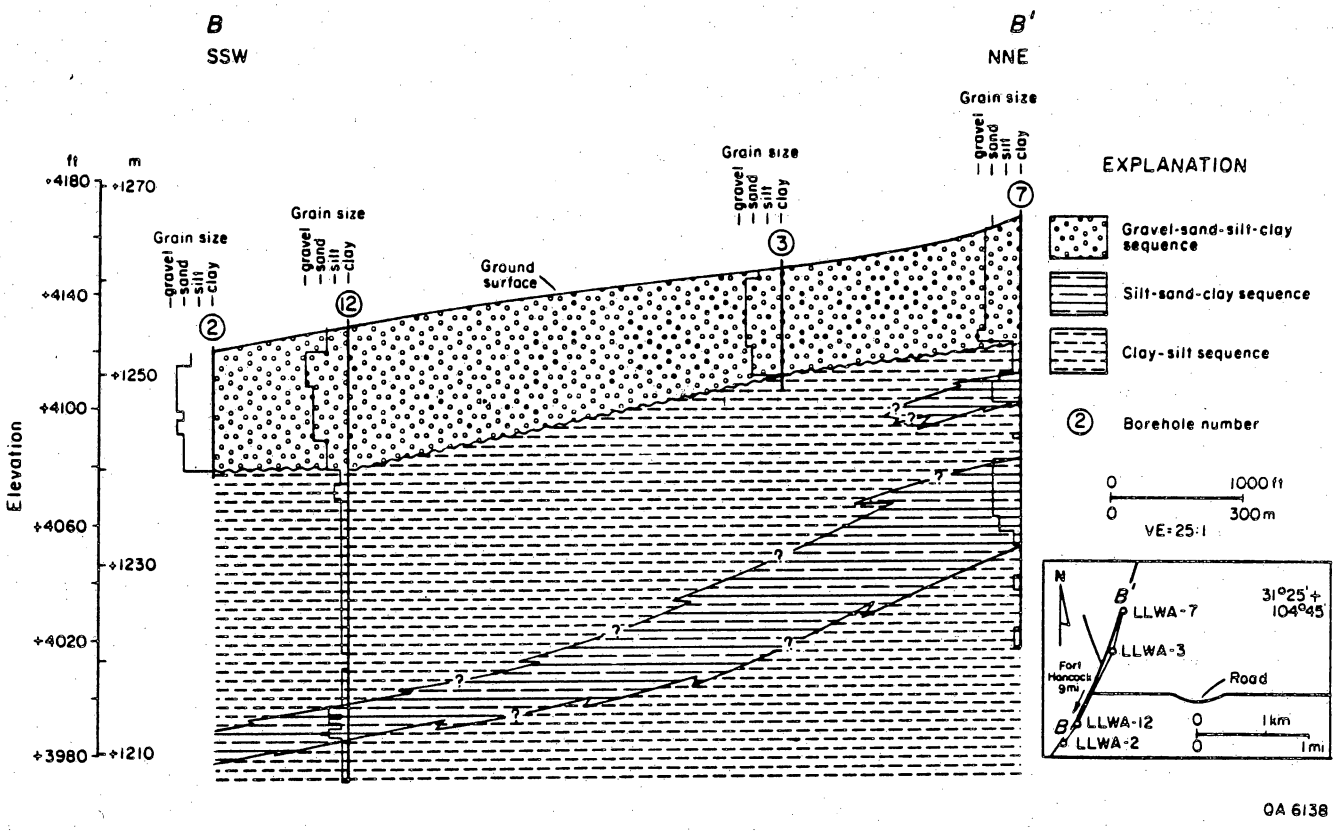

Figure 26. Cross section B-B' (north-northeast to south-southwest) across primary study site in Hudspeth County. Well locations are shown in figure 23.

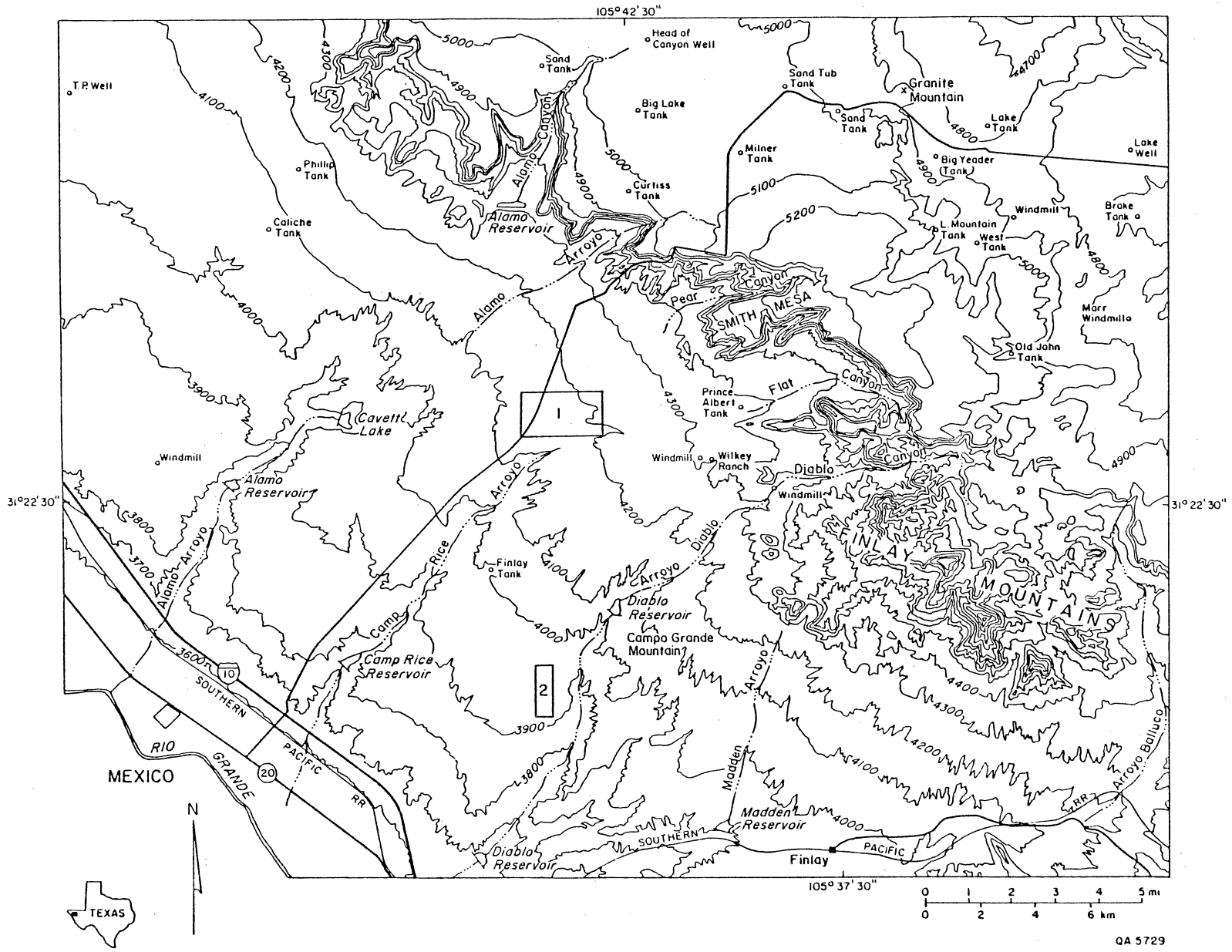

Figure 27. Base map for the Hudspeth County study area. Bold line approximately locates the primary (1) and second (2) site areas.

plateau's escarpment they cut into Cretaceous formations such as Finlay limestone, Cox sandstone, and Bluff Mesa limestone. The water in the arroyos changes its course from one flash flood to another. The depth of the alluvial fill in the arroyos is not known. However, little bolson fill is exposed in the riverbeds, which may suggest an alluvium thickness of several tens of feet. The abundance of earth dams, which are constructed on these arroyos (two reservoirs on Diablo Arroyo, one on Camp Rice Arroyo, and three on Alamo Arroyo, fig. 27), as well as the presence of water storage tanks, suggests that surface water flow occurs on a regular basis in this area. Residents (S. Wilkey and D. Walker, personal communication, 1986) say that these reservoirs receive water every year by August or September and hold water until January or February. No records about water depths in these reservoirs were available. Active floodplains are indicated in plate 4 (U.S. Department of Housing and Urban Development, Flood Insurance Administration, 1985).

Hydrologic Setting

Three aquifers underlie the site and the general Hudspeth study area. Cretaceous rocks form a plateau and underlie the lower area that is being considered for the potential site (fig. 27). Several wells in the plateau and the lower areas penetrate Cretaceous rocks of the Finlay, Cox, or Bluff Mesa Formations. It is not clear if there is one aquifer in the Cretaceous rocks or several aquifers in various formations. However, for simplicity, the rest of the discussion will refer to only one aquifer in the Cretaceous rocks. Because of regional faulting and overthrusting, various parts of the aquifer in the area west and south of the plateau may not be interconnected. A second aquifer occurs within the overlying Cenozoic bolson fill. Most of the wells being completed in this aquifer pump from sand lenses that occur between the clays and silty clays

that are more common in the older bolson fill. Basin and Range faults may cut the basin fill and could cause hydrologic discontinuities in this aquifer. The bolson fill is characterized by a variety of clastic materials that pinch out or grade into materials of different grain size laterally and vertically, which could be another reason for hydrologic discontinuities (Guyton and Associates, 1971). Lateral continuity of the bolson fill at the proposed site is discussed in the geologic investigations section. The third aquifer is in the young Quaternary Rio Grande alluvium that stretches along the Rio Grande from the El Paso area to Fort Quitman.

Water-bearing Characteristics

No porosity or hydraulic conductivity data were available for any of the three aquifers in the study area before the present study was initiated.

Cretaceous Formations

A minimum value of 27 gpd/ft (0.33 m^2/d) was estimated for the transmissivity coefficient of the Cretaceous aquifer based on a short pumping test in the water well drilled at the site by the Texas Low-level Radioactive Waste Disposal Authority (app. 7). No data are available on the thickness of the saturated zone of the Cretaceous aquifer in the area.

Bolson Fill

The thickness of the bolson fill in the site is approximately 400 to 500 ft (122 to 152 m). The bolson fill may thicken significantly across the Campo Grande fault toward the Rio Grande. Near Fabens, transmissivity of the bolson is 25,000 gpd/ft (310 m^2/d), and the storativity coefficient is 0.0003 (Leggat, 1962). Near El Paso, where the artesian bolson-fill aquifer provides the city with large

amounts of water, transmissivities range from 50,000 to 120,000 gpd/ft (620 to 1,500 m^2/d), and the storativity coefficient is 0.0004. In situ permeability measurements in shallow boreholes within the unsaturated zone of the bolson fill indicate values of 0.25 inch/d (0.63 cm/d) for the upper 40 to 50 ft (12 to 15 m) of sand and gravels and 0.12 inch/d (0.32 cm/d) for the 100-ft (30-m) interval of clays and thin sand lenses below these gravels (app. 12). These values represent horizontal permeabilities and therefore reflect the higher values of the sand lenses in the section. Vertical permeability values, more critical for flow in an unsaturated section, would be expected to be lower. Dames and Moore (1985) reported clay permeability in a core sampled in their test hole at the site, and their value was 0.002 inch/d (5.8×10^{-8} cm/s, or 0.005 cm/d). URM analyzed 6 silty clay (less than 20% sand) bolson cores taken from borehole LLWA 7 (fig. 23a) for vertical permeability and their results varied from 3.4×10^{-5} to less than 4.7×10^{-6} inch/d (1×10^{-9} to less than 5×10^{-11} cm/s, or 9×10^{-5} to less than 4.3×10^{-6} cm/d) (app. 6).

Total porosity values in the bolson fill were determined in four boreholes (7, 11, 12, and 13, fig. 23), using LDT-CNL cross plots (app. 10). They ranged between 16 and 54%. Lower values (16 to 30%) characterize the gravel cover and higher values (45 to 54%) are typical of the older fine grained bolson beneath the gravels. Effective porosity in the older bolson is expected to be much lower.

Rio Grande Alluvium

The thickness of the Rio Grande alluvium is about 200 ft (60 m) (Alvarez and Buckner, 1980). The alluvium is permeable but no aquifer tests are known to have been conducted within this aquifer. Assumed specific yield of 0.2 and

transmissivity value of 30,000 gpd/ft (370 m^2/d) was used for this aquifer in the verification stage of the Hueco Bolson model study (Alvarez and Buckner, 1980).

Recharge

Cretaceous Formations

Recharge into the Cretaceous aquifer is considered to be predominantly from direct precipitation on the outcrops in the plateau area. Tritium data of wells located in the Diablo Plateau (such as head of Canyon well or Wilkey No. 2 well, fig. 28) indicate the presence of a recent recharge component (as indicated by 11.8 and 20.67 TU) mixed with older recharge sources identified by ^{14}C analyses (resulting in a mixture that has 42 to 60 Percent Modern Carbon [PMC]) or corrected ^{14}C "age" of 833 to 865 yr) (fig. 28). However, water from Gunsight No. 1 well, which is located farther east in the Finlay Mountains, does not show any indications of recent recharge (0 TU, ^{14}C age of 13,071 yr, and the most depleted values of $\delta^{18}O$ and $\delta^{2}H$). This water sample may be regarded either as the end member of the older flow component in the Cretaceous aquifer in the plateau area or as a sample from a separate aquifer whose current recharge is very slow or nonexistent. Recharge may also occur where the Cretaceous crops out in arroyos that cut the Campo Grande fault.

Bolson Fill

The bolson aquifer can be recharged by (1) precipitation that falls on the gravel veneer that covers the finer grained bolson fill, (2) surface water that flows during flash floods in the arroyos, (3) ground water moving upward from the underlying Cretaceous aquifer (Davis and Leggat, 1973), or by (4) ground water in the overlying Rio Grande alluvium, which may recharge bolson fill by vertical or lateral flow.

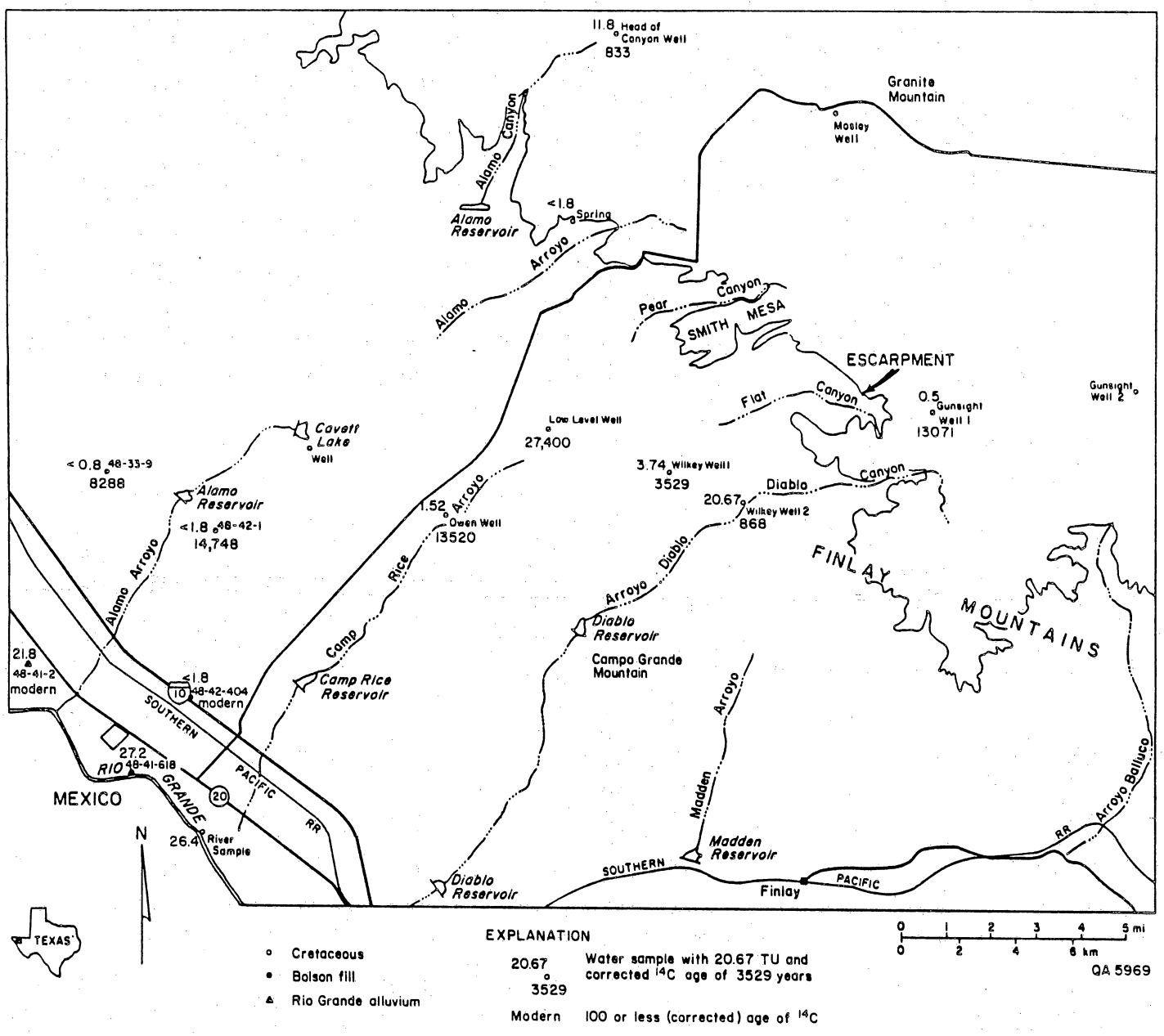

Figure 28. Tritium activity and ^{14}C corrected ages in ground water of the Hudspeth County study area.

Recharge by upwelling water from the underlying Cretaceous aquifer is a viable possibility in the site area and its vicinity. Both Cretaceous and bolson aquifers contain old water, based on ^{14}C analyses ranging from 3,529 to 27,400 yr old in the Cretaceous wells (Wilkey No. 1 well, Low-level well, and Owen well) and from 8,000 to 15,000 yr old in the bolson wells (48-33-9 and 48-42-1). However, in the Rio Grande valley this is not considered a dominant recharge process. ^{14}C results from bolson well 48-42-404 indicate modern (less than 100 yr old) water, whereas the water from Cretaceous wells in the area is probably much older.

The annual rate of recharge through desert soils can be estimated by the distribution of chloride in the unsaturated soil zone. Qualitatively, if recharge rates are high, Cl is flushed from the soils. Conversely, if recharge is low, Cl will accumulate in the soil section, similarly to calcrete. Theory and equation are available (Allison and Hughes, 1978) and are used in this study to estimate recharge through the sand and gravel that overlie the bolson fill. (See app. 13 for detailed description of techniques.) Samples of the sand and gravel (taken from five boreholes, LLWA 1 through 5, figs. 23a and 24a) augured by the BEG staff in the site area to total depth of 50 ft (15 m) were analyzed for their chloride concentrations (app. 13). Chloride concentration in soil profiles varied considerably from one borehole to another, ranging between 560 and 9,000 mg/l. Different distributions of chloride concentration with depth were observed in various boreholes (fig. 29). To determine the correlation between chloride distribution (and thereby the estimated recharge) and grain size of soil particles, soil samples from two boreholes (LLWA1 and 4, figs. 23 and 24) were analyzed for grain-size distribution (fig. 29). The soil profile of borehole LLWA1 has the lowest chloride concentration (560 mg/l) and no salinity peaks can be observed with depth. Chloride concentration of borehole LLWA4 is the highest (~9,000 mg/l) and several

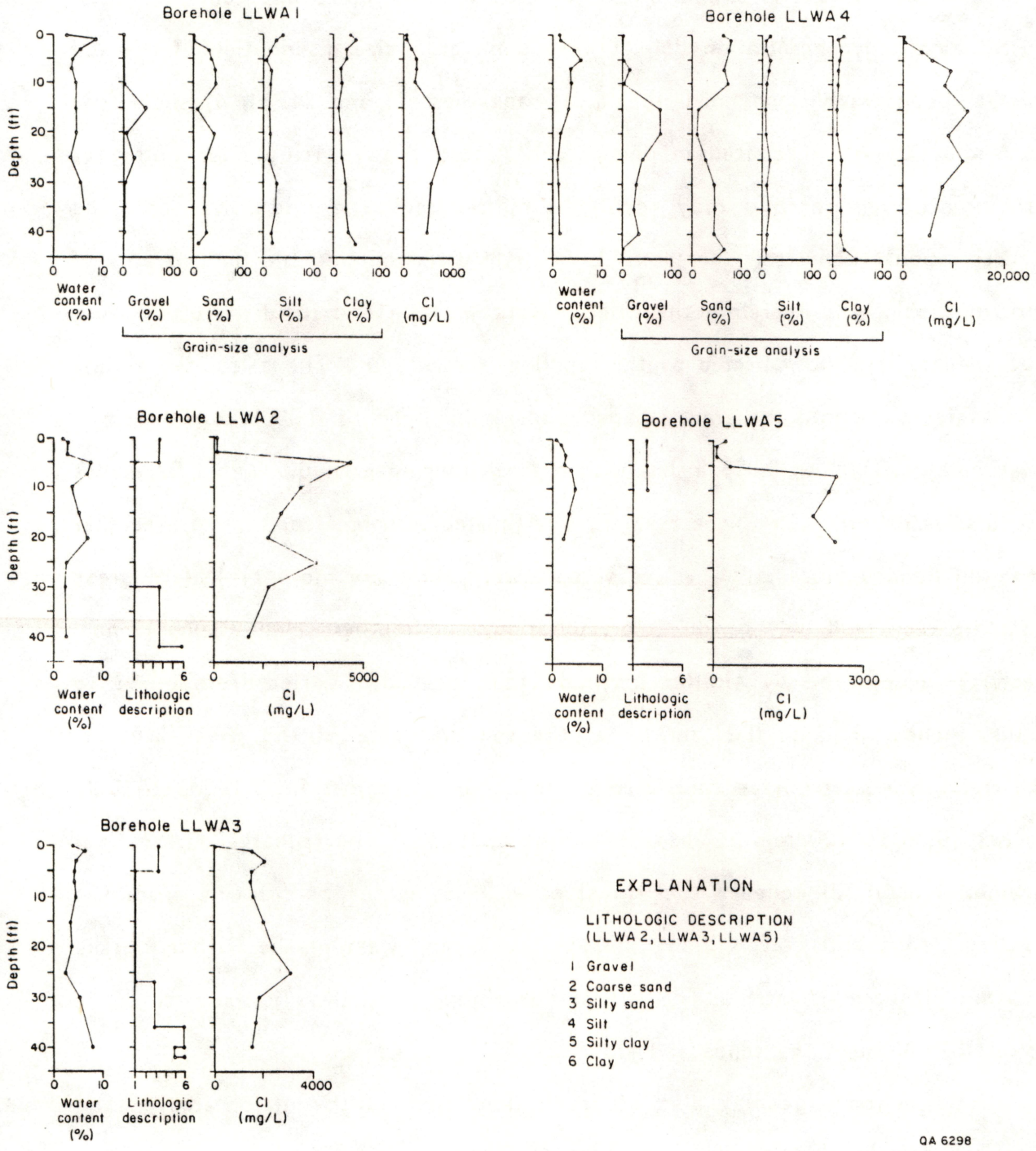

Figure 29. Variations of grain size, water content, and chlorides in soil cores of five boreholes in the bolson gravel cover. Borehole location shown in figure 23.

salinity peaks can be observed in the soil profile. Based on grain-size analysis, clay and silt content is similar in both holes and therefore apparently chloride distribution and concentration do not depend on grain-size distribution of the soil profile. Topographic and flood-prone-area maps (figs. 23 and 24, pl. 4) show that borehole LLWA1 is located in one of the Alamo Arroyo tributaries and that flooding of this arroyo may result in higher recharge and lower chloride concentration. Conversely, borehole LLWA4 is located outside the flooded area of Arroyo Diablo, and therefore the chloride concentration and its distribution along the soil profile is not affected by the runoff in the arroyo. The calculated annual flux of rainwater into the gravels varies from a minimum of 0.0005 to 0.003 to a maximum of 0.009 to 0.053 inches with a mean ranging from 0.003 to 0.02 inches (0.07 to 0.5 mm). The higher values for estimated recharge represent arroyos that may be flooded more often, whereas the lower values are more typical of areas that are recharged only by direct precipitation. In Southern High Plains, annual recharge calculated by similar methods (Stone, 1985) varied from 0.007 to 0.009 inches (0.18 to 0.24 mm). In the semiarid area of the River Murray, Australia, annual recharge calculated by this method ranged from 0.002 to 3.93 inches (0.06 to 100 mm) (Allison and others, 1985). The recharge of the fine-grained bolson fill beneath the gravel cover from water percolating from the overlying sand and gravels along the area south and west of the Diablo Plateau has not yet been assessed. The annual flux through the clays is expected to be lower than through the sands and gravels.

Bolson recharge may also occur by flood flow in the major arroyos and from the bottom of reservoirs such as the Alamo Reservoir.

In the Rio Grande valley, recharge occurs by the water stored in the Rio Grande alluvium that overlies the bolson fill near the Rio Grande. Both the Rio Grande and Rio Grande alluvium are characterized by modern ^{14}C activities and therefore agree with the ^{14}C data that indicate modern water in the bolson fill in the Rio Grande valley. However, the tritium data of the water in the bolson fill there (0 TU in well 48-42-404) indicate that the bolson was recharged before 1952 and that the recharge process is slow.

Rio Grande Alluvium

Water in the Rio Grande alluvium is recharged by the water of the Rio Grande (Guyton and Associates, 1971; Davis and Leggat, 1973; Alvarez and Buckner, 1980). When the flow of the Rio Grande is sufficient, Rio Grande water is used for irrigation on the cultivated land adjacent to the river. Some of this water recharges the alluvium and then discharges to local drain canals and returns to the river. This assumption is supported by the rise of water levels in the aquifer since the irrigation practice with river water was begun (Guyton and Associates, 1971) and by the results of ^{14}C and tritium analyses of water sampled from the Rio Grande and from wells that penetrate the Rio Grande alluvium. The water in the Rio Grande alluvium shows high ^{14}C and high tritium activities (21.8 and 27.2 TU), similar to the Rio Grande water (24.4 TU) (fig. 28).

Discharge

Cretaceous Formations

Discharge from the Cretaceous aquifer occurs through pumpage from a few water wells that penetrate the aquifer and possibly through natural outlets such as leakage into the overlying bolson fill and Rio Grande alluvium in the Rio Grande valley. The amount that discharges into the Rio Grande alluvium or bolson fill in

this area cannot be evaluated because no Cretaceous wells are located within the Rio Grande valley and therefore the difference between the potentiometric surface of the water in the Cretaceous aquifer and the water levels in the overlying aquifers in this area is not known. If such vertical leakage occurs it must be very small because in the Rio Grande valley water in both bolson and alluvium aquifers is modern, whereas water in the Cretaceous aquifer beneath the bolson fill is relatively old (fig. 28, app. 2). Discharge from the Cretaceous aquifer into the bolson fill at the site area and its vicinity is possible, considering the low tritium activities and old ^{14}C ages observed in two wells that pump from the bolson (48-33-9 and 48-41-1).

Bolson Fill

Discharge from the bolson fill occurs through pumpage from a few wells in the site area (toward the northwest the bolson fill is a major water supply source for the El Paso area). Water levels in the bolson fill (fig. 30) near the Rio Grande are similar to those in the Rio Grande alluvium and may suggest interconnectedness between both aquifers.

Rio Grande Alluvium

Water from the Rio Grande alluvium discharges (1) by evapotranspiration through the shallow water table or the crops, (2) through pumping wells, (3) through return flows into the Rio Grande by drainage channels, and (4) by leakage into the bolson fill.

Potentiometric Surface

Cretaceous Formations

The potentiometric surface of the water in the Cretaceous rocks (fig. 30) ranges between 4,679 ft (1,427 m) at the Diablo Plateau, where water flow is assumed to be under water-table conditions, to 3,745 ft (1,142 m) at the site

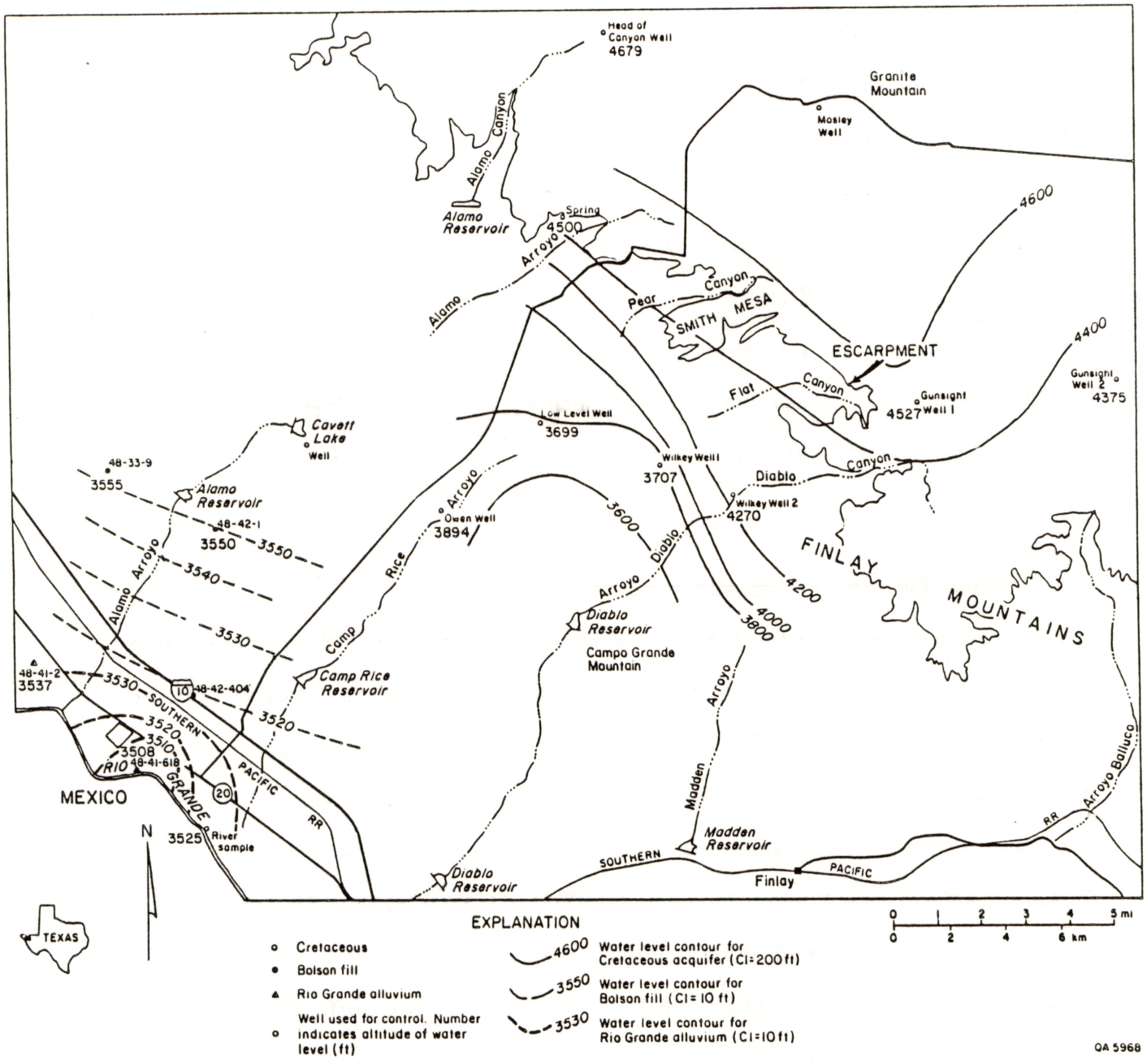

Figure 30. Potentiometric surfaces of ground water in the aquifers in Hudspeth County study area (ft).

area, where water is confined by the bolson fill. Ground water flows from the plateau toward the southwest. The gradient of the potentiometric surface ranges from 42 ft/mi (8 m/km) in the water-table area to 327 ft/mi (63 m/km) in the confined water area. The large gradient in the confined water zone may not reflect a decline in a potentiometric surface of a continuous aquifer but may indicate two hydrologic systems separated by possible faulting along the escarpment of the Diablo Plateau. Another possibility is that the aquifers that are exposed at the Diablo Plateau (Cox and Finlay Formations) are truncated, and that the Cretaceous aquifer beneath the bolson fill south and west of the plateau is in the deeper Bluff Mesa Formation. Calculated horizontal flow velocity based on ^{14}C data (Vogel, 1970) is 2.8 ft/yr (0.85 m/yr), assuming a continuous aquifer.

Bolson Fill

Ground-water flow in the bolson aquifer is probably under water-table conditions in the area south and west of the Diablo Plateau. Water may be confined in the Rio Grande valley, where the Rio Grande alluvium aquifer overlies the bolson aquifer (Alvarez and Buckner, 1980). Sixty mi (90 km) to the north and west in the El Paso area, the water in the bolson is artesian (Alvarez and Buckner, 1980). Where the bolson fill is very thick near Fabens (20 mi [30 km] to the northwest), a second artesian water zone was reported at a depth of 1,300 ft (400 m) (Alvarez and Buckner, 1980). The potentiometric surface of the water in bolson fill within the study area (fig. 30) ranges from 3,555 to 3,520 ft (1,084 to 1,073 m). Ground water follows the regional dip from northeast to the southwest with a rather small gradient of 8.6 ft/mi (2.6 m/km). In the vicinity of the study area, water levels in the bolson aquifer are lower than in the

underlying Cretaceous aquifer by 200 to 300 ft (60 to 90 m) and have water levels similar to those in the Rio Grande alluvium aquifer. It is assumed, therefore, that in the area of Fort Hancock, the bolson fill and the Rio Grande alluvium aquifer are hydrologically connected (Alvarez and Buckner, 1980).

Rio Grande Alluvium

Ground water in the Rio Grande alluvium aquifer flows under water table conditions along the Rio Grande valley from northwest to southeast (fig. 30; Alvarez and Buckner, 1980). Near Fort Hancock, the gradient of the water table is about 8 ft/mi (1.6 m/km). Water levels have risen since irrigation with Rio Grande water began in 1916 and it became necessary to construct drains. Water levels in the aquifer now fluctuate with the availability of Rio Grande water for irrigation and seasonal application of the water. Ground-water levels decline as a result of intensive pumpage from the aquifer but recover when the flow in the river is at a higher stage. As a result, no long-term declines of water levels are encountered in the aquifer.

Ground-water Geochemistry

Cretaceous Formations

Ground water in the Cretaceous aquifer is slightly brackish, with TDS ranging from 801 to 1,850 ppm (fig. 31). Along the flow path from the escarpment to the confined ground-water zone south and west of it, water facies change from Na-mixed-cations or Ca-mixed-cations in the outcrop area (in head of Canyon well, Thaxton Spring, and Wilkey No. 2 well) to Na-SO_4 facies in the confined water zone (Wilkey No. 1 and Owen wells) (fig. 32). These changes are also accompanied by increasing temperatures and age of

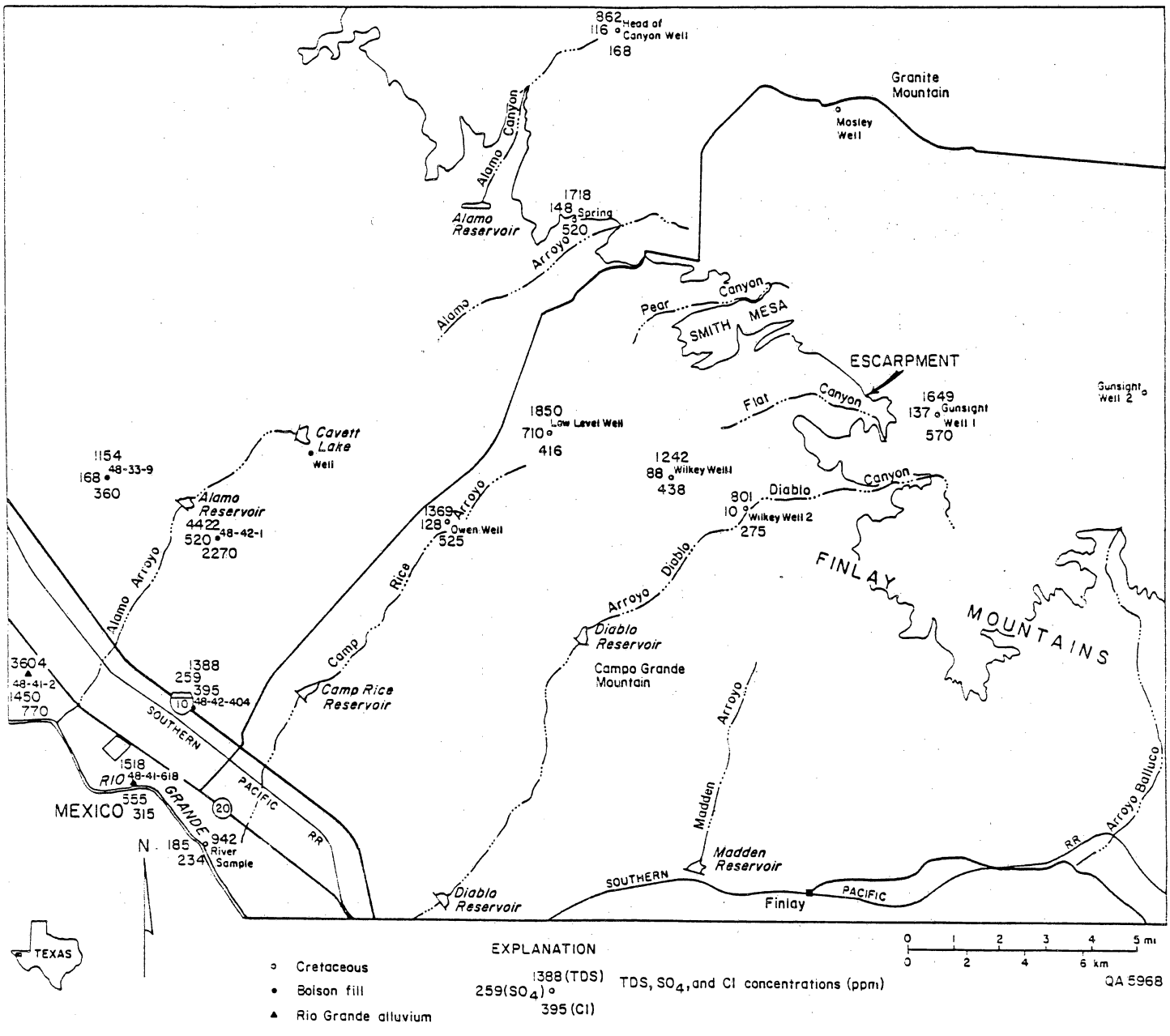

Figure 31. Total dissolved solids (TDS), SO_4^{2-}, and Cl^- (mg/l) distribution in ground water of Hudspeth County study area.

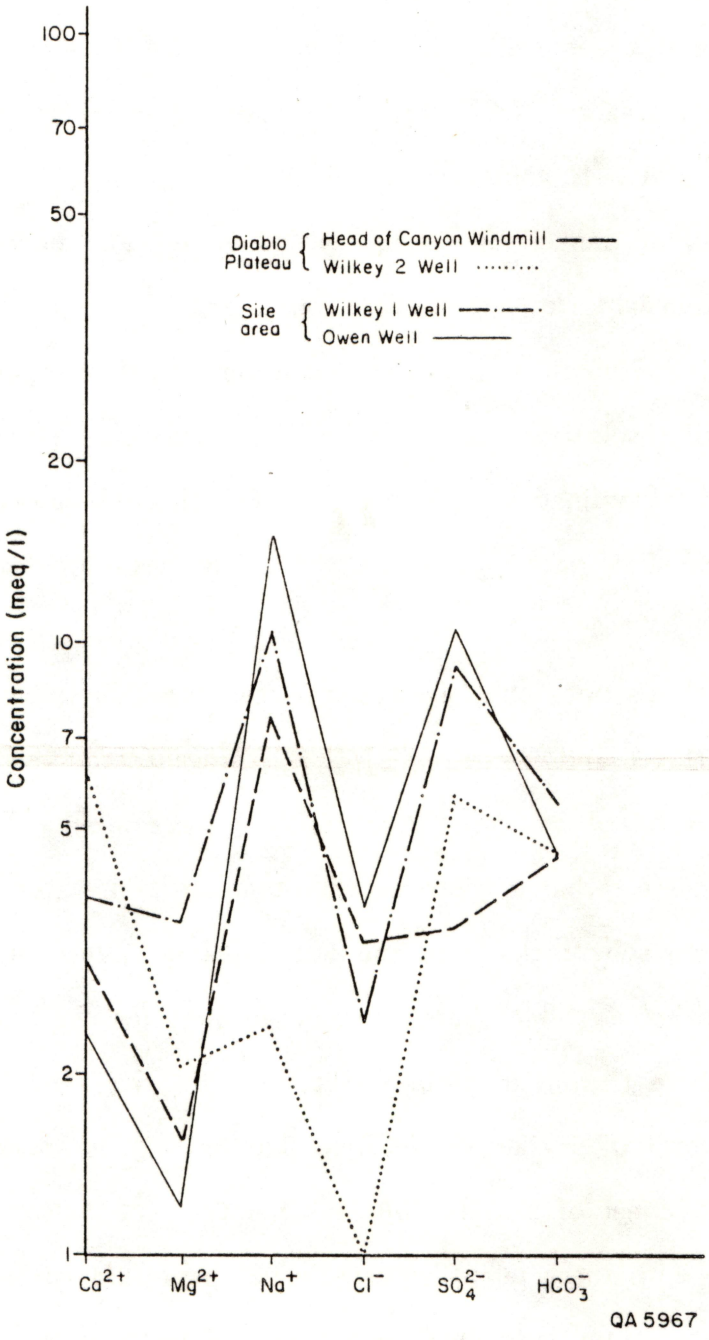

Figure 32. Salinity diagram of ground water from the Cretaceous aquifer in the Hudspeth County study area. Well location is shown in figure 31.

ground water, reflected by a decrease of tritium activity from 20.67 and 11.8 TU (head of Canyon and Wilkey No. 2 wells, respectively) to 3.75 and 1.52 TU (Wilkey No. 1 and Owen wells) and an increase in ^{14}C ages from about 800 yr in the outcrop area to 27,000 yr in the confined water zone (figs. 28, 33, and 34). $\delta^{18}O$ and $\delta^{2}H$ values (figs. 35, 36, and 37) are heavier at the Diablo Plateau (head of Canyon or Wilkey No. 2 wells) and become lighter along flow paths. Gunsight No. 1 well, with very light $\delta^{18}O$ and $\delta^{2}H$ values, is an exception in the Plateau area. The above-mentioned changes in water chemical facies could result from evolution of the water chemistry from the recharge zone into the confined water zone but may also indicate a hydraulic discontinuity along the flow path of water in the aquifer resulting from faulting or separate aquifers.

It is important to note that even the water samples in the confined water zone (Wilkey No. 1 and Owen wells) that represent relatively old water (3,530 and 13,520 yr based on low ^{14}C activities) have a small amount of tritium that may indicate recharge sources other than ground water flowing all the way into the Cretaceous rocks from the outcrop area. Vertical movement of water through the bolson fill probably cannot account for the fast recharge rate needed to preserve tritium in ground water at the site area. (A water flux range of 0.003 to 0.02 inches/yr [0.07 to 0.5 mm/yr] was calculated for the upper permeable veneer of gravels, whereas most of the bolson has lower permeabilities. Even with these relatively high values, it would take more than 6,000 yr to get water from land surface across the unsaturated section of 485 ft [148 m] into the Cretaceous. By that time, no tritium can be preserved in ground water.) If the Campo Grande fault zone is permeable, it could provide a shortcut for some recent recharge from surface water and precipitation into the aquifer.

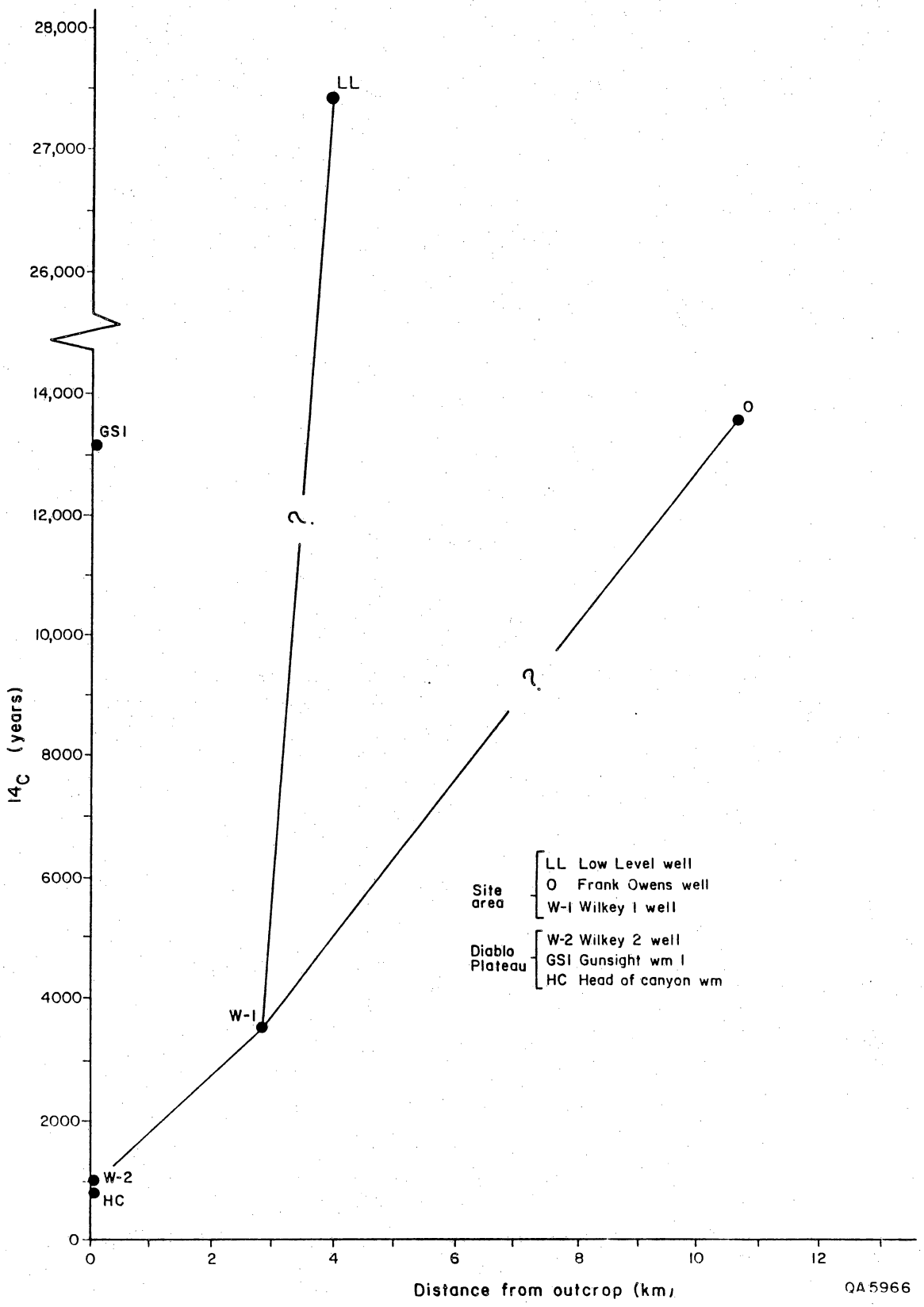

Figure 33. ^{14}C corrected ages (yr) in ground water sampled from wells that penetrate the Cretaceous aquifer versus the distance (km) of these wells from the recharge area at the Diablo Plateau. Well location is shown in figure 28.

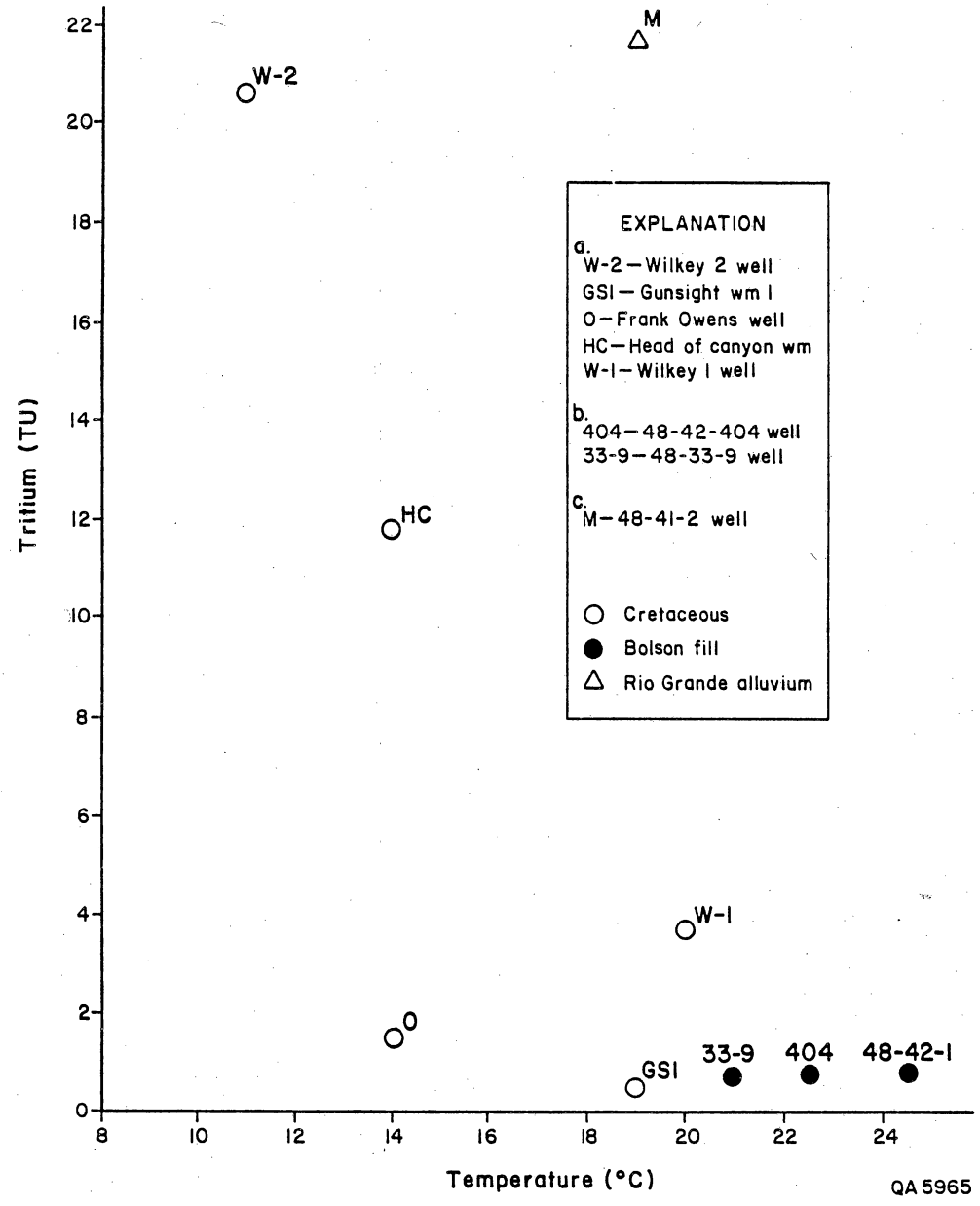

Figure 34. Tritium activity (TU) versus temperature (^{o}C) in ground-water samples in Hudspeth County study area. Well location is shown in figure 28.

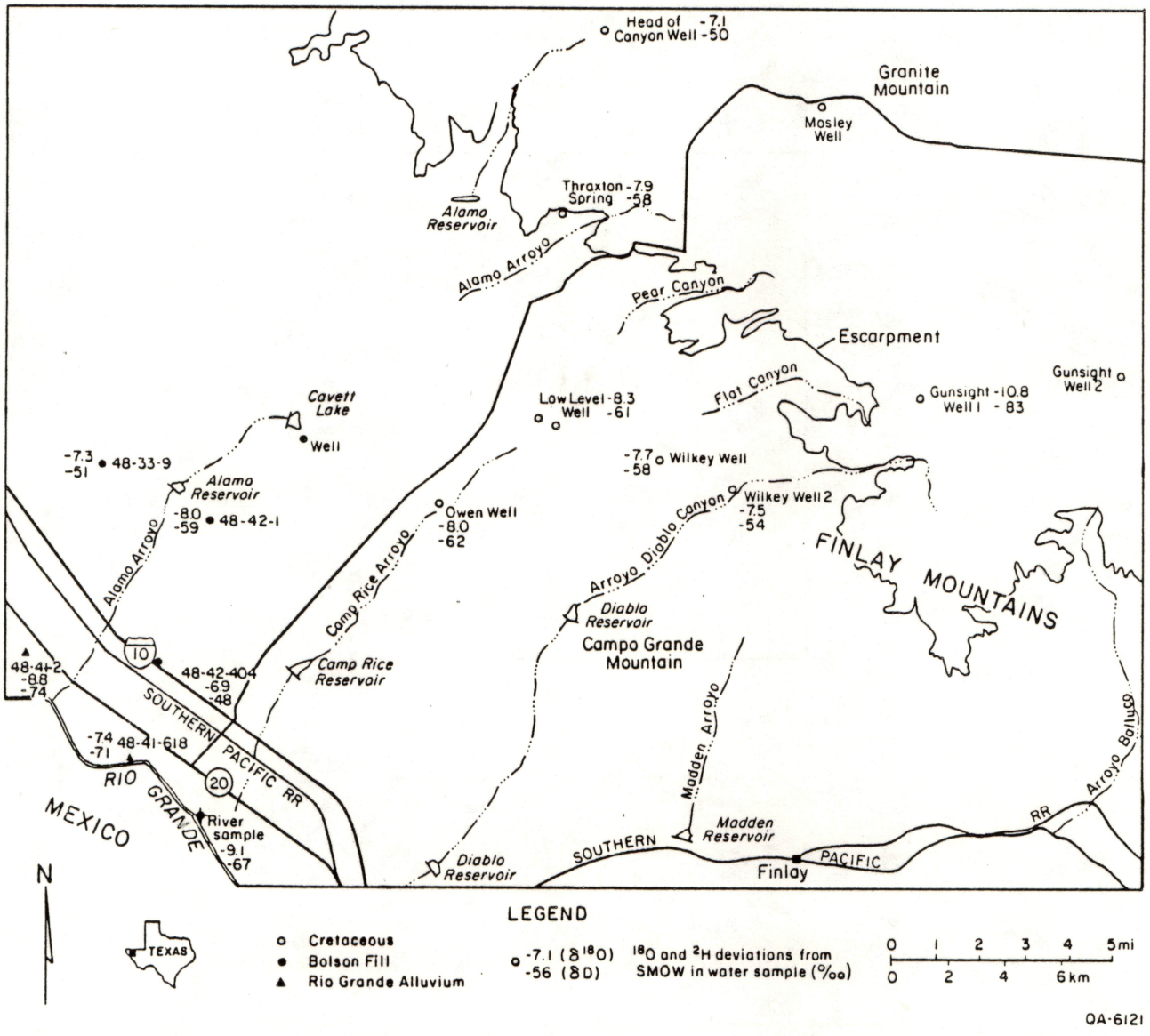

Figure 35. $\delta^{18}O$ and $\delta^{2}H$ distribution in ground water in Hudspeth County study area (in $^{o}/oo$ deviation from SMOW).

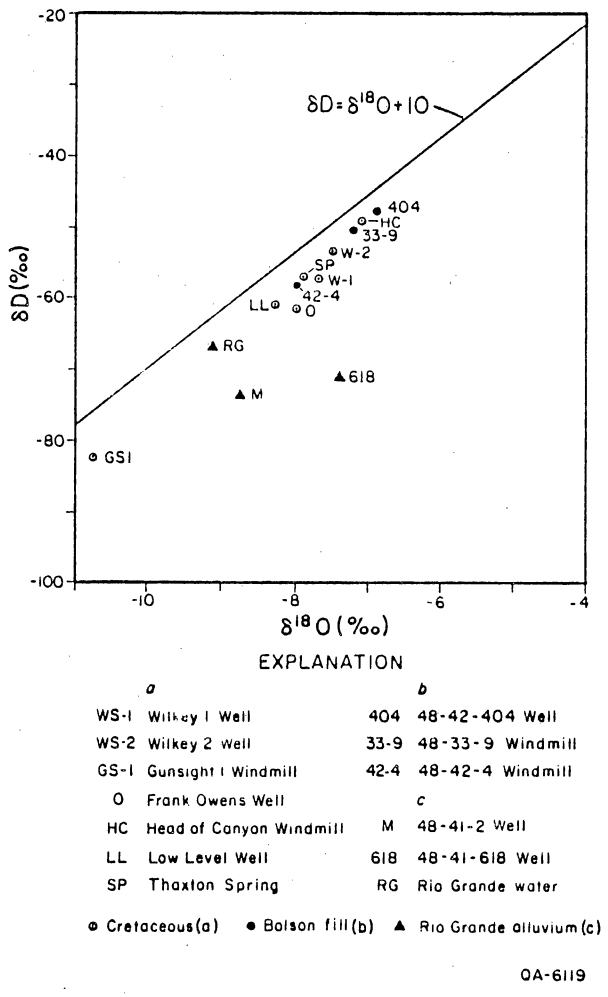

Figure 36. $\delta^{18}O$ versus $\delta^{2}H$ ($^{o}/oo$) in ground water of Hudspeth County study area (in $^{o}/oo$ deviation from SMOW). Well location is shown in figure 35.

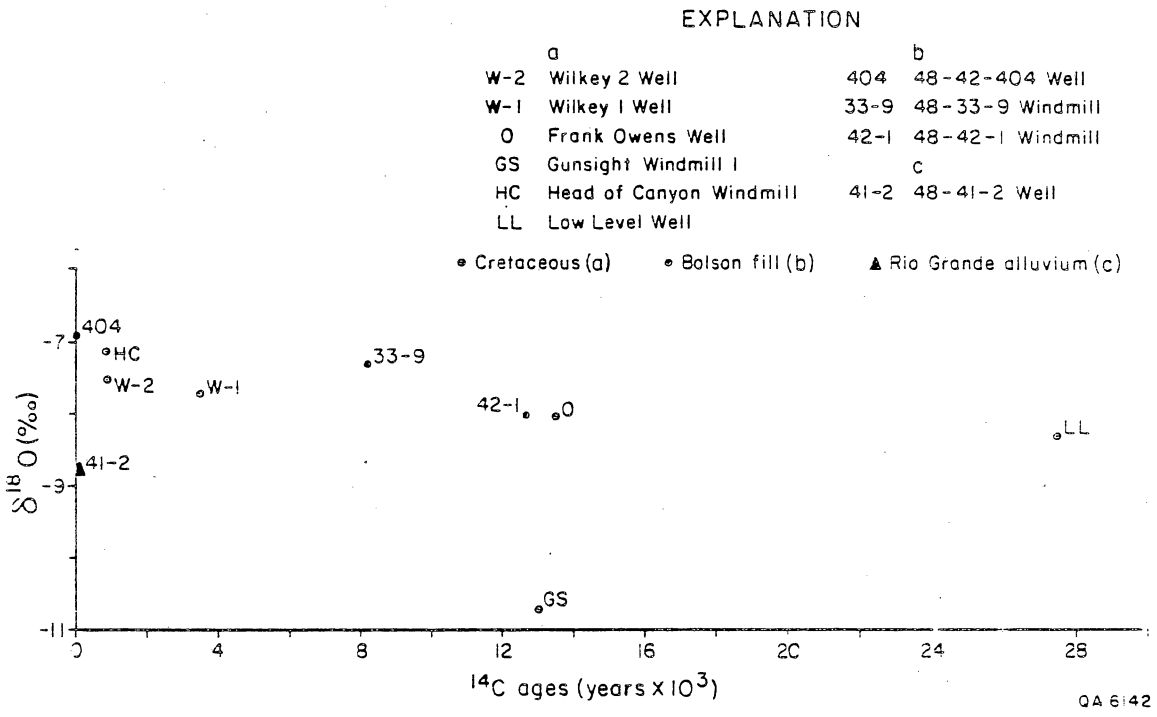

Figure 37. $\delta^{18}O$ ($^{o}/oo$) versus ^{14}C corrected ages (yr) in ground water of Hudspeth County study area. Well location is shown in figure 35.

Another interesting observation is the different chemical and isotopic features of the water sampled in Gunsight No. 1 well. The well is located in the outcrop area, but nevertheless its water exhibits characteristics of old water (0.5 TU and ^{14}C age of 13,071 yr), with Na-SO_4 chemical facies similar to the water in the confined water zone and the most depleted $\delta^{18}O$ and $\delta^{2}H$ values (-10.8 °/oo and -83 °/oo, respectively).

Bolson Aquifer

Water in the bolson aquifer is brackish, with TDS varying from 1,154 to 4,421 ppm (fig. 31). Its chemical facies vary from Na-mixed-cations type to Na-SO_4 type (fig. 38). Brackish Na-SO_4 water was also found in the deep bolson aquifer near Fabens, northwest of Fort Hancock (Guyton and Associates, 1971). Ground water in the Cretaceous aquifer that underlies the bolson fill has similar Na-SO_4 water facies. Soluble material in the fine-grained, predominantly playa-lake deposits and the low level of interconnectedness between the sandy lens that prevents efficient flushing of the salts from the bolson fill probably account for the mineralization of the water in this aquifer (Gates and others, 1980). Where horizontal movement is restricted, increase in dissolved salts may occur because there is no lateral influx of fresh water. Where vertical movement is constrained, zones of saline water may occur above or below zones of fresher water (Alvarez and Buckner, 1980). The tritium and ^{14}C activities of the water in the bolson aquifer near the site area indicate a very long residence time of ground water in the aquifer (8,000 to 15,000 yr and 0 TU), whereas in the Rio Grande valley they indicate recharge that occurred between 35 and 100 yr ago (0 TU and modern water, app. 2). The large difference in ^{14}C ages between two adjacent bolson wells (48-42-1 with 14,800 yr and 48-33-9 with 8,000 yr) can indicate a hydraulic

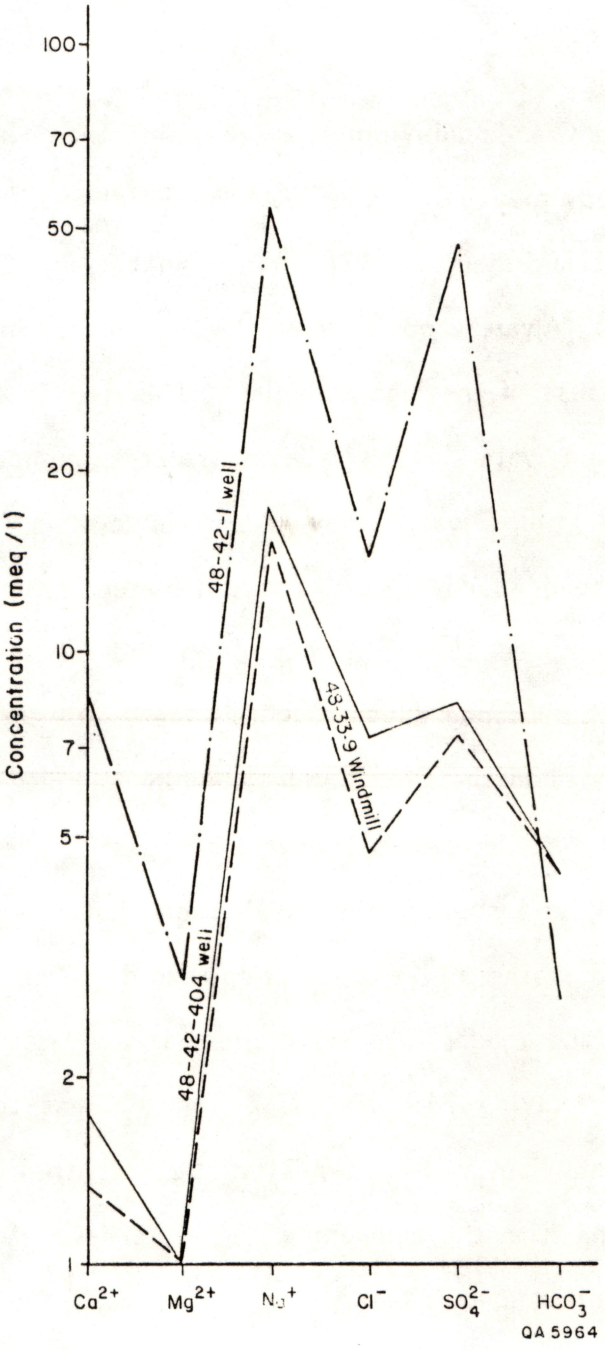

Figure 38. Salinity diagram of ground-water samples of the bolson-fill aquifer in the Hudspeth County study area. Well location is shown in figure 31.

discontinuity between them, resulting from either tectonic movements or the lenticular nature of the bolson.

Rio Grande Alluvium

Water in the Rio Grande alluvium is more saline than water in the bolson aquifer, and in the study area TDS varies between 1,500 and 7,500 ppm (fig. 31; Alvarez and Buckner, 1980, their fig. 12). Water in the Rio Grande alluvium is fresher to the northwest (Alvarez and Buckner, 1980). Irrigation with Rio Grande water is probably the cause of the high salinities. The river is the source of and also the sink for irrigation water in the valley. Water is pumped from the river, but tail water and any ground water above a certain level in the alluvium drain back to the river by the open channels. The tail water is typically more saline than the regular water because of evapotranspiration and, as a result, contributes more minerals into the Rio Grande alluvium in this area. All chemical analyses of water from wells completed in the Rio Grande alluvium sampled for this study or older analyses taken from the Texas Water Commission files indicate Na-Cl chemical facies (fig. 39) and support the assumption that the salinity source is evaporation of recycled water and evapotranspiration. The tritium and ^{14}C activities of water from the aquifer (fig. 28) suggest a very fast recharge rate from the river (modern water having 21.8 and 27.2 TU, whereas the river has 24.4 TU). The Rio Grande alluvium water chemistry suggests that not much of the bolson-fill water is mixing with the alluvium water; water-level data of Rio Grande alluvium suggest that mixing is possible.

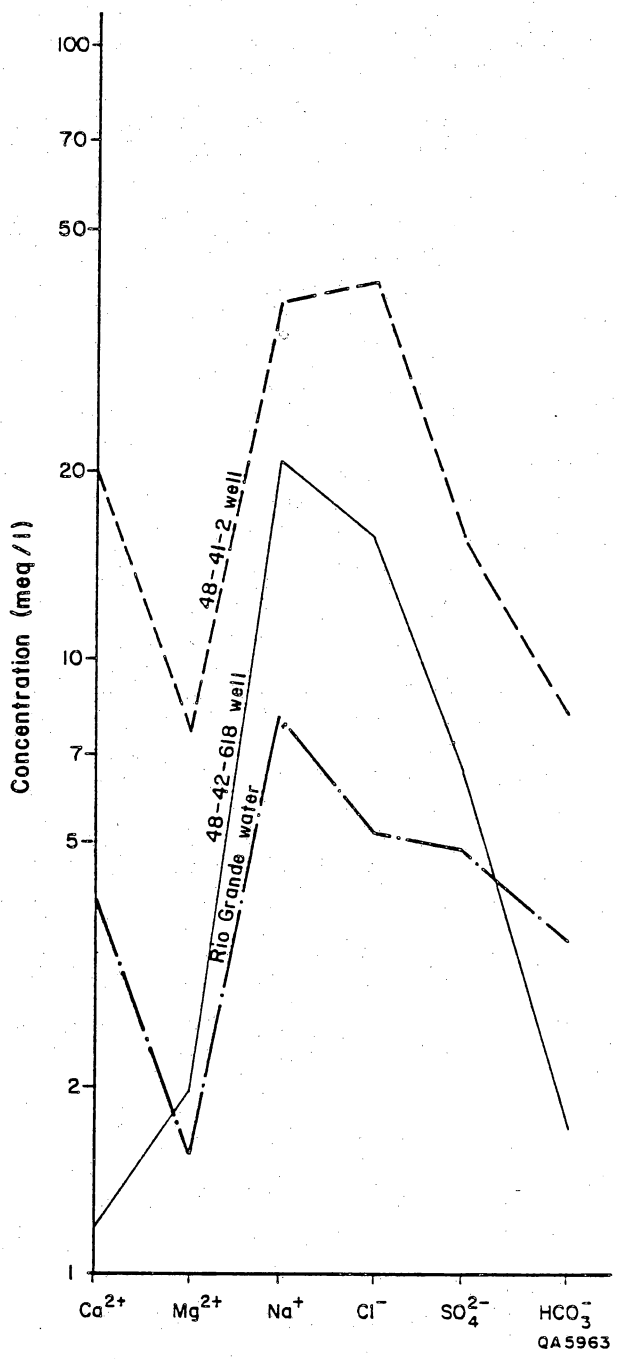

Figure 39. Salinity diagram of ground-water samples of the Rio Grande alluvium in the vicinity of the Hudspeth County study area. Well location is shown in figure 31.

Summary

Based on the geochemistry of the water in the Cretaceous, bolson, and Rio Grande alluvium aquifers, the Cretaceous and bolson formations appear to contain the oldest water but still receive some current recharge in areas that allow faster movement of water. A hydraulic discontinuity in the Cretaceous and bolson aquifers as a result of faulting is possible in the study area. Based on geochemical and isotopic data, there is a possibility of upward movement of water from the Cretaceous aquifer into the bolson aquifer (this movement may also be hypothesized based on differences in potentiometric surfaces between these aquifers). On the other hand, water from the Rio Grande alluvium aquifer, mainly replenished by the Rio Grande, possibly recharges the bolson aquifer in the Rio Grande valley. Recharge to the bolson is slower than recharge to the Rio Grande alluvium aquifer and is governed by the lower permeabilities of the bolson fill.

Site-specific Hydrologic Features

No ground water was encountered in the bolson fill in the site area. The permeability and porosity of the bolson fill are expected to be heterogeneous because of the lenticular nature of the bolson clastics. The annual recharge from precipitation into the gravel cover of the bolson was estimated to range from 0.003 to 0.02 inches/yr (0.07 to 0.5 mm/yr). No information is available now about the recharge rate into the finer bolson sediments below the gravels. Another source of recharge into the bolson fill in the site area is flash floods in the Alamo and Camp Rice Arroyo that drain the land surface toward the Rio Grande valley.

The only aquifer observed at the site is the Cretaceous. Two wells are located near the site area (Wilkey No. 1 and Owen wells). The thickness of the aquifer is not known. The aquifer is confined in the site area and its potentiometric surface is 478 ft (145.7 m) below land surface. The estimated age of the ground water in the Cretaceous aquifer near and at the site area ranges from 3,500 and 27,400 yr old, which may suggest either a very low permeability of the aquifer or a hydraulic disconnection as a result of the regional fault. However, the presence of a small amount of tritium in the ground water may indicate shortcut paths of recent recharge. Water from the well that was drilled at the site is Na-SO_4 and brackish (TDS=1,850 ppm). Ground water flows from the site area to the southwest toward the Rio Grande valley. A small part of the site was indicated as a flood-prone area. Based on an earlier geologic reconnaissance, the site area was mapped as being within the extended outcrop of major and minor aquifers (Dames and Moore, 1985, their fig. 3.2). The hydrochemical, potentiometric, and geologic data from this investigation, however, suggest no significant hydrologic connection between the bolson deposits in the site area and the bolson deposits closer to the Rio Grande where it is used as a water supply.

HUDSPETH COUNTY--CONCLUSIONS

The Hudspeth County study area is underlain by bolson-fill sediments deposited on Cretaceous bedrock. The older bolson-fill deposits consist of a series of interbedded fine sands, silts, and clays. The younger bolson deposits contain coarser sediments, including conglomerates, whose upper surface has been eroded to form a pediment surface. The only absolute date on the bolson deposits, about 2

million yr. is from an ash bed near the base of the younger bolson fill. The total thickness of the bolson fill is variable due to the highly irregular surface of the Cretaceous bedrock but is about 400 ft (120 m) or more thick in the vicinity of the primary study area.

The bolson-fill sediments are cut by the Campo Grande fault. The Campo Grande fault is a high-angle normal fault that strikes northwesterly across the bolson-fill deposits to the south of the primary study area. Several meters of displacement are present in the older bolson fill, but the amount of displacement of the younger bolson deposits and the age of last movement along the fault are not known. The fault zone is a relatively discrete and easily mappable feature. Other faults are present in Cretaceous rocks exposed along the margin of the Diablo Plateau and in the outcrops of the Finlay Mountains area.

Conclusions on the hydrogeology of the Hudspeth County site are as follows:

(1) Three regional aquifers, located in the Cretaceous rocks, the bolson fill, and the Rio Grande alluvium, underlie the proposed site or its vicinity.

(2) The uppermost aquifer near the site area is the bolson fill, but at the site no water was encountered in its sediments while drilling the water well. However, within a few miles of the site area, water levels in the bolson fill vary from 90 to 360 ft (27 to 110 m) below land surface. In the site area, the uppermost aquifer is in the Cretaceous formations, 478 ft (145.7 m) below land surface.

(3) The flow direction of the water in the Cretaceous and bolson aquifers is to the southwest toward the Rio Grande valley. The Campo Grande fault may isolate aquifers beneath the site from aquifers in the Rio Grande valley. Flow

direction in the Rio Grande alluvium is along the valley and parallel to the river. Flow directions in the Rio Grande alluvium fluctuate depending on whether ground water or river water is being used for irrigation.

(4) The residence time of water in the Cretaceous aquifer varies from hundreds to thousands of years. The water in the bolson is old near the site area (8,000 to 15,000 yr) and modern (40 to 100 yr old) in the Rio Grande valley; the water in the Rio Grande alluvium is the current Rio Grande water.

(5) Recharge to the Cretaceous aquifer is from precipitation on the Cretaceous outcrop area. Presence of tritium in water of the Cretaceous aquifer beneath the bolson suggests mixing of young water with an older component of ground water. In the Rio Grande valley recharge to the Rio Grande alluvium and the bolson aquifers is through the Rio Grande. Recharge from the Cretaceous aquifer into the bolson fill in the vicinity of the site is a reasonable possibility based on the differences in potentiometric surfaces and on chemical and isotopic similarities. Based on the very low vertical permeability core values, vertical diffusion of rainwater into the bolson through the clays is extremely low. However, the presence of sand lenses and perhaps faults can result in shortcuts for vertical movement of water into the system.

(6) Water wells pump water from the Rio Grande alluvium, the bolson fill, and the Cretaceous aquifers in the site area and its vicinity. Hydraulic continuity probably exists between the bolson and the Rio Grande alluvium in the Rio Grande valley, and the alluvium water discharges into the river. The water in the Cretaceous aquifer probably does not discharge into the upper aquifers in the Rio Grande valley because of the Campo Grande fault. In the site area, chemical and isotopic similarities suggest that water in the Cretaceous discharges into the bolson fill.

ACKNOWLEDGMENTS

We would like to thank Wheeler Wilson, Josef W. Mussey, Joe Crawford, and John Peters of the Pennzoil Sulphur Mine in Culberson County for the valuable information regarding ground water and land subsidence at the mine area and for their help in ground-water sampling during this study. Kenneth Moore of the University Lands Office was a great help during the sampling of ground water in the Block 46 area in Culberson County. Many people and well owners in Hudspeth County provided information and help. However, we owe special thanks to Mr. and Mrs. Scott Wilkey for their help and care, Mr. and Mrs. Dennis Walker for information and equipment, Mr. E. Franklin for information about well locations and owners, and Mr. J. Galvan for help in locating wells.

Saleem M. Akhter of the Bureau of Economic Geology helped with data processing and drafting. Bernd Richter reviewed the report. Word processing was by Dorothy C. Johnson and Rosanne M. Wilson under the supervision of Lucille C. Harrell. Base maps were drafted by Richard L. Dillon. Figures were drafted by Nan Minchow-Newman, Don W. Thompson, and Marty Thompson, under the supervision of Richard L. Dillon. The report was edited by Mary Ellen Johansen. Funding for this study was provided by the Texas Low-level Radioactive Waste Disposal Authority under contract no. IAC(86-87)-0828.

REFERENCES

Adams, J. E., 1944, Upper Permian Ochoa series of the Delaware Basin, west Texas and southeastern New Mexico: American Association of Petroleum Geologists Bulletin, v. 28, no. 11, p. 1596-1625.

Albritton, C. C., Jr., and Smith, J. F., 1965, Geology of the Sierra Blanca area, Hudspeth County, Texas: U.S. Geological Survey Professional Paper 479, 131 p.

Allison, G. B., and Hughes, M. W., 1978, The use of environmental chloride and tritium to estimate total recharge to an unconfined aquifer: Australian Journal of Soil Research, v. 16, p. 181-195.

Allison, G. B., Stone, W. J., and Hughes, M. W., 1985: Recharge in karst and dune elements of semi-arid landscape as indicated by natural isotopes and chloride, Journal of Hydrology 76, p. 1-25.

Alvarez, H. J., and Buckner, A. W., 1980, Ground-water development in the El Paso region, Texas, with emphasis on the Lower El Paso Valley: Texas Department of Water Resources Report 246, 346 p.

Anderson, R. Y., Dean, W. E., Jr., Kirkland, D. W., and Snider, H. I., 1972, Permian Castile varved evaporite sequence, West Texas and New Mexico: Geological Society of America Bulletin, v. 83, p. 59-86.

Askew, Bonny, and Algermissen, S. T., 1983, An earthquake catalog for the Basin and Range province, 1803-1977: U.S. Geological Survey Open-File Report 83-86, 21 p.

Asquith, G. B., 1982, Basic well log analysis for geologists: Tulsa, Oklahoma, American Association of Petroleum Geologists, 210 p.

Bachman, G. O., and Machette, M. N., 1977, Calcic soils and calcretes in the southwestern United States: U.S. Geological Survey Open-File Report 77-794, 162 p.

Barnes, V. E., 1983, Van Horn - El Paso Sheet: The University of Texas at Austin, Bureau of Economic Geology, Geologic Atlas of Texas, scale 1:250,000.

Boersma, L., 1965, Field measurement of hydraulic conductivity above water table, in Black, L. A., ed., Methods of soil analysis: American Society of Agronomy, p. 222-234.

Bomar, G. W., 1983a, 1982--When a tornado hit Paris, a review of Texas' weather during the year: Texas Department of Water Resources Publication LP-195, 117 p.

_____ 1983b, Texas weather: Austin, University of Texas Press, 265 p.

Brown, J. B., Rogers, L. T., and Baker, B. B., 1973, Reconnaissance investigation of the ground water resources of the middle Rio Grande Basin, Texas: Texas Water Commission Bulletin 6502, p. M-1 - M-80.

Brune, G., 1981, The springs of Texas: Fort Worth, Branch-Smith, 566 p.

Carr, J. T., 1967, The climate and physiography of Texas: Texas Water Development Board Report 53, 27 p.

Craig, H., 1961, Isotopic variations in meteoric waters: Science, v. 133, p. 1702-1703.

Dames and Moore, 1985, Siting of a low-level radioactive waste disposal facility in Texas: Evaluation of State-owned lands, part III, appendix B.

Davis, M. E., and Leggat, E. R., 1973, Reconnaissance investigation of the ground water resources of the upper Rio Grande Basin, Texas: Texas Water Commission Bulletin 6502, p. U-1 - U-99.

Dumas, D. B., 1980, Seismicity in the Basin and Range province of Texas and northeastern Chihuahua, Mexico, in Dickerson, P. W., Hoffer, J. M., and Callender, J. F., eds., Trans-Pecos region, southeastern New Mexico and west Texas: New Mexico Geological Society 31st Annual Field Conference Guidebook, p. 77-81.

Gardner, J. S., and Dumanoir, J. L., 1980, Litho-density log interpretation: Society of Professional Well Log Analysts Transactions v. 21, p. I-1 - I-23.

Gates, J. S., and Stanley, W. D., 1976, Hydrologic interpretations of geophysical data from the southeastern Hueco Bolson, El Paso and Hudspeth Counties, Texas: U.S. Geological Survey Open-File Report 76-650, 37 p.

Gates, J. S., White, D. E., Stanley, W. D., and Ackermann, H. D., 1980, Availability of fresh and slightly saline ground water in the basins of westernmost Texas: Texas Department of Water Resources Report 256, 108 p.

Gile, L. H., Hawley, J. W., and Grossman, R. B., 1981, Soils and geomorphology in the Basin and Range area of southern New Mexico--guidebook to the Desert Project: New Mexico Bureau of Mines and Mineral Resources Memoir 39, 222 p.

Groat, C. G., 1972, Presidio Bolson, Trans-Pecos Texas and adjacent Mexico: geology of a desert basin aquifer system: The University of Texas at Austin, Bureau of Economic Geology Report of Investigations No. 76, 46 p.

Guyton, W. F., and Associates, 1971, Availability of brackish water from Mesa area of Hueco Bolson, El Paso County, Texas: report prepared for El Paso Electrical Company, El Paso, Texas, 26 p.

Henry, C. D., and Price, J. G., 1985, Summary of the tectonic development of Trans-Pecos Texas: The University of Texas at Austin, Bureau of Economic Geology Miscellaneous Map No. 36, 8 p.

Hoefs, J., 1973, Stable isotope geochemistry: New York, Springer-Verlag, 112 p.

Izett, G. A., and Wilcox, R. E., 1982, Map showing localities and inferred distributions of the Huckleberry Ridge, Mesa Falls, and Lava Creek ash beds (Pearlette family ash beds) of Pliocene and Pleistocene age in the western United States and southern Canada: U.S. Geological Survey Miscellaneous Investigations Series Map I-1325.

Kruseman, G. P., and De Ridder, N. A., 1976, Analysis and evaluation of pumping test data: International Institute for Land Reclamation and Improvement, Waglninger, The Netherlands, Bulletin 11 p. 160-169.

King, P. B., 1948, Geology of the southern Guadalupe Mountains, Texas: Washington, D.C., U.S. Department of the Interior, Geological Survey Professional Paper 215, 183 p.

_____ 1949, Regional geologic map of parts of Hudspeth and Culberson Counties, Texas: U.S. Geological Survey Oil and Gas Investigations Preliminary Map 90.

Larkin, T. J., and Bomar, G. W., 1983, Climatic atlas of Texas: Texas Department of Water Resources Publication LP-192, 151 p.

Leggat, E. R., 1962, Development of ground water in the El Paso district, Texas, 1955-1960, Progress Report 8: Texas Water Commission Bulletin 6204, 56 p.

Lodge, J. P., Jr., Pate, J. B., Basbergill, W., Swanson, G. S., Hill, K. C., Lorange, E., and Lazrus, A. L., 1968, Chemistry of United States precipitation, final report on the national precipitation sampling network: Boulder, National Center for Atmospheric Research, 66 p.

Mazor, E., in press, Tracing ground water by its chemical, physical and isotopic parameters, a practical approach to field data.

Miller, R. R., 1977, Composition and derivation of the native fish fauna of the Chihuahuan Desert region, in Wauer, R. H., and Riskind, D. H., eds., Transactions of the Symposium on the Biological Resources of the Chihuahuan Desert Region, United States and Mexico: Washington, D.C., U.S. Department of the Interior, National Park Service Transactions and Proceedings Series No. 3, p. 365-381.

Motsch, S. A., 1951, Culberson County, Texas: The University of Texas at Austin, Master's thesis, 51 p.

Muehlberger, W. R., Belcher, R. C., and Goetz, L. K., 1978, Quaternary faulting in Trans-Pecos Texas: Geology, v. 6, no. 6, p. 337-340.

National Climatic Data Center, 1985, Texas, 1984: Asheville, North Carolina, National Oceanic and Atmospheric Administration, Climatological Data Annual Summary, v. 89, no. 13, 78 p.

Obert, L., and Duvall, W. L., 1967, Rock mechanics and the design of structures in rock: New York, John Wiley, 650 p.

Olive, W. W., 1957, Solution-subsidence troughs, Castile Formation of Gypsum Plain, Texas and New Mexico: Geological Society of America Bulletin, v. 68, p. 351-358.

Orton, R. B., 1969, Climates of the states -- Texas: Washington, D.C., United States Department of Commerce, Environmental Data Center, Climatography of the United States No. 60-41, 46 p.

_____ 1964, The climate of Texas and adjacent Gulf waters: Washington, D.C., U.S. Department of Commerce, Weather Bureau, 195 p.

Pearson, F. J., Jr., and White, D. E., 1967, Carbon-14 ages and flow rates of water in Carrizo Sands, Atascosa County, Texas: Austin, Water Resources Research, v. 3, p. 251-261.

Porsch, E. L., Jr., 1917, The Rustler Springs sulphur deposits: University of Texas, Austin, Bulletin, 1722, 71 p.

Reagor, B. G., Stover, C. W., Algermissen, S. T., 1982, Seismicity map of the state of Texas: U.S. Geological Survey Miscellaneous Field Studies, map MF-1388, U.S. Geological Survey, Denver, Colorado.

Rightmire, C. T., 1967, A radioactive study of the age and origin of caliche deposits: The University of Texas at Austin, Master's thesis.

Sanford, A. R., and Toppozada, T. R., 1974, Seismicity of proposed radioactive waste disposal site in southeastern New Mexico: New Mexico Bureau of Mines and Mineral Resources Circular 143, 15 p.

Schlumberger, 1974, Log interpretation manual/application, v. II: Houston, Schlumberger Well Services, Inc.

_____ 1984, Log interpretation charts: Houston, Schlumberger Well Services, Inc., 106 p.

Smith, A. R., 1980, Sulfur deposits in Ochoan rocks of the Gypsum Plain, southeast New Mexico and West Texas, in Dickerson, P. W., and Hoffer, J. M., eds., Trans-Pecos region, southeastern New Mexico and West Texas: New Mexico Geological Society 31st Field Conference Guidebook, p. 277-283.

Snyder, R. P., and Gard, L. M., Jr., 1982, Evaluation of breccia pipes in southeastern New Mexico and their relation to the waste isolation pilot plant (WIPP) site: U.S. Geological Survey Open File Report 82-968.

Stone, W. J., 1985, Recharge through calcrete, in Hydrogeology of rocks of low permeability: IAH conference, Tucson, Arizona, Memoires.

Strain, W. S., 1966, Blancan mammalian fauna and Pleistocene formations, Hudspeth County, Texas: Texas Memorial Museum Bulletin No. 10, 55 p.

Thornthwaite, C. W., 1931, The climates of North America according to a new classification: Geographical Review, v. 21, p. 633-655.

U.S. Department of Housing and Urban Development, Federal Insurance Administration, 1985, Flood hazard boundary maps, Hudspeth County, Texas Community Panel Nos. 480361 0650B, 480361 0800B.

Vogel, J. C., 1970, ^{14}C dating of ground water, in Isotope hydrology: Vienna, IAEA, p. 225-239.

Appendix 1. Records of wells and springs in Culberson and Hudspeth sites (ft).

ID1	ID2	Coordinates		Ground-level altitude	Water-level depth	Water-level altitude	Total depth	Perforated interval
CULBERSON								
Wells: S-15 Area								
LL100	Kohen Windmill	31°40'12"	104°10'50"	3331	75	3256	80	
LL101	Smilin Jack Windmill	31°40'23"	104°12'22"	3480	70	3410	140	
LL104	Monument Windmill	31°38'13"	104°10'52"	3455	150	3305	200	
LL119	S-15 W. Windmill	31°39'10"	104°19'02"	3712				
LL120	Philips Windmill	31°40'06"	104°14'41"	3575				
LL121	S-15 N. Windmill	31°43'55"	104°14'59"	3560				
LL001	S-15 Scott Windmill	31°41'44"	104°09'48"	3348	115	3233	200	
LL002	S-15 South Windmill	31°40'04"	104°08'09"	3310	58	3252	110	
Wells: S-46 Area								
LL123	S-46 Seven L. Windmill	31°44'53"	104°28'18"	4055	20	4035		
LL124	S-46 High L. Windmill	31°42'46"	104°27'46"	4265				
LL125	S-46 Cave Well	31°40'03"	104°26'23"	4108	30	4078		
Springs: S-15 area								
LL102	Rustler Spring	31°38'42"	104°13'33"	3493		3493		
LL117	S-15 W. Sp	31°41'13"	104°17'33"	3780		3780		
LL118	S-15 S. Sp	31°38'43"	104°17'25"	3680		3680		
LL122	S-15 N. WM Sp	31°44'57"	104°15'19"	3572		3572		
LL400	Spring	31°50'43"	104°14'54"	3525		3525		
LL401	Toy Springs	31°49'16"	104°09'25"	3280		3280		
LL402	Springs	31°49'10"	104°10'37"	3355		3355		
LL403	Cotton Wood Sp	31°48'26"	104°11'50"	3445		3445		
LL404	Spring	31°45'48"	104°12'37"	3460		3460		
LL405	Springs	31°44'55"	104°12'38"	3485		3485		
LL406	Springs Well	31°44'42"	104°13'07"	3485		3485		
LL407	Horseshoe Spring	31°44'20"	104°09'52"	3275		3275		
LL408	Spring	31°46'30"	104°16'10"	3600		3600		
LL409	Spring	31°45'10"	104°18'23"	3700		3700		
LL413	Springs	31°39'33"	104°12'46"	3415		3415		
Springs: S-46 Area								
LL412	Burro Spring	31°46'41"	104°28'37"	4006		4006		
LL414	Spring	31°41'20"	104°26'06"	4130		4130		
LL415	Spring	31°39'26"	104°20'38"	3720		3720		

Appendix 1. (cont.)

ID1	ID2	Coordinates		Ground-level altitude	Water-level depth	Water-level altitude	Total depth	Perforated interval
HUDSPETH								
Wells:								
LL107	48-42-1 Windmill	31°22'12"	105°50'52"	3355	335	3550	450	
LL108	48-42-404 Well	31°18'56"	105°51'27"	3610	90	3530	267	146-267
LL109	48-41-618 Well	31°17'31"	105°52'45"	3523	10	3513	305	45-305
LL110	48-41-2 Well	31°19'37"	105°54'55"	3545	8	3536	160	40-160
LL111	48-33-9 Windmill	31°23'18"	105°53'18"	3882	327	3555	367	300-340
LL112	Head of Canyon WM	31°31'42"	105°42'05"	5059	380	4679	720	
LL113	Wilkey Well no. 1	31°23'23"	105°40'48"	4307	600	3707	730	700-735
LL114	Wilkey Well no. 2	31°22'48"	105°39'07"	4346	76	4270	200	
LL115	Gunsight Windmill no. 2	31°25'03"	105°30'20"	4780	405	4375	480	
LL116	Owens Well	31°22'31"	105°45'50"	4014	120	3894	300	
LL126	Low Level Well	31°24'14"	105°43'32"	4179	478	3699	530	
LL127	Gunsight Windmill no. 1	31°25'03"	105°30'20"	5154	627	4527	690	
Springs:								
LL105	Rio Grande Water	31°16'23"	105°51'14"					
LL106	Thaxton Sp	31°28'11"	105°42'57"	4500		4500		

Appendix 2. Chemical and isotopic composition of ground-water samples.

Culberson County site: Major ions (mg/l) and temperatures (°C).

ID1	ID2	Coordinates		Ca^{2+}	Mg^{2+}	Na^{+}	K^{+}	HCO_3^{-}	SO_4^{2-}	Cl^{-}	NO_3^{-}	TDS	Temp.
Wells: S-15 Area													
LL100	Kohen Windmill	31°40'12"	104°10'50"	517	229.0	367.0	16.2	223	2310	283	36.1	3993.9	17.6
LL101	Smilin Jack Windmill	31°40'23"	104°12'22"	587	83.3	38.0	7.3	121	1650	50	79.7	2627.7	19.0
LL104	Monument Windmill	31°38'13"	104°10'52"	277	115.0	45.0	3.2	258	900	40	10.3	1655.8	21.0
LL119	S-15 W. Windmill	31°39'10"	104°19'02"	577	120.0	227.0	21.0	114	2040	190	22.6	3322.7	18.0
LL120	Phillips Windmill	31°40'06"	104°14'41"	614	34.0	47.9	4.6	84	1590	31	60.0	2476.0	19.0
LL121	S-15 N. Windmill	31°43'55"	104°14'59"	600	107.0	218.0	4.5	160	1900	221	35.5	3256.8	20.0
Wells: S-46 area													
LL123	S-46 Seven L. Windmill	31°44'53"	104°28'18"	618	72.2	70.4	7.3	190	1680	73	<0.5	2724.4	17.0
LL124	S-46 High L. Windmill	31°42'46"	104°27'46"	634	25.8	68.4	10.2	201	1480	74	39.6	2539.9	18.0
LL125	S-46 Cave Well	31°40'03"	104°26'23"	676	55.9	73.2	13.0	320	1540	104	104.0	2898.9	
Springs: S-15 Area													
LL102	Rustler Spring	31°38'42"	104°13'33"	595	49.8	68.7	6.7	133	1580	70	22.1	2534.2	14.9
LL117	S-15 W. Sp	31°41'13"	104°17'33"	634	25.6	34.0	5.3	151	1500	34	26.5	2419.2	11.0
LL118	S-15 S. Sp	31°38'43"	104°17'25"	714	12.3	11.5	16.6	448	1490	13	<0.5	1203.0	14.0
LL122	S-15 N. Windmill Sp	31°44'57"	104°15'19"	620	50.6	163.0	7.4	126	1730	127	44.6	2879.7	13.0

Culberson County site: Trace ions (mg/l) and isotope composition[1] in ground-water samples.

ID1	ID2	Coordinates		As^{3+}	Cd^{2+}	Li^{+}	Fe^{2+}	Sr^{2+}	Ba^{2+}	Br^{-}	F^{-}	$\delta^{18}O$	$\delta^{2}H$	Tritium	$\delta^{34}S$	$\delta^{13}C$	PMC[2]	^{14}C Age[3]
Wells: S-15 Area																		
LL100	Kohen Windmill	31°40'12"	104°10'50"	<0.010	<0.03	0.10	0.02	9.79	0.01	1.17	1.50	-7.1	-47	13.7	+9.3			
LL101	Smilin Jack Windmill	31°40'23"	104°12'22"	<0.010	<0.03	0.05	0.24	9.78	0.01	0.18	1.05	-6.1	-42	12.0	+9.9			
LL104	Monument Windmill	31°38'13"	104°10'52"	<0.010	<0.03	0.04	0.07	4.65	0.02	0.22	2.37	-6.7	-43	6.3	+5.8			
LL119	S-15 W. Windmill	31°39'10"	104°19'02"	<0.010	<0.03	0.07	0.02	9.15	0.02	0.72	1.10	-6.7	-51	9.84	+9.4	-14.4	82	314
LL120	Phillips Windmill	31°40'06"	104°14'41"	<0.010	<0.03	0.03	0.04	9.35	0.01	0.24	0.80	-6.7	-51	8.67	+9.6	-17.0		
LL121	S-15 N. Windmill	31°43'55"	104°14'59"	<0.010	<0.03	0.06	0.07	8.27	0.01	1.10	1.30	-7.2	-54	13.46	+9.8	-18.0	90	1358

Appendix 2. (cont.)

Culberson County site (cont.)

ID1	ID2	Coordinates		As^{3+}	Cd^{2+}	Li^{+}	Fe^{2+}	Sr^{2+}	Ba^{2+}	Br^{-}	F^{-}	$\delta^{18}O$	$\delta^{2}H$	Tritium	$\delta^{34}S$	$\delta^{13}C$	PMC^{2}	^{14}C Age[3]
Wells: S-46 Area																		
LL123	S-46 Seven L. WM	31°44'53"	104°28'18"	<0.010	<0.03	0.04	1.09	9.90	0.03	0.53	1.40	-7.4	-53	28.04	+11.5	-19.5	56	5906
LL124	S-46 High L. WM	31°42'46"	104°27'46"	<0.010	<0.03	0.03	0.04	5.86	0.03	0.33	0.60	-5.8	-40	11.35	+10.5	-12.0		Modern
LL125	S-46 Cave W.	31°40'03"	104°26'23"	<0.010	<0.03	0.05	0.07	11.00	0.03	0.66	0.90	-6.5	-50	21.78	+11.3	-18.8	110	Modern
Springs: S-15 Area																		
LL102	Rustler Sp	31°38'42"	104°13'33"	<0.010	<0.03	0.04	0.03	11.20	0.01	0.22	1.45	-6.6	-48	6.7	+9.9			
LL117	S-15 W. Sp	31°41'13"	104°17'33"	<0.010	<0.03	0.09	<0.02	7.62	0.02	0.23	0.70	-6.9	-51	15.76	+9.9			
LL118	S-15 S. Sp	31°38'43"	104°17'25"	<0.010	<0.03	0.03	0.07	4.16	0.07	0.19	0.30	-6.3	-48	13.16	+17.2			
LL122	S-15 N. Windmill Sp	31°44'57"	104°15'19"	<0.010	<0.03	0.04	0.02	9.22	0.01	0.74	1.10	-6.7	-56	16.33	+9.9			

Hudspeth County site: Major ions (mg/l) and temperatures (°C).

ID1	ID2	Coordinates		Ca^{2+}	Mg^{2+}	Na^{+}	K^{+}	HCO_3^{-}	SO_4^{2-}	Cl^{-}	NO_3^{-}	TDS	Temp.
LL107	48-42-1 Windmill	31°22'12"	105°50'52"	169.0	35.3	1250	7.7	161	2270	520	1.3	4421.6	24.5
LL108	48-42-404 Well	31°18'56"	105°51'27"	34.7	11.9	410	4.5	263	395	259	5.1	1388.1	22.5
LL109	48-41-618 Well	31°17'31"	105°52'45"	23.8	23.9	486	14.6	96	315	555	<0.5	1517.5	
LL110	48-41-2 Well	31°19'37"	105°54'55"	387.0	91.7	881	12.8	495	770	1450	<0.5	3604.1	19.0
LL111	48-33-9 Windmill	31°23'18"	105°53'18"	26.8	10.5	327	4.2	242	360	168	11.4	1154.4	21.0
LL112	Head of Canyon WM	31°31'42"	105°42'05"	61.6	19.3	177	5.4	282	168	116	26.5	861.7	14.0
LL113	Wilkey Well no. 1	31°23'23"	105°40'48"	77.1	43.1	237	3.4	336	438	88	11.8	1241.5	20.0
LL114	Wilkey Well no. 2	31°22'48"	105°39'07"	131.0	24.6	55	1.5	284	275	10	11.3	801.4	11.0
LL115	Gunsight Windmill no. 1	31°25'03"	105°30'20"	37.3	22.1	454	7.4	411	570	137	<0.5	1649.2	19.0
LL116	Owens Well	31°22'31"	105°45'50"	48.4	15.3	362	3.5	278	525	128	<0.5	1369.4	14.0
LL126	Low Level Well	31°24'14"	105°43'32"	70.7	6.9	549	4.4	60	710	416	18.3	1850.	17.0
Springs:													
LL105	Rio Grande Water	31°16'23"	105°51'14"	86.9	18.5	186	7.8	214	234	185	6.6	941.9	11.0
LL106	Thaxton Sp	31°28'11"	105°42'57"	26.8	22.9	475	4.6	501	520	148	11.3	1718.3	9.0

Appendix 2. (cont.)

Hudspeth County site: Trace ions (mg/l) and isotope composition[1] in ground-water samples.

ID1	ID2	Coordinates		As^{3+}	Cd^{2+}	Li^{+}	Fe^{2+}	Sr^{2+}	Ba^{2+}	Br^{-}	F^{-}	$\delta^{18}O$	$\delta^{2}H$	Tritium	$\delta^{34}S$	$\delta^{13}C$	PMC[2]	^{14}C Age[3]
LL107	48-42-1 Windmill	31°22'12"	105°50'52"	0.012	<0.03	0.26	0.04	3.20	0.02	2.66	1.05	-8.0	-59	<0.8	+1.0	-16.8	16.6	14,748
LL108	48-42-404 Well	31°18'56"	105°51'27"	0.017	<0.03	0.10	0.05	1.01	0.04	1.25	2.37	-6.9	-48	<0.8	+3.8	-9.6	61	Modern
LL109	48-41-618 Well	31°17'31"	105°52'45"	<0.010	<0.03	0.21	0.02	1.43	0.01	0.59	0.39	-7.4	-71	27.2	+16.9			
LL110	48-41-2 Well	31°19'37"	105°54'55"	<0.010	<0.03	0.26	1.35	6.69	0.06	2.27	0.61	-8.8	-74	21.8	+4.7	-12.0	116	Modern
LL111	48-33-9 Windmill	31°23'18"	105°53'18"	<0.010	<0.03	0.10	0.49	0.81	0.02	1.01	2.03	-7.3	-51	<0.8	+7.2	-10.1	21.8	8,288
LL112	Head of Canyon Windmill	31°31'42"	105°42'05"	<0.010	<0.03	0.06	0.10	1.72	0.02	1.14	2.79	-7.1	-50	11.8	+5.8	-8.0	43	833
LL113	Wilkey Well no. 1	31°23'23"	105°40'48"	<0.010	<0.03	0.05	0.71	3.90	0.03	0.77	1.60	-7.7	-58	3.74	+5.2	-9.4	36	3,529
LL114	Wilkey Well no. 2	31°22'48"	105°39'07"	<0.010	<0.03	0.03	<0.02	7.50	0.03	0.44	0.90	-7.5	-54	20.67	+10.9	-11.3	60	868
LL115	Gunsight Windmill no. 1	31°25'03"	105°30'20"	<0.010	<0.03	0.12	2.15	3.32	0.03	1.15	3.10	-10.7	-83	0.5	-0.5	-7.9	9.6	13,071
LL116	Owens Well	31°22'31"	105°45'50"	<0.010	<0.03	0.07	0.20	2.87	0.12	1.10	4.30	-8.0	-62	1.52	+7.0	-7.8	8.9	13,520
LL126	Low Level well	31°24'14"	105°43'32"	<0.050	<0.03	0.10	0.13	8.30	0.19	2.10	4.30	-8.3	-61	no data[4]	+4.1	-18.1	3.3	27,400
Springs:																		
LL105	Rio Gr. Water	31°16'23"	105°51'14"	<0.010	<0.03	0.11	0.69	1.36	0.06	0.22	0.66	-9.1	-69	24.4	+1.1			
LL106	Thaxton Sp	31°28'11"	105°42'57"	<0.010	<0.03	0.13	0.02	1.63	0.02	1.34	5.57	-7.5	-58	<0.8	-1.8			

1) $\delta^{18}O$ and $\delta^{2}H$ defined relative to SMOW. $\delta^{34}S$ is given as deviation from the Canyon Diablo Meteorite standard. $\delta^{13}C$ defined relative to Pee Dee Belemnite carbonate.
2) PMC is percent of modern carbon
3) ^{14}C age was corrected by using $\delta^{13}C$ values (app. 5) except for sample LL126
4) Tritium data for the Low Level well were not available by the time this report was submitted. Data will be provided in an addendum.

Appendix 3. Application of isotope techniques to hydrology.

Stable Hydrogen and Oxygen Isotopes (modified from Mazor, in press)

Two oxygen isotopes are commonly measured in water samples, ^{16}O and ^{18}O. The concentration of the heavy and rare ^{18}O is expressed as percent deviation from an international standard (Standard Mean Ocean Water [SMOW]). Similarly, two stable hydrogen isotopes are measured: a light one, ^{1}H, and a heavy, rare one, ^{2}H. These ^{18}O and ^{2}H concentrations are commonly written as $\delta^{18}O$ °/oo and $\delta^{2}H$ °/oo, respectively, as an expression of their relative abundance in °/oo deviation from the named SMOW standard. Craig (1961) published a $\delta^{2}H$ - $\delta^{18}O$ diagram based on about 400 water samples from rivers, lakes, and precipitation in various countries. These data follow a best-fit line of $\delta^{2}H = 8\delta^{18}O + 10$ called the meteoric water line. Isotope data from all over the world fall on this line. The meteoric water line is very convenient as a reference for the understanding and tracing of local ground-water origins and movement. Commonly, ground-water data are plotted on a $\delta^{2}H$ - $\delta^{18}O$ diagram, with the meteoric line of local precipitation as a reference. Large isotopic deviations from present meteoric water isotopic composition indicate that ground water was recharged under different climatic conditions and therefore may indicate ancient water. Other deviations from the meteoric line occur when precipitation partly evaporates before reaching the water table. Water molecules with light hydrogen and oxygen, $^{1}H_{2}{}^{16}O$, are more volatile and upon evaporation pass more efficiently from the liquid to the vapor phase. As a result, the residual evaporating water gets relatively enriched with the heavier and less mobile

molecules. Enriched ground water may indicate evaporation that the rain and/or surface water go through before infiltration occurs (and therefore may indicate low permeability of the soil cover) or evaporation of ground water directly from a shallow water table. In deep aquifers, it may also indicate the equilibrium state between ground water and the host rock.

Tritium (modified from Mazor, in press)

Hydrogen has a radioactive isotope, ^{3}H, called tritium in addition to its stable isotopes, ^{1}H and ^{2}H. Cosmic rays that interact with the upper part of the atmosphere produce secondary neutrons that interact with nitrogen, producing tritium. Tritium is formed constantly, oxidized to water, $^{1}H^{3}HO$, and washed down by rains. The half-life of tritium is 12.43 yr. The concentration of tritium in water is expressed by the ratio of tritium atoms to ^{1}H atoms. A ratio of $^{3}H/^{1}H=10^{-18}$ is defined as one tritium unit (TU). The natural tritium abundance was completely masked by the hydrogen bomb tests that began in 1952 in the northern hemisphere because large concentrations of tritium were added to the atmosphere, reaching a peak in 1963 with up to 10,000 TU in a single monthly rain sample in the U.S. When the anthropogenic tritium was noticed, it was hoped that the specific tritium pulses contributed by the individual tests would provide a means of accurate dating of ground water; however, the input values in precipitation varied greatly from one location to another and from one season and year to the next in each place. Semiquantitative dating, however, is possible and very informative:

(a) Ground water with less than the amount of natural tritium left after decay indicates all or a major part is pre-1952, i.e., several decades old. The

statement "all or a major part" refers to the possibility of old water with 0 TU being mixed with a small amount of post-1952 water.

(b) Ground water with 0 TU is all pre-1952, i.e., several decades or more old.

(c) Ground water with elevated tritium values indicates that all or a major part is post-1952.

Tritium in ground water may be compared with the local tritium-precipitation curve to find its age range.

Radioactive Carbon, ^{14}C (modified from Mazor, in press)

Carbon has three isotopes in nature:

^{12}C - common, stable

^{13}C - rare, stable

^{14}C - very rare, radioactive, 5,730-year half-life.

^{14}C is formed in the upper parts of the atmosphere by secondary neutrons interacting with common nitrogen. ^{14}C decays radioactively into ^{14}N. The ^{14}C is oxidized upon production to CO_2 and then mixed into the large atmospheric CO_2 reservoir. The concentration of ^{14}C is expressed relative to $^{14}C/^{12}C$ in an international standard (oxalic acid). The ^{14}C concentration in the bulk carbon of the standard is defined as 100 Percent Modern Carbon (PMC).

Large amounts of fossil fuels are continuously combusted, so far causing an increase of about 10% in the concentration of atmospheric CO_2. This added fossil CO_2 is devoid of ^{14}C and correspondingly lowers the $^{14}C/^{12}C$ ratio in the air. The nuclear bomb test introduced ^{14}C into the atmosphere, similarly to the increase of tritium, but the elevated values have decreased since, and present values are around 140 PMC. Rain and water dissolve small amounts of CO_2. Significantly more CO_2 is added to water percolating through the soil layer

because soil-air contains around 100 times more CO_2 compared with free air owing to biological action in the soil zone. This CO_2 is tagged by the atmospheric ^{14}C concentrations, i.e., around 100 PMC in pre-nuclear-bomb test years and up to 140 and even 160 PMC in post-bomb test years. Once water reaches the saturated zone it is isolated from the atmosphere and its ^{14}C decays with a half-life of 5,730 years. Thus, ^{14}C can serve as an age indicator of rain and surface water that reached the water table up to 30,000 to 40,000 yr ago. Interactions of ground water with carbonate rocks that form the aquifer or that are on the way to the aquifer (such as caliche layers) can add "dead" CO_2 (i.e., devoid of ^{14}C) to ground water. Limestone and dolomite contain no ^{14}C because they were formed a long time ago compared with the ^{14}C half-life. Recharged CO_2 containing water reacts with the carbonates to form dissolved bicarbonate:

$$\underset{}{H_2O} + \underset{\uparrow}{CO_2} + \underset{\uparrow}{CaCO_3} \longrightarrow Ca^{2+} + \underset{\uparrow}{2HCO_3^-}$$

100 PMC 0 PMC 50 PMC

Thus the dissolved CO_2 with 100 PMC reacts with the rock with 0 PMC to produce a 50 PMC bicarbonate.

The abundance of ^{13}C in rocks, organic material, or ground water is expressed in $^{o}/oo$ deviation of the $^{13}C/^{12}C$ ratio in the sample that is a standard (PDB, a Belemnite carbonate from the Pee Dee Formation of South Carolina). Most marine carbonate rocks have $\delta^{13}C=0$ $^{o}/oo$, whereas frequent values for organic material and CO_2 in soil are -25 $^{o}/oo$ to -20 $^{o}/oo$. The concentration of $\delta^{13}C$ in ground water is determined by the input with recharged water and by reactions with rocks. For example, the reaction of water charged with CO_2 of $\delta^{13}C=-25$ $^{o}/oo$ with marine carbonate rock of $\delta^{13}C=0$ $^{o}/oo$ is:

$$H_2O + CO_2 + CaCO_3 \longrightarrow Ca^{2+} + 2HCO_3^-$$
$$\delta^{13}C=-25^{o}/oo \quad \delta^{13}C=0^{o}/oo \quad \delta^{13}C=12.5^{o}/oo$$

whereas in reactions with silicates the original (organic) $\delta^{13}C$ is retained because no carbon is contributed from silicate dissolution. It has been suggested that $\delta^{13}C$ values may be applied to evaluate the extent to which ^{14}C in ground water is altered by reaction with the aquifer matrix. Three values are needed: (a) the $\delta^{13}C$ value of local soil material, representing the initial composition of ground water prior to the reaction with rocks, (b) the $\delta^{13}C$ value of the local aquifer rocks, and (c) the $\delta^{13}C$ value of the studied ground water. This correction technique has been applied in this study as explained in appendix 5.

The main importance of carbon-14 isotopes in hydrologic studies is to determine relative ages; leading to aquifer flow velocities; to check the continuity of proposed regional aquifers; and to study mixing of ground water from different sources. Because of the complexities of the ^{14}C and its interactions with the aquifer minerals, ^{14}C ages represent approximations.

^{34}S (modified from Hoefs, 1973)

Sulfur has four stable isotopes with the following abundance:

^{32}S: 95.02 $^{o}/oo$

^{33}S: 0.75 $^{o}/oo$

^{34}S: 4.21 $^{o}/oo$

^{36}S: 0.02 $^{o}/oo$

The reference standard commonly used is sulfur from troilite of the Canyon Diablo iron meteorite with a $^{32}S/^{34}S$ ratio of 22.22. Variations in concentrations of sulfur isotopes have been observed. The "heaviest" sulfates show $\delta^{34}S$ values

reactions produce sulfur variations:

1) a kinetic effect during the bacterial reduction of sulfate to isotopically "light" H_2S, which gives by far the largest fractionations in the sulfur cycle and

2) various chemical exchange reactions, e.g., between sulfate and sulfides on the one hand and between the sulfides themselves on the other. In this mechanism, sulfides are being depleted in $\delta^{34}S$ by amounts up to 75% relative to sulfates.

Ground water flowing in marine rocks may reach chemical and isotopic equilibrium with the host rocks. $\delta^{34}S$ of sulfates in marine rocks has not remained constant during the geologic past. The general trends of evaporite $\delta^{34}S$ evolution are: high del-values (+20 to +30 $^{o}/oo$) in the early Paleozoic, decreasing to +11 $^{o}/oo$ in Permian time, rapidly increasing in the early Mesozoic, and later on slightly oscillating around the present value of +20 $^{o}/oo$. The trend of del-values of sulfate evolution in the world's oceans is so consistent, especially the very narrow range of Permian del-values, it has been successfully used to determine the age of unknown salt deposits and the origin of sulfate-containing formation water.

The $\delta^{34}S$ of ground-water sulfate may indicate whether SO_4 originated as sulfides or sulfates, and possibly the age of the formations through which ground water passed.

Appendix 4. Karst features of the Gypsum Plain.

Karst landforms and landforms possibly indicative of ancient karst processes are common throughout both of the potential low-level radioactive waste sites in Culberson County. These features include, from smallest to largest, karren, swallow holes, collapse sinks, dolines, blind valleys, and subsidence basins. A landform resulting from karst processes, but not a true karst feature, is the castile. Trough-like features in the western part of the study area also have been attributed to solution and subsidence (Olive, 1957).

Karren

Karren are small solution channels formed on fracture surfaces in gypsum and other soluble rocks and they occur in many parts of the study area where gypsum of the Permian Castile Formation is exposed. The channels commonly exceed 1 cm in width and are separated by a knifelike ridge. Karren are oriented parallel to the slope of the exposed bedrock surface; they formed as surface waters infiltrated the gypsum and moved downward through fractures or across exposed surfaces. The presence of karren on fracture surfaces indicates that the process of dissolution of gypsum and solution widening of joints has occurred.

Sinkholes

The three types of sinkholes that occur in the study area are dolines, collapse sinks, and swallow holes (fig. 4). Sinkholes result from the collapse or subsidence of sediments overlaying subsurface solution channels. Dolines are a special form of sinkhole that result either from surface solution beneath a soil mantle or from

subsidence of an area over caverns. They are broad, closed, surface depressions that show no evidence of abrupt collapse. Collapse sinkholes, on the other hand, are generally steep-sided and floored with rocky debris resulting from the collapse of the roof of a cavern. Another special form of sinkhole is the swallow hole. Swallow holes occur in stream valleys and mark the point where the discharge carried in the stream valley moves underground.

Several hundred sinkholes have been mapped from aerial photographs of the study area, and collapse sinkholes are far more common than dolines. It is likely that many additional sinkholes exist in the area, but they have not been recognized on the aerial photographs because of their small size.

The largest collapse sinkhole recognized in the area is more than 820 ft (250 m) long. The presence of numerous sinkholes indicates that an extensive system of caverns is present in the subsurface. Large collapse sinkholes suggest the former presence of large cavern rooms.

Blind Valleys

Blind valleys occur where the surface drainage carried by a stream is diverted underground through a swallow hole. Surface runoff and erosion produce valley incision, but where valley incision ends at a swallow hole a blind valley results. Blind valleys are common in the terrain underlain by the Castile Formation, and some of the larger blind valleys and associated sinkholes are shown in figure 4. The largest blind valley in the study area is nearly 1.2 mi (2 km) long.

Subsidence Basins

Subsidence basins, unlike sinkholes, are interpreted to have resulted from dissolution of soluble rocks over a large region. Two types of regional subsidence basins have been recognized: basins with extensive alluvial fill and basins with no appreciable alluvial fill.

The alluvium-filled subsidence basins illustrated in figure 4 are distinguished from other areas containing Quaternary alluvium by their low slope and unusually broad valley development. Drainage from these features is restricted and in some cases they are internally drained. The three larger subsidence basins are oriented east-west and are bounded on either the north or south by abrupt erosional escarpments. The floors of these features are heavily vegetated, and the alluvial fill is dark, suggesting a soil with a significant organic content. This is in contrast to the stark-white gypsite that mantles much of the Castile Formation that surrounds the basins. Alluvial fans have formed locally along the margins of the basins. Sinkholes are uncommon in the subsidence basins. Field observations and interpretations of aerial photographs indicate that these areas resulted from the gradual alluviation of broad basins. Basin shape, restricted or internal drainage, and the presence of numerous karst landforms in areas surrounding the basins suggest that these features resulted from solution of soluble rocks and subsidence of overlying strata.

A second type of subsidence basin with no evidence of alluvial filling consists of numerous small, irregularly shaped, closed depressions (fig. 4). The depressions are separated by irregular low ridges, and the entire group of ridges and depressions lies in a closed topographic basin. These features may become alluvium-filled subsidence basins if a source of alluvium is available.

Castiles

Numerous small, typically conical hills are present throughout the Gypsum Plain. Those that developed strictly within the Castile Formation are typically capped by a resistant carbonate mass either formed by secondary processes or occurring as erosional remnants of limestone-rich portions of the Castile Formation. Other hills, commonly developed in the upper Castile Formation near the eastern margin of the Gypsum Plain, are not true castiles because they contain exotic lithologies from units overlying the Castile Formation, particularly the Salado and Rustler Formations. These hills are capped by erosionally resistant sedimentary rocks, mostly Permian sandstones, limestones, and dolomites or siliceous gravels of unknown age. In some places the erosionally resistant material only partially caps the hills or castiles and provides only a partial measure of protection from the processes of erosion.

Well-exposed castiles were examined in the eastern half of Block 46 and along U.S. Highway 652 approximately 6 mi (10 km) west of Texas Highway FM 2185. All are capped by resistant bodies of carbonate, but the origins of the carbonate may be diverse and are open to interpretation. Textures within the carbonate vary from clearly secondary to apparently primary and from nearly massive to well bedded to brecciated. The castiles along U.S. 652 are capped by a very well bedded but highly brecciated rock that appears to be a limestone-rich unit within the Castile Formation. The brecciation is interpreted to be the result of downward collapse into the throat of a sinkhole, with each castile in this cluster of hills apparently representing an individual sinkhole. Evidence of collapse is not as apparent in the castiles examined in Block 46. Some appear to have clearly secondary or replacement carbonate present, although the degree to which these processes have occurred may be variable and is open to further study. Many of

the hills shown in figure 2 were recognized from aerial photographs and are interpreted to be castiles, although their origin has not been determined. Where collapse chimneys have been recognized, these features are identified in figure 4.

Troughs

A series of ridges oriented approximately N 85 E is located in the western Gypsum Plain within the outcrop area of the Castile Formation (King, 1949). Commonly, these ridges occur in pairs and bound a trough (fig. 4). The western ends of the pairs of ridges are open, and in several cases the eastern ends of the pairs of ridges converge to a blunt, rounded ridge. The trough between the ridges is usually topographically lower than the terrain beyond the ridges. These landforms range up to 9 mi (15 km) in length and up to 0.6 mi (1 km) from ridge crest to ridge crest. The ridges are underlain by gypsite or by disturbed and weathered bedded gypsum. Thin alluvium, gypsite, or relatively unweathered gypsum usually underlies the trough. The troughs and bounding ridges are at a high angle to the northeast-striking faults that occur near the western ends of these features. Olive (1957) suggested that these "solution-subsidence troughs" resulted from subsidence following solution of gypsum along joints in the Permian Castile Formation.

In one area, where a deeply incised stream channel cuts across a trough and its associated pair of ridges, only a few joints parallel to the trend of the trough were observed in exposures of bedrock along the stream. The incised stream channel is nearly normal to the orientation of the trough, and the stream follows joints nearly normal to the trend of the trough. There is no evidence of collapse or of significant dissolution of gypsum in the beds exposed beneath the ridges or in the intervening trough.

From the interpretation of aerial photographs, sinkholes are known to occur in troughs, but the concentrations of sinkholes in troughs are no higher than in areas outside of troughs. Evidence in the literature (Olive, 1957) that pertains to the possible formation processes of these features is apparently contradictory to field observations made during this study. Although these features are an important aspect of the landscape of the study area, their origin cannot be determined from available data.

Distribution of Sinkholes

The widespread occurrence of sinkholes suggests that much of the area is underlain by a system or systems of caverns. Sinkholes are distributed throughout much of the study area without any recognizable relationship to fracture systems or other structural features. Locally, however, groups of sinkholes appear to occur preferentially along the northeasterly extensions of northeast-striking normal faults exposed in the western part of the study area. In certain cases, castiles and subsidence basins are associated with aligned groups of sinkholes. The aligned groups of sinkholes occur preferentially on the upthrown side of the faults. Small flexures or monoclines are commonly associated with these northeast-striking normal faults. The flexures were most often recognized on the upthrown side of the faults. Development of the flexures parallel to and on the upthrown side of the faults apparently allowed fractures parallel to the faults to open. Solution of gypsum along these fractures and later collapse or subsidence of overlying strata resulted in the formation of subsidence basins, castiles, and sinkholes.

Surface Drainage of the Gypsum Plain

The surface drainage of the study region is intermittent and has formed a karst-deranged pattern (fig. 4). Sinkholes, swallow holes, sinking streams, and blind valleys constitute the karst drainage system. The remainder of the area is characterized by a deranged pattern of larger streams flowing into and out of alluvial and subsidence basins. These streams and the alluvial basins also have numerous short tributaries. Deranged drainage patterns indicate that insufficient time has passed for an integrated drainage to develop. The lack of an integrated drainage system suggests also that the surface of the study region is not stable and is changing as dissolution-induced subsidence continues.

Structural and topographic control of segments of streams has been recognized both in the field and from interpretation of aerial photographs. First- and second-order stream segments locally parallel or follow joints. In some places joint sets apparently weaken the rocks, and these rocks are preferentially eroded. In other areas joints widened by solution have been occupied by streams. Many drainage elements are aligned nearly east-west. These include numerous east-west stream segments and parts of the margins of most of the subsidence basins. In most of these areas it appears that valley or basin development has been influenced by jointing.

Appendix 5. Calculation of ground-water age in Hudspeth and Culberson Counties using ^{14}C and ^{13}C data.

The percentage of modern carbon in each ground-water sample (PMC in app. 2) was corrected by using $\delta^{13}C$ data to evaluate the age of the water. $\delta^{13}C$ value of the water sample, together with assumed $\delta^{13}C$ value of -17 °/oo of soil air CO_2 (measured in West Texas by Rightmire, 1967), were used. Correction was based on the following equation (Pearson and White, 1967):

$$\text{Age} = -k \ln \left[\frac{^{14}C \text{ \% modern}}{100\ P}\right]$$

where:

k = 5,730 yr/ln 2

P = $\delta^{13}C_{sm}/\delta^{13}C_{cr}$. This is a ratio of atmospheric-derived carbon to total carbon in the system.

$\delta^{13}C_{sm}$ = $\delta^{13}C$ °/oo PDB of the water sample.

$\delta^{13}C_{cr}$ = typical $\delta^{13}C$ value of recharge water (was assumed to be -17 °/oo PDB).

The results of the corrected ages of the ground-water samples are reported in appendix 2.

Appendix 6. Permeability of bolson fill based on core and grain-size analyses.

Three boreholes (B-7, B-12, and B-13--fig. 23a) were cored by URM in the bolson fill from below the gravel cover to a total depth of 150 ft for grain-size and vertical permeability analyses. Samples from B-7 were analyzed. B-7 was selected for the analysis because an in situ permeability test on nearly the same section was performed earlier in an adjacent borehole (B-8). It is assumed that the permeability measured in the in situ test is mainly horizontal permeability of the more permeable sandy layers. Conversely, lab tests are biased toward the finer grain sized samples because the sandy samples are not cohesive enough for handling and measurement. As a result, a complementary set of data was achieved. Following are the results of the lab tests performed by URM for B-7:

Sample #	Depth below land surface (ft)	Sand (%)	Silt (%)	Clay (%)	Vertical perm. (cm/sec)
3	65-70	45	30	25	
4	73.5-74	23	47	30	
5	77-77.5	22	38	40	1×10^{-9}
6	82-82.5	0	18	82	$< 1 \times 10^{-10}$
7	85-90	6	49	45	2×10^{-10}
8	100-101	41	26	33	
9	105-110	22	25	53	
10	110-111	27	40	33	
11	116-116.5	0	5	95	$< 5 \times 10^{-11}$
12	120-125	3	21	76	$< 4 \times 10^{-10}$
13	126-126.5	16	30	54	
14	142-142.5	5	23	72	2×10^{-10}

Sand percentage varies from 0 to 45 within this section, whereas clay percentage varies from 25 to 95 (fig. 40). The upper limit of sand percentage for the lab permeability test in these samples was 22 and resulted with the highest vertical permeability value of 1×10^{-9} cm/sec. The in situ test that measured the horizontal permeability of the entire section between 48 and 149.8 ft below land surface yielded a higher value of 3.7×10^{-6} cm/sec (app. 12). Horizontal permeability is usually higher than vertical permeability. The sandy layers, whose permeability could not be tested in the lab, apparently dominated the field test. Dames and Moore (1985) reported a clay permeability of 5.8×10^{-8} cm/sec in a core sampled in their test hole at this site. Porosity data derived from the geophysical logs of B-7 showed negative correlation with core vertical permeability data (fig. 41), as was expected from the high percentage of clay and silt present in the cores.

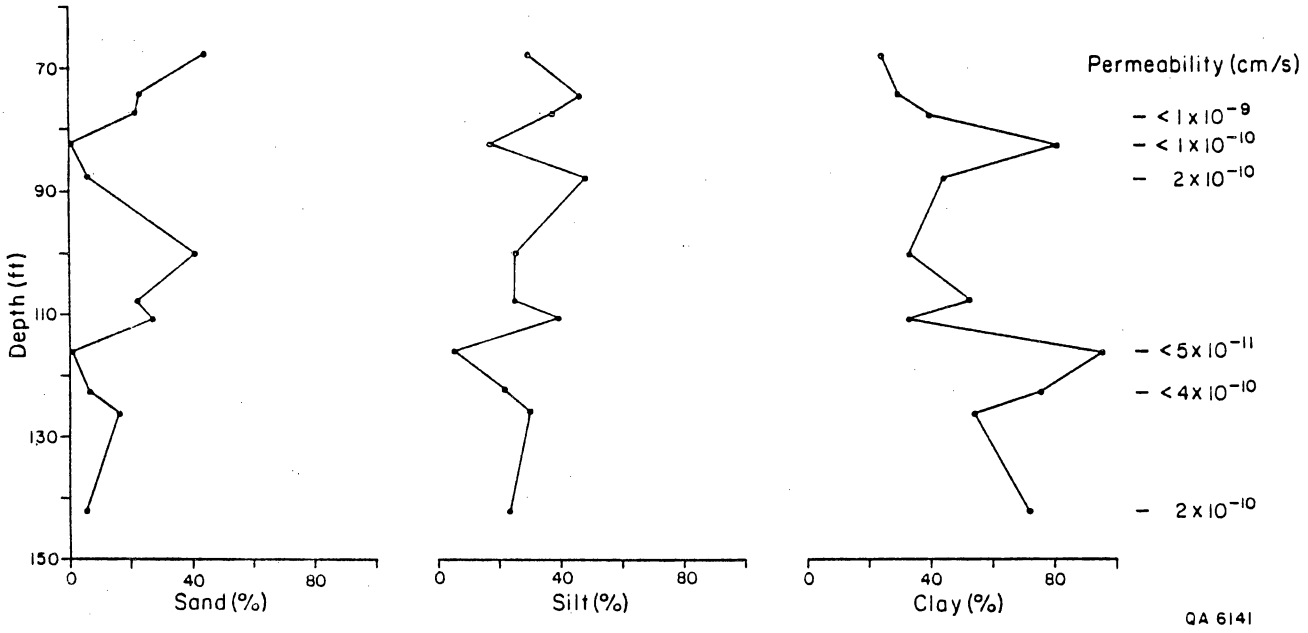

Figure 40. Variations in grain size (%) and vertical permeability (cm/s) with depth (ft) in bore-hole 7. Location of the borehole is shown in figure 23a.

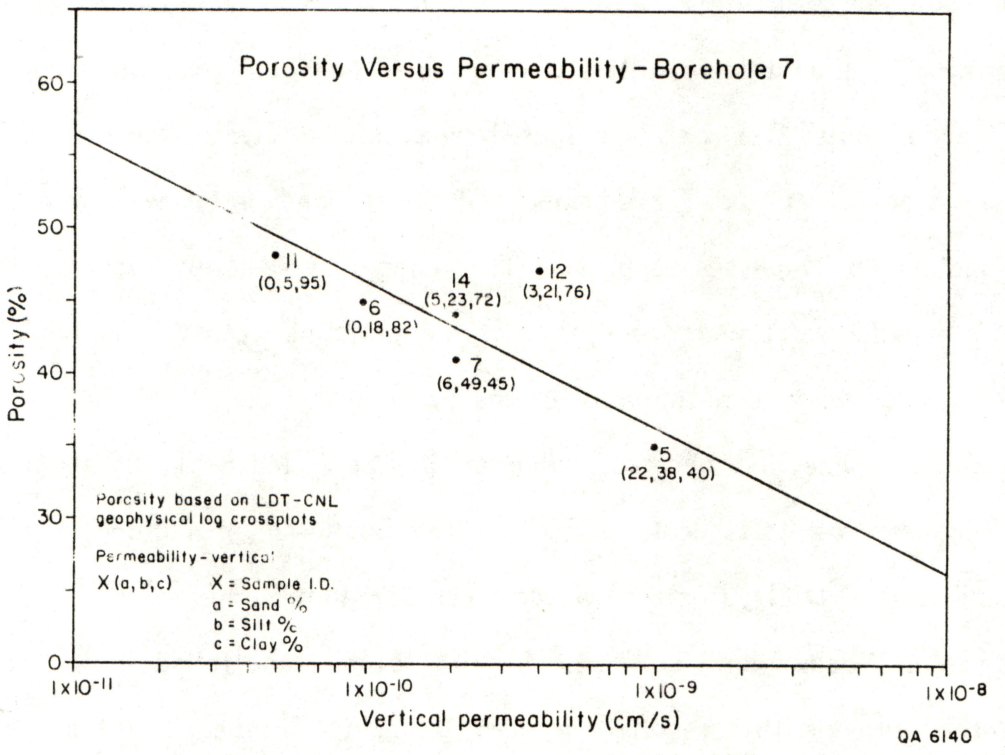

Figure 41. Correlation of porosity (%) and vertical permeability (cm/sec) in borehole 7. Location of the borehole is shown in figure 23a.

Appendix 7: Hydrological parameters of the Cretaceous aquifer, Hudspeth site, derived from a short-term pump test.

The drilling of the water well in the Hudspeth site involved three major objectives in the following order of priority: measuring static water level in the Cretaceous aquifer, sampling its ground water for chemical and isotope analyses, and performing a pump test in order to determine the aquifer transmissivity. The first and second objectives were completed successfully: water level at the well was measured at 478 ft (145.7 m) below land surface and water was sampled for chemical and isotopic analyses (app. 2). The pump test was not accomplished as previously planned. A detailed description of the pumping activities is included in appendix 11. Following is a summary of the pump test.

Ground water was first observed while drilling at a depth of 485 ft (148 m). Drilling continued to a total depth of 530 ft (161 m) at an open borehole of 3.875 inches (9.84 cm) O.D. Hydrostatic water level was monitored for a few days at 478 ft (145.7 m) below land surface. The first pump test failed owing to wall caving at the borehole that resulted in pump clogging. In the second attempt to pump the well, the pump was located at a depth of 489 ft (149 m) (it was not possible to lower it farther), only 11 ft (3.3 m) below water table. As a result, the pumpage rate had to be kept very low in order to prevent a large drawdown, which would have left the pump dry. Pumpage started at a rate of 0.26 gpm (0.98 lpm) (discharge was measured with 15-gallon containers) and lasted 68 minutes with no drawdown. At that point the pump plugged and had to be raised 5 ft (1.5 m) in an attempt to increase borehole clearance and to continue to clear up formation water for sampling. Pumpage was resumed at an increased and constant production rate of 0.789 gpm (2.98 lpm) with no drawdown for another 159 minutes. At that point, the pumping rate decreased to 0.75 gpm (2.83 lpm) and stopped at 167 minutes because the pump plugged again.

To calculate an approximate transmissivity, conventional solutions could not be used because no drawdown occurred in the borehole. A steady-state approximation method was used but provides only a minimum value for transmissivity. A minimum transmissivity of 27 gpd/ft (0.33 m^2/d) was calculated.

Logan's method for a steady-state flow in confined aquifers (Kruseman and De Ridder, 1976) represents an approximation of the Thiem formula for a confined aquifer and was used for the calculation of transmissivity. The ground water in the aquifer is assumed to be confined. The constant rate of pumpage and the absence of drawdown justify a steady-state condition.

$$kD = \frac{2.30Q \log r_{max}/r_w}{2\pi s_{mw}}$$

where

kD = transmissivity of the aquifer, m^2/d

Q = well discharge, m^3/d

r_w = radius of the pumped well, m

r_{max} = radius of influence (=radius of depression cone, m)

s_{mw} = maximum drawdown in the pumped well, m.

The ratio of r_{max}/r_w cannot be accurately determined without the use of additional piezometers. However, although the variations in r_{max} and r_w may be substantial, the variation in the logarithm of their ratio is much smaller and can be approximated with an average value of 3.33. Substituting this value into the above equation yields

$$kD = \frac{1.22Q}{S_{mw}}$$

As was mentioned earlier, no drawdown was observed in the well but a drawdown is needed to calculate transmissivity with this equation. The maximum drawdown possible at the well is 52 ft (15.85 m). Using the same discharge as in the pump test (0.789 gpm [4.3 m^3/d, or 2.98 lpm]) with this maximum drawdown yields a minimum value of 27 gpd/ft (0.33 m^2/d). Transmissivity must be higher because there was no drawdown.

Appendix 8. Stratigraphic sections of bolson deposits cropping out in Hudspeth County study region. (Locations of measured sections described in this appendix shown in figure 22.)

Section 1. Located on Arroyo Diablo ~ 0.63 mi (1 km) NE of Diablo Reservoir No. 2 at 31°15'13" N, 105°45'26" W, ~ 4.75 mi (7.6 km) SSW of the Campo Grande Fault.

Depth Below Surface	
	YOUNGER BOLSON DEPOSITS
0 m	
	Pedogenic calcrete. Surface eroded.
0.75	
	Matrix- to clast-supported limestone pebble to cobble gravel with clasts up to 20 cm in longest dimension. Gravels fine upward to flat-bedded medium to coarse gravelly sand. Hornblende diorite clasts common. This unit contains ~ 8 fining-upward sequences.
2.7	
	$CaCO_3$-cemented, pale-brown, laminated clayey silt.
3.0	
	Laminated, strongly bioturbated clayey silt. Many plant fragments in lower 30 cm.
5.0	
	Medium sand with vague laminations. Pedogenic $CaCO_3$ nodules up to 5 cm. Dispersed pebbles.
7.3	
	Pebbly flat-bedded sand. Pebbles up to 5 cm. Pebbles mostly crystalline volcanics.
8.0	
	Flat-bedded fine pebbly sand.
9.9	
	Section covered by Recent alluvium.

Section 2. Located on Arroyo Diablo ~1 mi (1.75 km) WSW of Diablo Reservoir No. 2 at 31°19'46" N, 104°44'04" W, ~ 300 ft (100 m) WSW of the Campo Grande Fault.

Depth Below Surface	
	YOUNGER BOLSON DEPOSITS
0 m	
	Stage V calcrete with recemented fractures. Fracture fills are up 1 cm thick and laminated. Massive, dense; weathers to a tabular or platy appearance.

2.5	Flat-bedded, clast-supported, gray limestone pebble-cobble gravel deposited on an erosion surface and overlain by medium to coarse flat-bedded sand with calcrete nodules.
3.0	Flat-bedded, clast-supported, gray limestone pebble-cobble gravel deposited on an erosion surface and overlain by medium to coarse flat-bedded sand with lenses of fine pebbles or granules.
4.2	Flat-bedded, clast-supported, gray limestone pebble-cobble gravel deposited on an erosion surface and overlain by medium to coarse flat-bedded sand with lenses of fine pebbles or granules.
5.75	Three sequences of flat-bedded, gray pebble gravels fining upward to flat-bedded coarse to medium sand. Numerous lithoclasts of calcrete nodules in the basal gravel.
7.0	Matrix- to clast-supported, flat-bedded, gray limestone pebble to cobble basal gravel. Gravel is overlain by fine sand with gravel lenses and isolated pebbles. No primary sedimenary structures are preserved in the sand. Pedogenic $CaCO_3$ nodules occur throughout the fine sand and three massive pedogenic calcretes composed of $CaCO_3$ nodules are preserved in the fine sands. $CaCO_3$ films up to several millimeters thick occur on the lower surface of pebbles and cobbles. Calcretes are probably Stage III calcretes in the classification of Bachman and Machette (1977).
9.75	Base of section covered by Recent alluvium.

Section 3. Located on Arroyo Diablo ~ 0.5 mi (0.8 km) S of Campo Grande Mountain at 31°19'07" N, 105°42'30" W, ~ 30 to 60 ft (10 to 20 m) WSW of the Campo Grande Fault.

Depth Below Surface	
	YOUNGER BOLSON DEPOSITS
0 m	Stage IV to V calcrete. Massive $CaCO_3$ weathering to a platy or tabular structure. Fracture fillings are laminated. $CaCO_3$ content and density increases upward.
1.25	Poorly exposed, interbedded flat-bedded sand and gravel. Gravel content increases upward. Sand and gravel overlie an an erosion surface developed on lower bolson deposits.

OLDER BOLSON DEPOSITS

26.5

Pale-brown, laminated clayey silt.

28.5

Pale-red-brown silty clay. Massive, blocky fracturing with no preserved primary sedimentary structures. Fractures with slickensides.

28.8

Pale-brown, laminated clayey silt.

31.8

Pale-red-brown silty clay. Massive, blocky fracturing with no preserved primary sedimentary structures. Fractures with slickensides.

34.8

Section covered by Recent alluvium.

Section 4. Located on Camp Rice Arroyo ~ 0.8 mi (1.3 km) N of the Lutich Ranch at 31°22'48" N, 105°46' W, ~ 1 mi (1.6 km) NE of the Campo Grande Fault.

Depth Below Surface

RECENT SEDIMENTS

0 m

Eolian sand.

YOUNGER BOLSON DEPOSITS

1.8

Stage V calcrete, slightly laminated.

2.7

Flat-bedded sand and sandy pebble gravel.

OLDER BOLSON DEPOSITS

4.6

Pale-red-brown silty clay, no preserved primary sedimentary structures, blocky fractures with slickensides.

7.0

Laminated pale-brown clayey silt.

7.3

Pale-red-brown silty clay, no preserved primary sedimentary structures, blocky fractures with slickensides.

9.4

Interbedded red-brown silty clay and pale-brown clayey silt. Characteristics of these beds are similar to those of silts and clays described above.

12.4

Base of section covered by Recent alluvium.

Section 5. Located on Arroyo Diablo ~1 mi (1.75 km) WSW of Diablo Reservoir No. 2 at 31°20'02" N. 104°44'06" W. ~ 300 ft (100 m) ENE of the Campo Grande Fault.

Depth Below Surface	
	YOUNGER BOLSON DEPOSITS
0 m	
	Stage IV to V calcrete. Dense, fractured, platy or tabular weathering. Fracture fillings laminated. Upper surface eroded.
0.5	
	Flat-bedded, partly clast-supported limestone pebble-cobble gravel with lenses of flat-bedded sand. Pedogenic $CaCO_3$ content increases upward. Gravel clasts up to 10 cm. Unit deposited on an erosion surface developed on lower bolson deposits.
	OLDER BOLSON DEPOSITS
2.5	
	Pale-brown laminated clayey silt with dispersed gravel clasts up to 10 cm.
3.5	
	Pale-red-brown silty clay. No preserved primary sedimentary structures. Fractures with slickensides.
3.75	
	Laminated clayey silt with clasts up to 8 cm at base.
4.3	
	Pale-red-brown silty clay. No preserved primary sedimentary structures. Blocky fracturing with slickensides on fracture faces.
5.1	
	Laminated, pale-brown clayey silt.
6.0	
	Pale-red-brown silty clay. No preserved primary sedimentary structures. Blocky fracturing with slickensides on fracture faces.
6.4	
	Laminated pale-brown clayey silt.
6.9	
	Pale-red-brown silty clay. No preserved primary sedimentary structures. Blocky fracturing with slickensides on fracture faces.
7.8	
	Laminated pale-brown clayey silt. $CaCO_3$-filled fractures.
8.4	
	Pale-red-brown silty clay. No preserved primary sedimentary structures. Blocky fracturing with slickensides on fracture faces.
9.25	
	Section covered by Recent alluvium.

Section 6. Located on Arroyo Diablo ~ 0.35 mi (0.6 km) NNW of Diablo Reservoir No. 1, at 31°20'34" N, 105°43' W.

Depth Below Surface	
	YOUNGER BOLSON DEPOSITS
0 m	
	Pedogenic calcrete, becomes more massive upward, tabular to platy, lamina in fractures, surface appears stripped. Probably a Stage IV to V calcrete.
1.1	
	Sandy matrix-supported pebble-cobble gravel with lenses of clast-supported pebble gravel.
4.0	
	Interbedded laminated silty sand and clayey silt. No primary sedimentary structures preserved in the clayey silt.
5.9	
	Red-brown, blocky-fracturing silty clay. Slickensides on fracture faces. No preserved primary sedimentary structures. $CaCO_3$ nodules up to 15 cm in diameter preserved near base.
6.4	
	Ripple-laminated fine silty sand.
6.4	
	Red-brown silty clay with $CaCO_3$ nodules.
6.6	
	Fine to medium horizontally laminated sand. Lower 2 m $CaCO_3$-cemented to form a ground-water calcrete. $CaCO_3$ nodules over a 0.5- to 1.0-cm-thick red-brown clay
9.9	
	$CaCO_3$ nodules overlying a 1.0-cm-thick clay. $CaCO_3$ nodules up to 8 cm in diameter.
10.0	
	Fine- to medium-laminated silty sand.
	OLDER BOLSON DEPOSITS
10.5	
	Red-brown, blocky-fracturing silty clay with $CaCO_3$ nodules. No preserved primary sedimentary structures. The upper contact of this unit is an erosional surface in which channels have been cut to a depth of as much as 2 m.
12.5	
	Laminated to ripple cross-laminated fine to medium sand. $CaCO_3$ nodules and thin $CaCO_3$-cemented lenses.
13.8	
	Horizontally bedded, fine to medium sand overlying Couplets of silty clay and fine sand inclined up to 30° south. Couplets range from centimeters to nearly a meter thick. Inclined lamina overlie horizontal silty sand and sands. This unit is interpreted as a Gilbertian delta.

16.1

Red-brown, blocky-fracturing silty clay. No preserved primary sedimentary structures. Slickensides on fracture faces. $CaCO_3$ nodules preserved throughout.

Section covered by Recent alluvium.

Section 7. Located on Camp Rice Arroyo 0.55 mi (0.9 km) NW of Lutich Ranch at 31°22'26" N, 105°46'24" W.

Depth Below Surface

YOUNGER BOLSON DEPOSITS

0 m

Massive calcrete, in part fractured with fracture fillings laminated. Nodular calcrete becoming massive upward. Surface of calcrete stripped. Probably a Stage IV or V calcrete.

1.6

Interbedded horizontally bedded sand and sandy clast-supported limestone gravel. Clasts up to 10 cm in long dimension.

3.6

Horizontally bedded silty fine sand.

4.4

Massive, silty fine sand. No preserved primary sedimentary structures. Lightly $CaCO_3$-cemented. $CaCO_3$ cement decreases upward.

OLDER BOLSON DEPOSITS

9.8

Red-brown, blocky-fracturing silty clay. No preserved primary sedimentary structures. Slickensides on fracture faces.

11.5

Thinly laminated clayey silt.

11.8

Red-brown, blocky-fracturing silty clay. No preserved primary sedimentary structures. Slickensides on fracture faces.

13.5

Thinly laminated silt.

13.6

Red-brown, blocky-fracturing silty clay. No preserved primary sedimentary structures. Slickensides on fracture faces.

15.4

Massive silty fine sand. Rare preserved lamina marked by black stains. $CaCO_3$ nodules. Popcorn texture on exposed surface suggests a high expansive clay content.

17.8

Red-brown, blocky-fracturing silty clay. No preserved primary sedimentary structures. Slickensides on fracture faces.

22.3

Ripple cross-laminated fine sand and clayey silt. Fine sand lamina mark ripples.

24

Red-brown, blocky-fracturing silty clay. No preserved primary sedimentary structures. Slickensides on fracture faces.

25.3

Silty sand. No preserved primary structures.

25.4

Red-brown, blocky-fracturing silty clay. No preserved primary sedimentary structures. Slickensides on fracture faces.

25.5

Section covered by Recent alluvium.

Section 8. Located on Arroyo Diablo ~0.5 mi (0.8 km) S of Campo Grande Mountain at 31°19'17" N, 105°42'30" W, ~ 30 to 60 ft (10 to 20 m) ENE of the Campo Grande fault.

Depth Below Surface

OLDER BOLSON DEPOSITS

0 m

Calcrete. $CaCO_3$ content increases upward. Stage of calcrete development unknown.

1

Interbedded red-brown, blocky-fracturing silty clay and pale-red-brown silty clay. Section partly obscured by colluvium.

12

Pale-red-brown clayey silt.

12.5

Red-brown silty clay.

16.5

Pale-red-brown clayey silt.

26.5

Section covered by Recent alluvium.

Section 9. Located in Alamo Arroyo ~ 0.6 mi (1 km) WNW of Cavett Lake dam at 31°24'20" N, 105°49'40" W.

Depth Below Surface

RECENT

0 m

Eolian sand

OLDER BOLSON DEPOSITS

3

Red-brown, blocky-fracturing silty clay. No preserved primary sedimentary structures. Slickensides on fracture faces.

4

Trough crossbedded silty sand. The base of this unit is an erosional surface.

5.5

Red-brown, blocky-fracturing silty clay. No preserved primary sedimentary structures. Slickensides on fracture faces.

6.0

Laminated to cross-laminated silty fine to medium sand. $CaCO_3$ nodules.

6.9

Red-brown, blocky-fracturing silty clay. No preserved primary sedimentary structures. slickensides on fracture faces. $CaCO_3$ nodules.

19.4

Laminated to cross-laminated silty fine sand. Some zones massive with no preserved primary sedimentary structures.

20.9

Section covered by Recent alluvium.

Appendix 9. Lithologic logs for Hudspeth County test holes.

LLWA 1

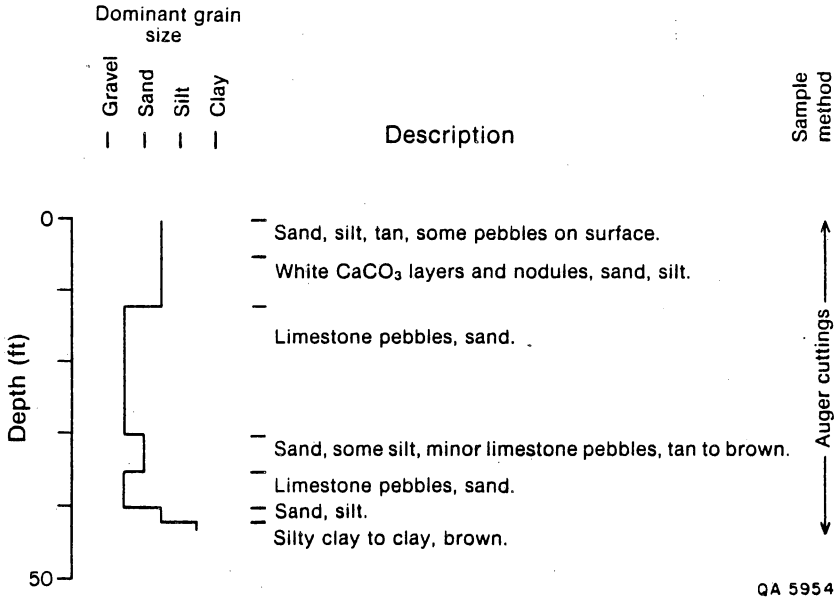
Dominant grain size
Gravel
Sand
Silt
Clay
Description
Sample method
Depth (ft)
0
50
Sand, silt, tan, some pebbles on surface.
White CaCO3 layers and nodules, sand, silt.
Limestone pebbles, sand.
Sand, some silt, minor limestone pebbles, tan to brown.
Limestone pebbles, sand.
Sand, silt.
Silty clay to clay, brown.
Auger cuttings
QA 5954

LLWA 2

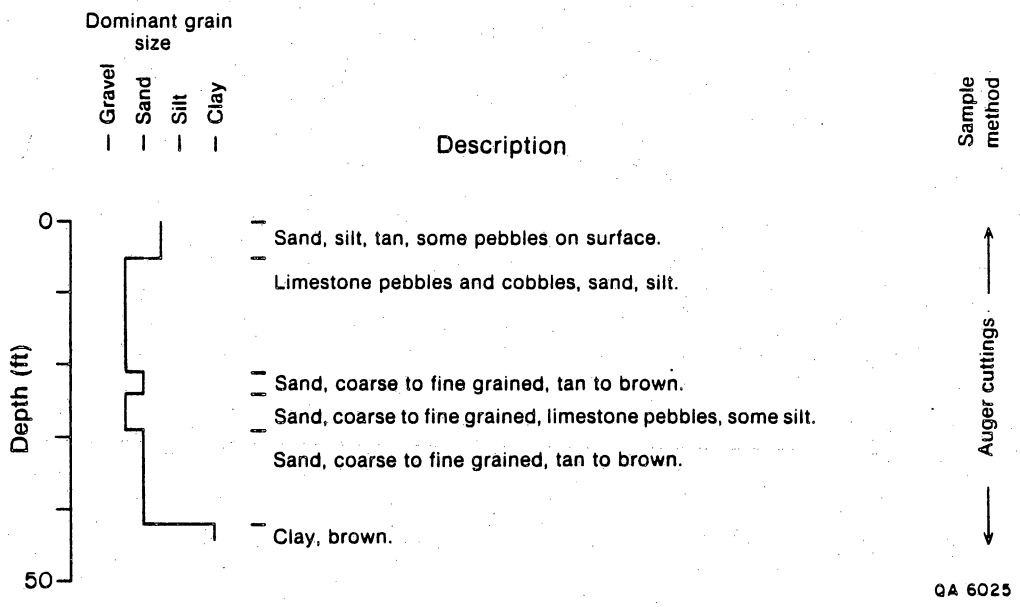
Dominant grain size
Gravel
Sand
Silt
Clay
Description
Sample method
0
Depth (ft)
50
Sand, silt, tan, some pebbles on surface.
Limestone pebbles and cobbles, sand, silt.
Sand, coarse to fine grained, tan to brown.
Sand, coarse to fine grained, limestone pebbles, some silt.
Sand, coarse to fine grained, tan to brown.
Clay, brown.
Auger cuttings
QA 6025

LLWA 3

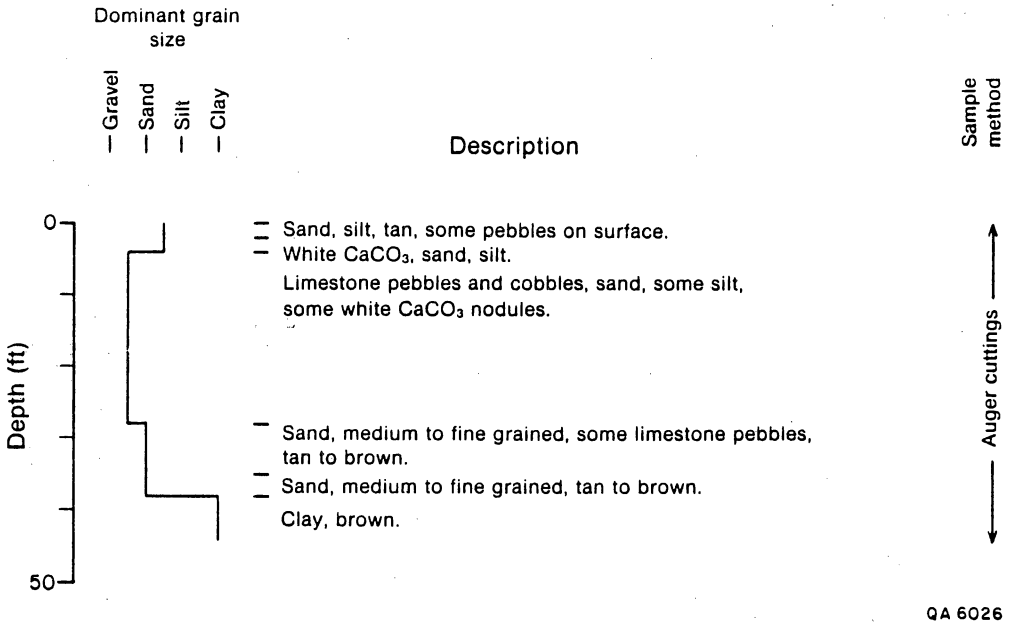
Dominant grain size
Gravel
Sand
Silt
Clay
Description
Sample method
Depth (ft)
0
50
Sand, silt, tan, some pebbles on surface.
White $CaCO_3$, sand, silt.
Limestone pebbles and cobbles, sand, some silt, some white $CaCO_3$ nodules.
Sand, medium to fine grained, some limestone pebbles, tan to brown.
Sand, medium to fine grained, tan to brown.
Clay, brown.
Auger cuttings
QA 6026

LLWA 4

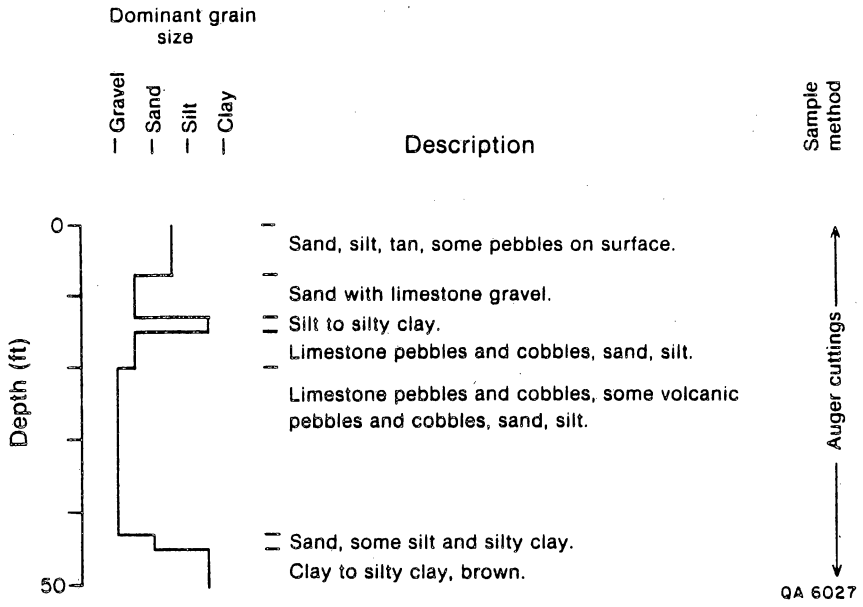
Dominant grain size
Gravel
Sand
Silt
Clay
Description
Sample method
Depth (ft)
0
50
Sand, silt, tan, some pebbles on surface.
Sand with limestone gravel.
Silt to silty clay.
Limestone pebbles and cobbles, sand, silt.
Limestone pebbles and cobbles, some volcanic pebbles and cobbles, sand, silt.
Sand, some silt and silty clay.
Clay to silty clay, brown.
Auger cuttings
QA 6027

LLWA 5

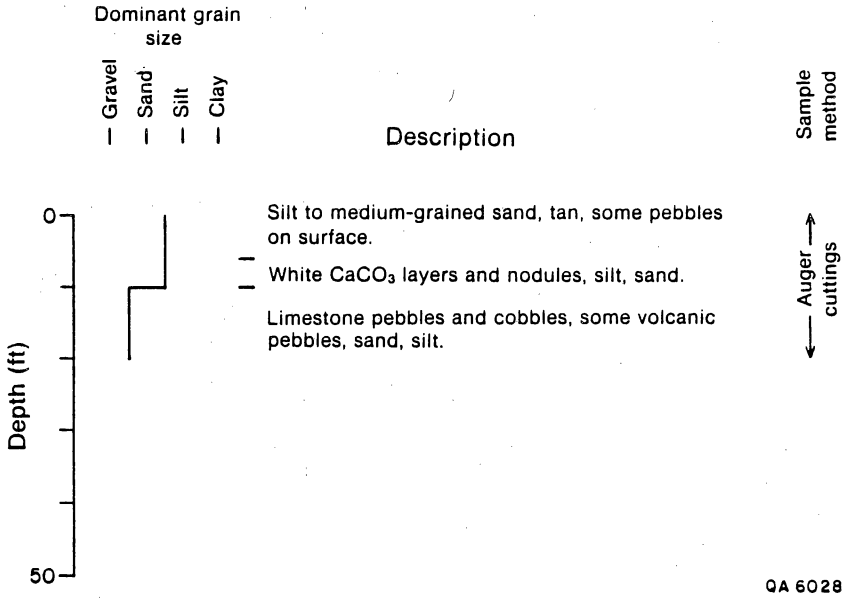
Dominant grain size
Gravel
Sand
Silt
Clay
Description
Sample method
Silt to medium-grained sand, tan, some pebbles on surface.
White $CaCO_3$ layers and nodules, silt, sand.
Limestone pebbles and cobbles, some volcanic pebbles, sand, silt.
Auger cuttings
Depth (ft)
0
50
QA 6028

LLWA 6

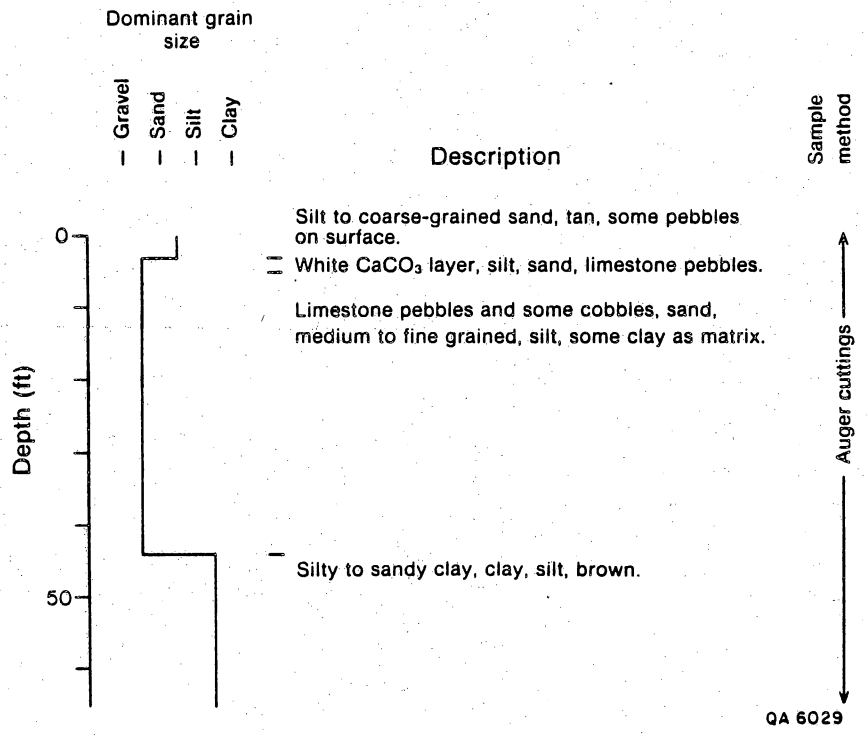
Dominant grain size
Gravel
Sand
Silt
Clay
Description
Sample method
Depth (ft)
0
50
Silt to coarse-grained sand, tan, some pebbles on surface.
White $CaCO_3$ layer, silt, sand, limestone pebbles.
Limestone pebbles and some cobbles, sand, medium to fine grained, silt, some clay as matrix.
Silty to sandy clay, clay, silt, brown.
Auger cuttings
QA 6029

LLWA 7

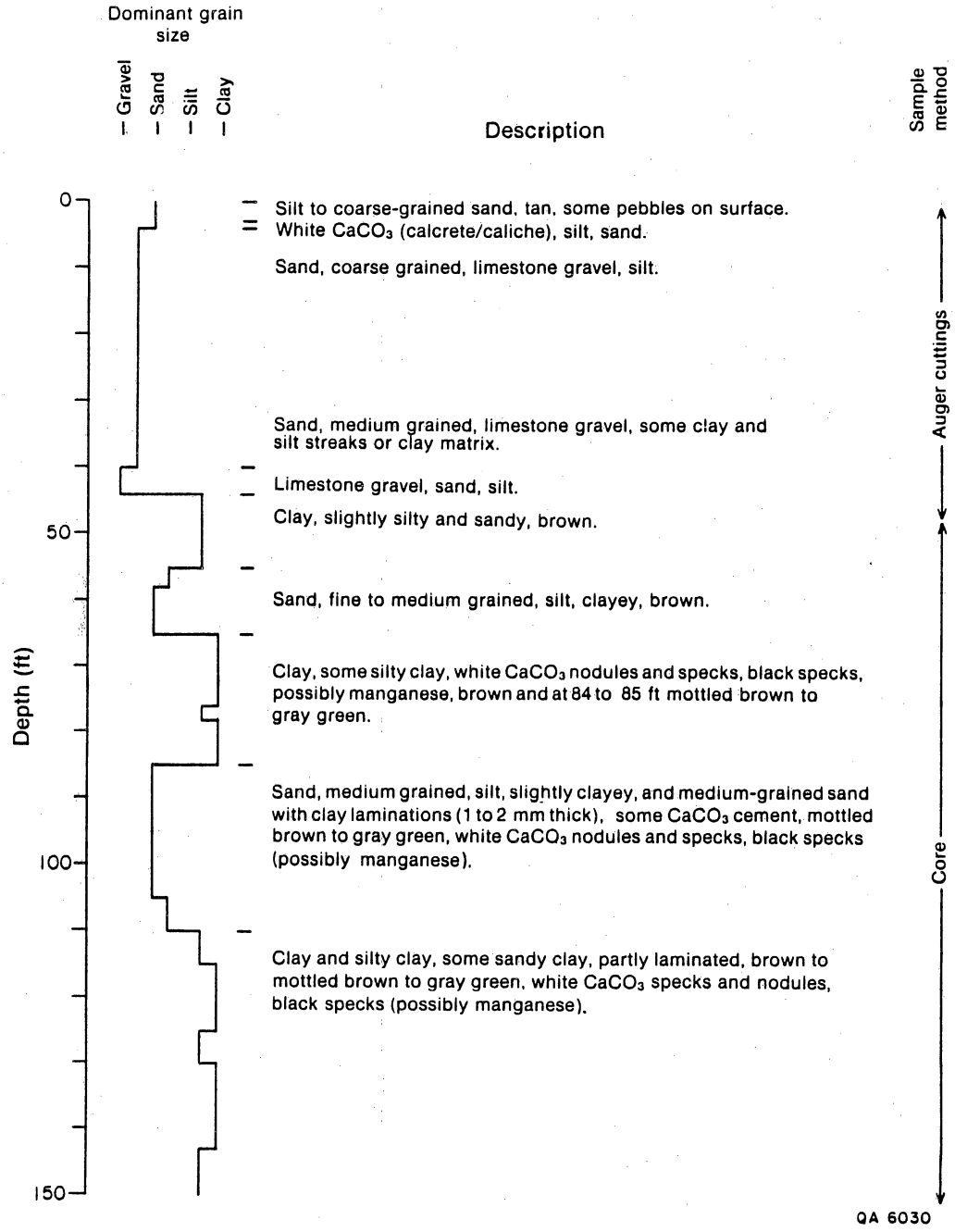
Dominant grain size
Gravel
Sand
Silt
Clay
Description
Sample method
Depth (ft)
0
50
100
150
Silt to coarse-grained sand, tan, some pebbles on surface.
White CaCO3 (calcrete/caliche), silt, sand.
Sand, coarse grained, limestone gravel, silt.
Sand, medium grained, limestone gravel, some clay and silt streaks or clay matrix.
Limestone gravel, sand, silt.
Clay, slightly silty and sandy, brown.
Sand, fine to medium grained, silt, clayey, brown.
Clay, some silty clay, white CaCO3 nodules and specks, black specks, possibly manganese, brown and at 84 to 85 ft mottled brown to gray green.
Sand, medium grained, silt, slightly clayey, and medium-grained sand with clay laminations (1 to 2 mm thick), some CaCO3 cement, mottled brown to gray green, white CaCO3 nodules and specks, black specks (possibly manganese).
Clay and silty clay, some sandy clay, partly laminated, brown to mottled brown to gray green, white CaCO3 specks and nodules, black specks (possibly manganese).
Auger cuttings
Core
QA 6030

LLWA 10

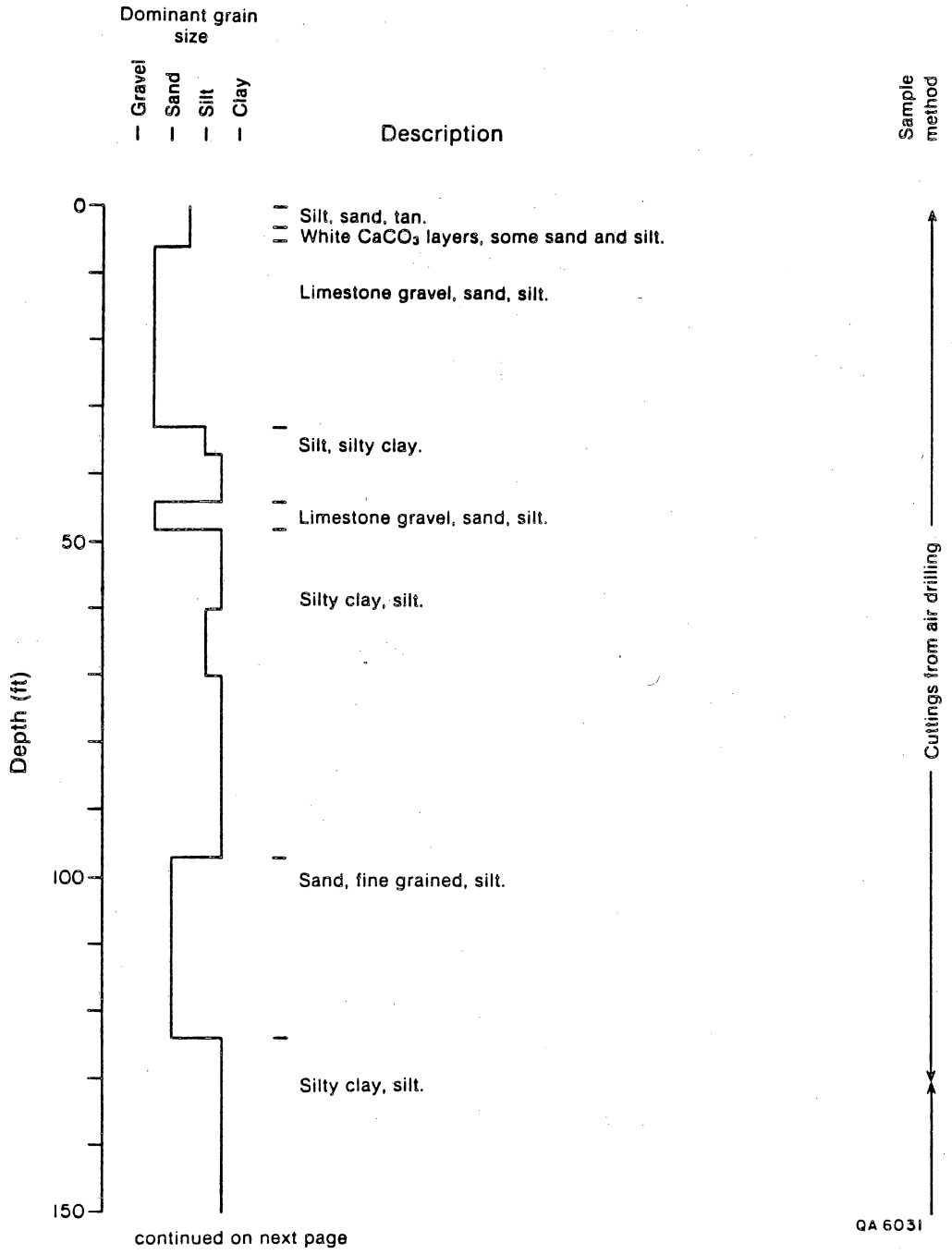

continued on next page

LLWA 10

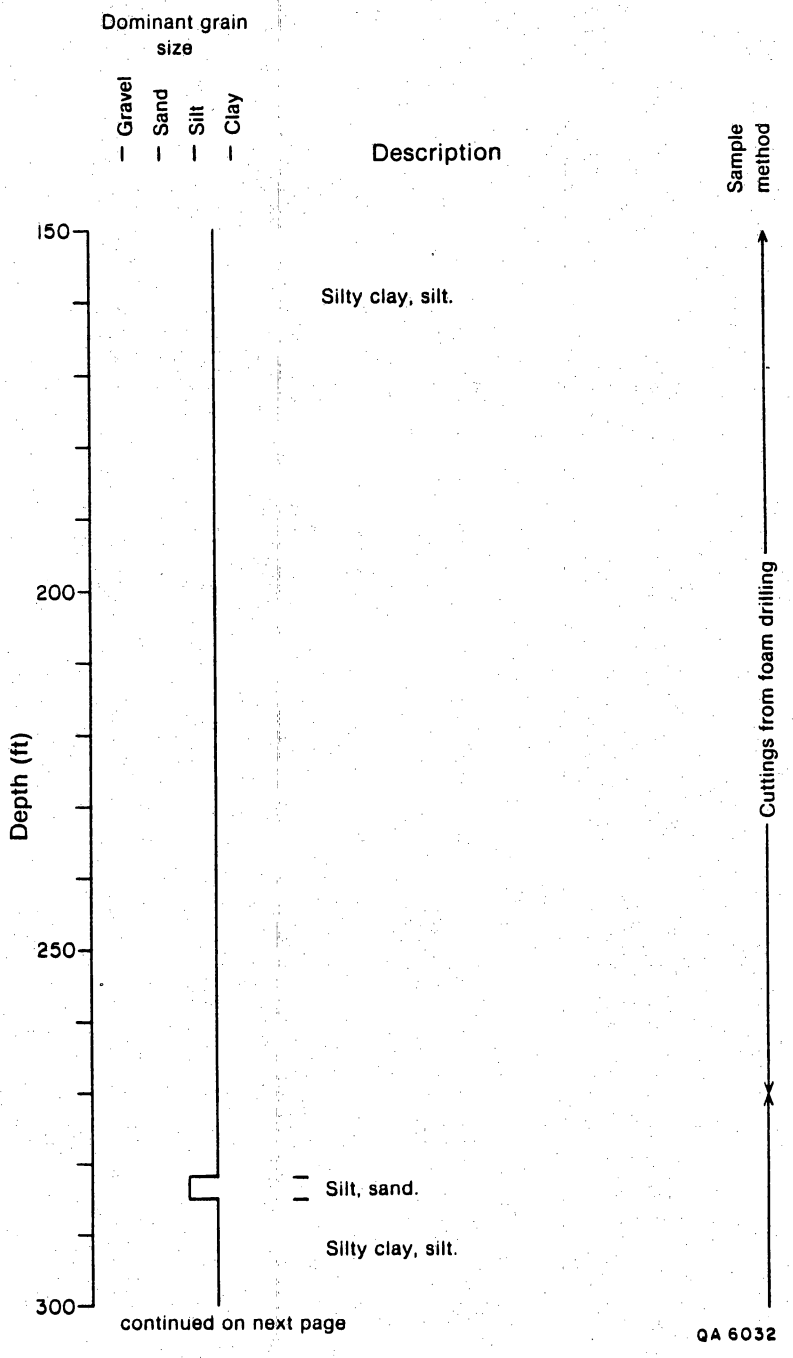
Dominant grain size
Gravel
Sand
Silt
Clay
Description
Sample method
150
200
250
300
Depth (ft)
Silty clay, silt.
Silt, sand.
Silty clay, silt.
Cuttings from foam drilling
continued on next page
QA 6032

LLWA 10

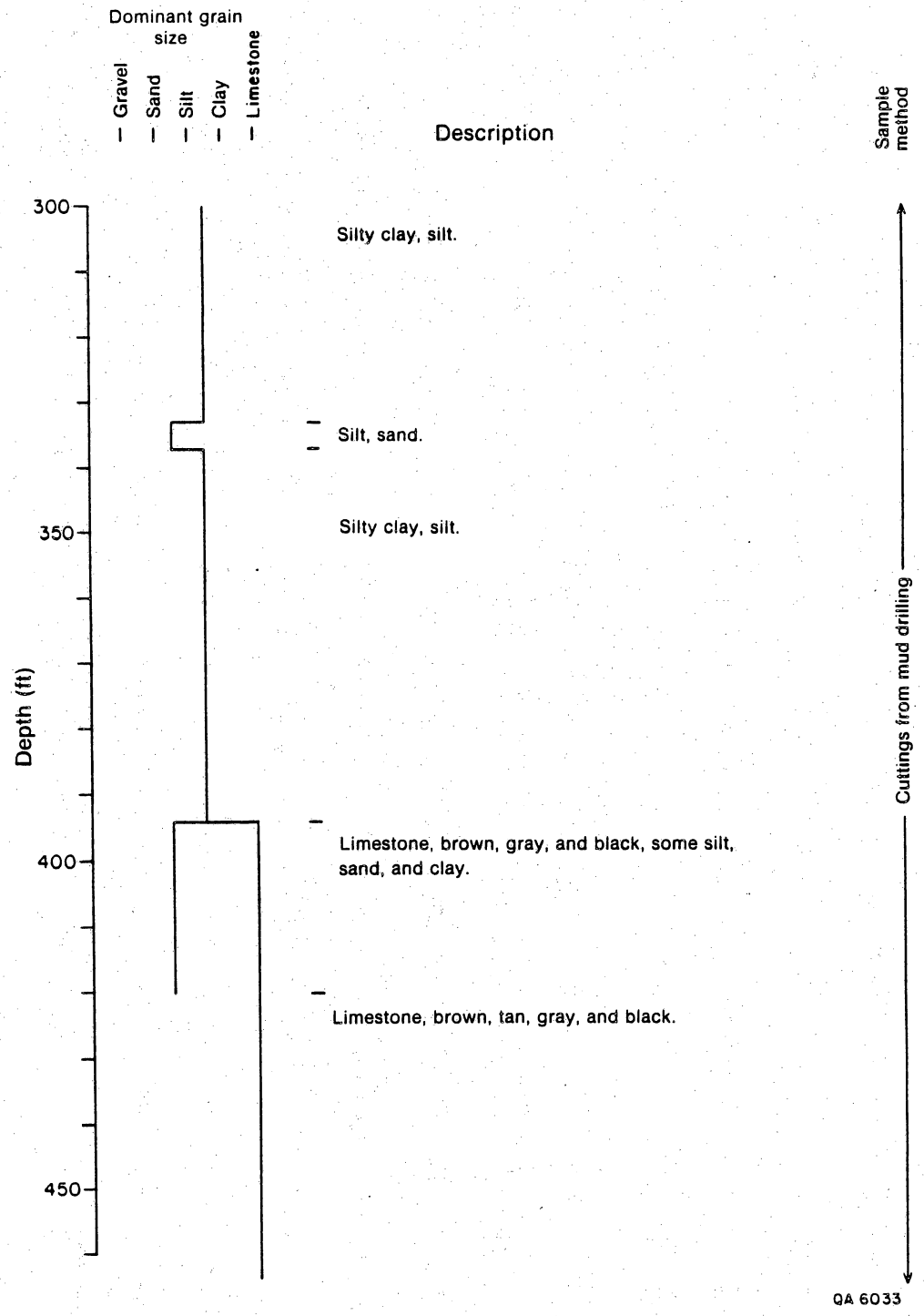
Dominant grain size
Gravel
Sand
Silt
Clay
Limestone
Description
Sample method
300
350
400
450
Depth (ft)
Silty clay, silt.
Silt, sand.
Silty clay, silt.
Limestone, brown, gray, and black, some silt, sand, and clay.
Limestone, brown, tan, gray, and black.
Cuttings from mud drilling
QA 6033

LLWA II

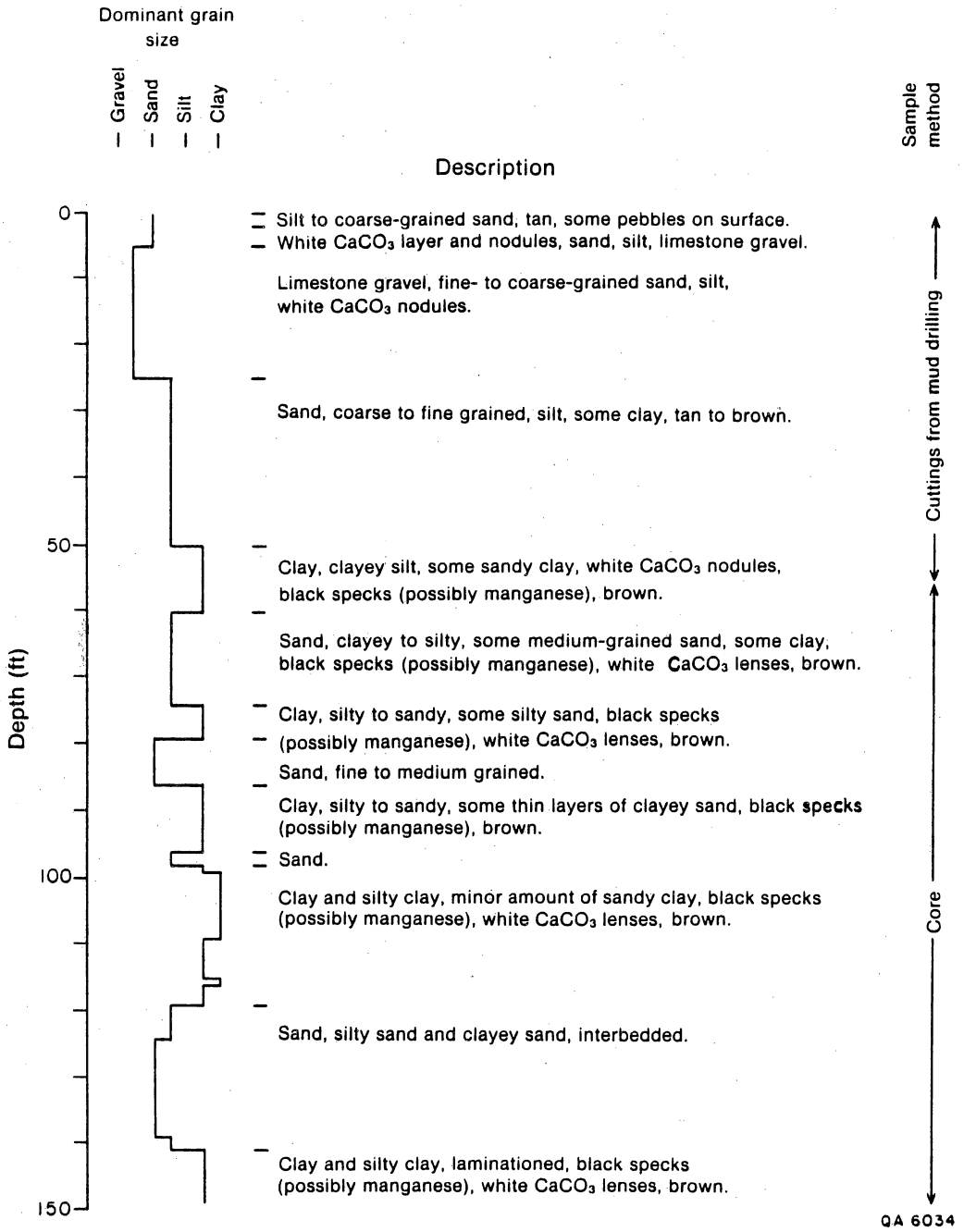
Dominant grain size
Gravel
Sand
Silt
Clay
Description
Sample method
Depth (ft)
0
50
100
150
Silt to coarse-grained sand, tan, some pebbles on surface.
White CaCO3 layer and nodules, sand, silt, limestone gravel.
Limestone gravel, fine- to coarse-grained sand, silt, white CaCO3 nodules.
Sand, coarse to fine grained, silt, some clay, tan to brown.
Clay, clayey silt, some sandy clay, white CaCO3 nodules, black specks (possibly manganese), brown.
Sand, clayey to silty, some medium-grained sand, some clay, black specks (possibly manganese), white CaCO3 lenses, brown.
Clay, silty to sandy, some silty sand, black specks (possibly manganese), white CaCO3 lenses, brown.
Sand, fine to medium grained.
Clay, silty to sandy, some thin layers of clayey sand, black specks (possibly manganese), brown.
Sand.
Clay and silty clay, minor amount of sandy clay, black specks (possibly manganese), white CaCO3 lenses, brown.
Sand, silty sand and clayey sand, interbedded.
Clay and silty clay, laminationed, black specks (possibly manganese), white CaCO3 lenses, brown.
Cuttings from mud drilling
Core
QA 6034

LLWA 12

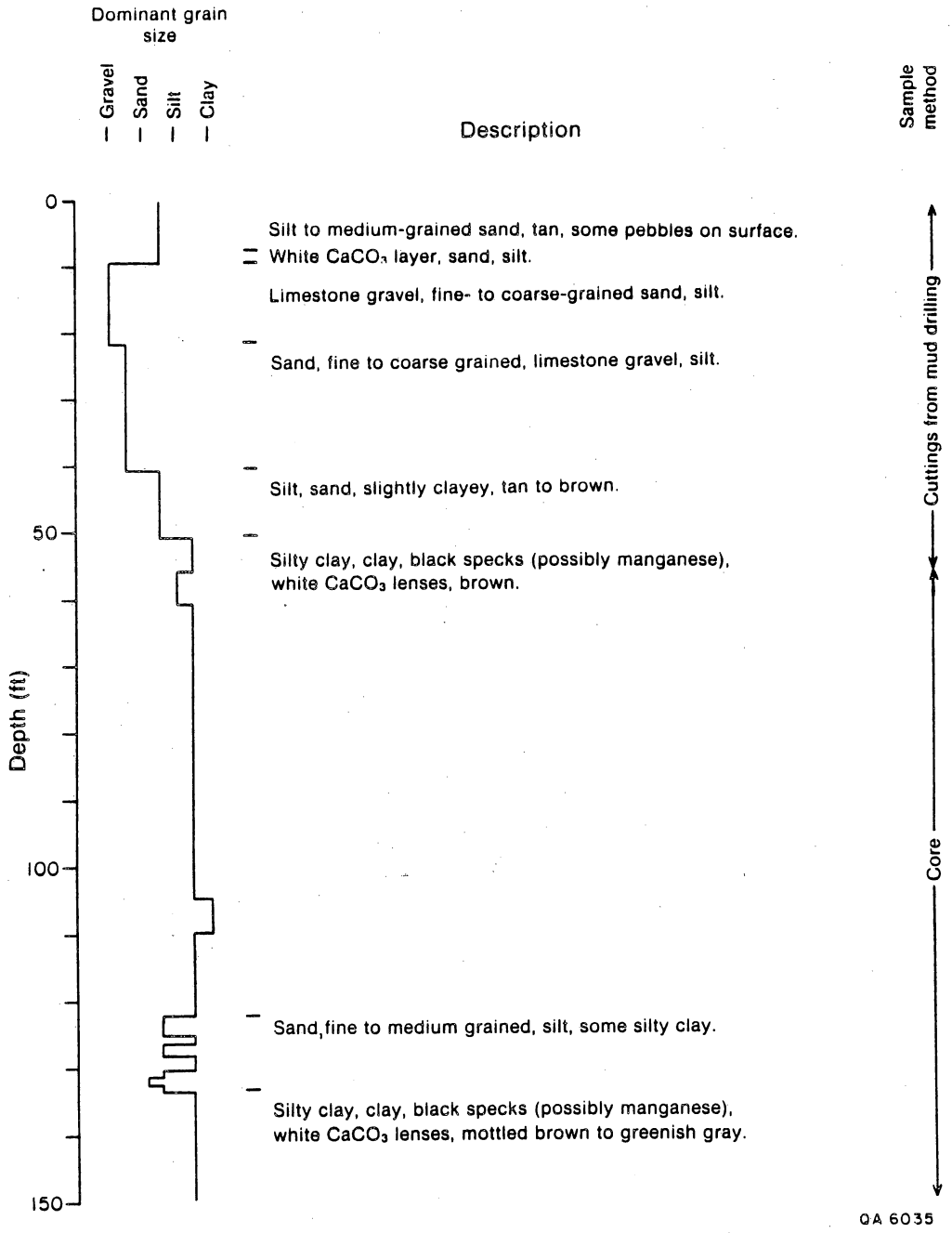
Dominant grain size
Gravel
Sand
Silt
Clay
Description
Sample method
Depth (ft)
0
50
100
150
Silt to medium-grained sand, tan, some pebbles on surface.
White CaCO3 layer, sand, silt.
Limestone gravel, fine- to coarse-grained sand, silt.
Sand, fine to coarse grained, limestone gravel, silt.
Silt, sand, slightly clayey, tan to brown.
Silty clay, clay, black specks (possibly manganese), white CaCO3 lenses, brown.
Sand, fine to medium grained, silt, some silty clay.
Silty clay, clay, black specks (possibly manganese), white CaCO3 lenses, mottled brown to greenish gray.
Cuttings from mud drilling
Core
QA 6035

LLWA 13

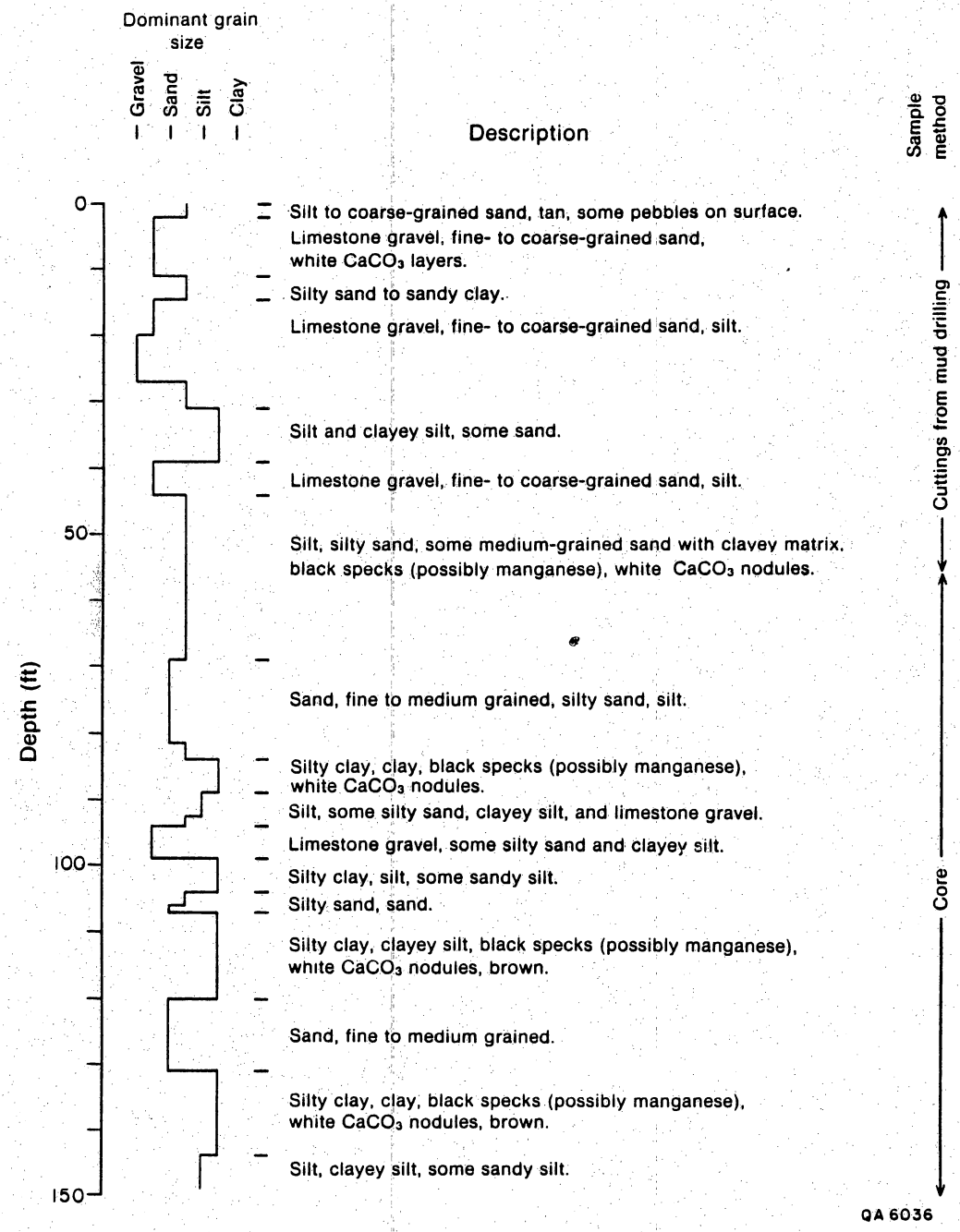
Dominant grain size
Gravel
Sand
Silt
Clay
Description
Sample method
Depth (ft)
0
50
100
150
Silt to coarse-grained sand, tan, some pebbles on surface.
Limestone gravel, fine- to coarse-grained sand, white $CaCO_3$ layers.
Silty sand to sandy clay.
Limestone gravel, fine- to coarse-grained sand, silt.
Silt and clayey silt, some sand.
Limestone gravel, fine- to coarse-grained sand, silt.
Silt, silty sand, some medium-grained sand with clayey matrix, black specks (possibly manganese), white $CaCO_3$ nodules.
Sand, fine to medium grained, silty sand, silt.
Silty clay, clay, black specks (possibly manganese), white $CaCO_3$ nodules.
Silt, some silty sand, clayey silt, and limestone gravel.
Limestone gravel, some silty sand and clayey silt.
Silty clay, silt, some sandy silt.
Silty sand, sand.
Silty clay, clayey silt, black specks (possibly manganese), white $CaCO_3$ nodules, brown.
Sand, fine to medium grained.
Silty clay, clay, black specks (possibly manganese), white $CaCO_3$ nodules, brown.
Silt, clayey silt, some sandy silt.
Cuttings from mud drilling
Core
QA 6036

Appendix 10. Geophysical log data.

The following data is based on analysis of geophysical logs run in four open boreholes and one cased borehole (figs. 42 through 46). Schlumberger Well Services performed the logging on April 17-18, 1986. It should be noted that all five boreholes were unsaturated (above the water table) and certain tools were directly affected by this environment.

Lithologic Determination

Three logging tools may be used to determine lithologies in open boreholes: the Spontaneous Potential curve (SP), the Gamma-Ray log (GR), and the Litho-Density log (LDT).

The SP log is commonly used to determine the presence of permeable beds, bed boundaries, formation water resistivity, and shale content (Asquith, 1982). The SP log may also be an effective tool in stratigraphic and structural correlations. Typically, the SP log measures the contrast in salinities between the drilling mud filtrate and formation water. In this case (boreholes at S-34), formation water is limited to the irreducible water content trapped between and coating grains of sand, silt, and clay. This factor essentially eliminates the potential for electrochemical conduction and contrast through the formation. The SP log may have limited use in stratigraphic and structural correlations but should be used in combination with other logs such as GR or DIL.

The GR log measures natural radioactivity of a formation. In typical sequences, radioactive materials tend to be concentrated in shales and clays. The higher GR readings indicate shalier units, whereas lower GR readings indicate cleaner sandstones and limestones. Since formation water is not a requirement for GR logs they are

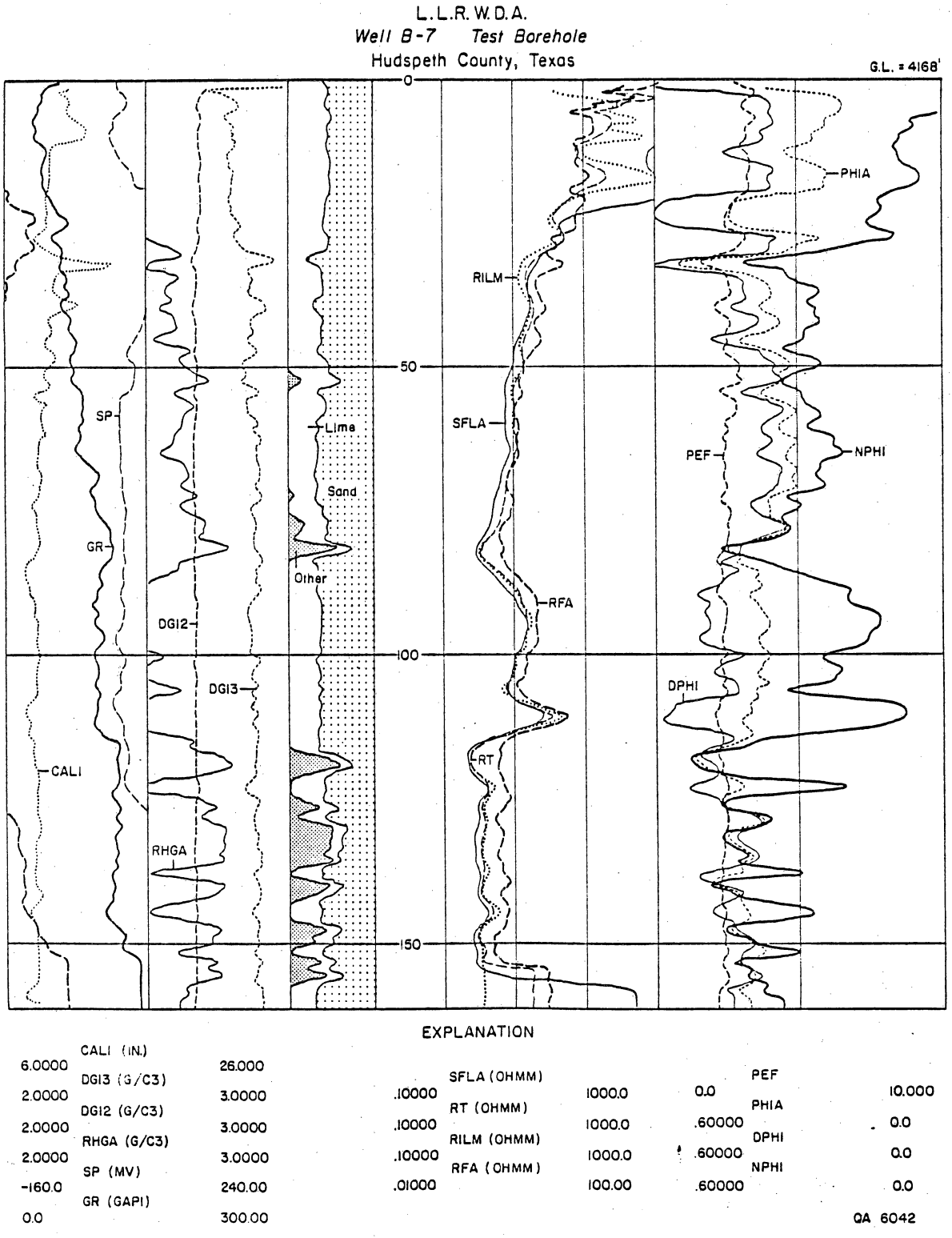

Figure 42. Composite geophysical log for borehole 7. Location of the borehole is shown in figure 23.

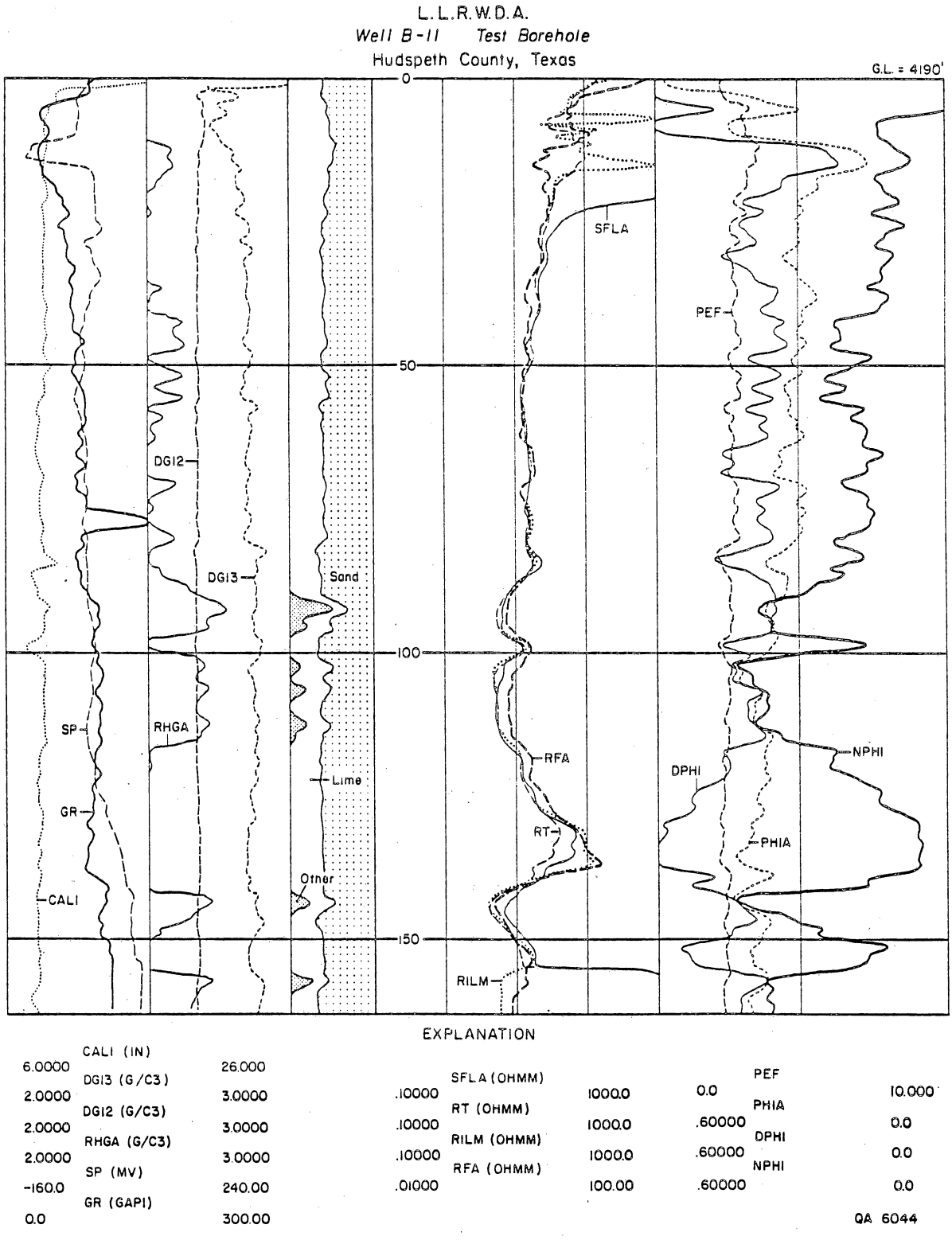

Figure 43. Composite geophysical log for borehole 11. Location of the borehole is shown in figure 23.

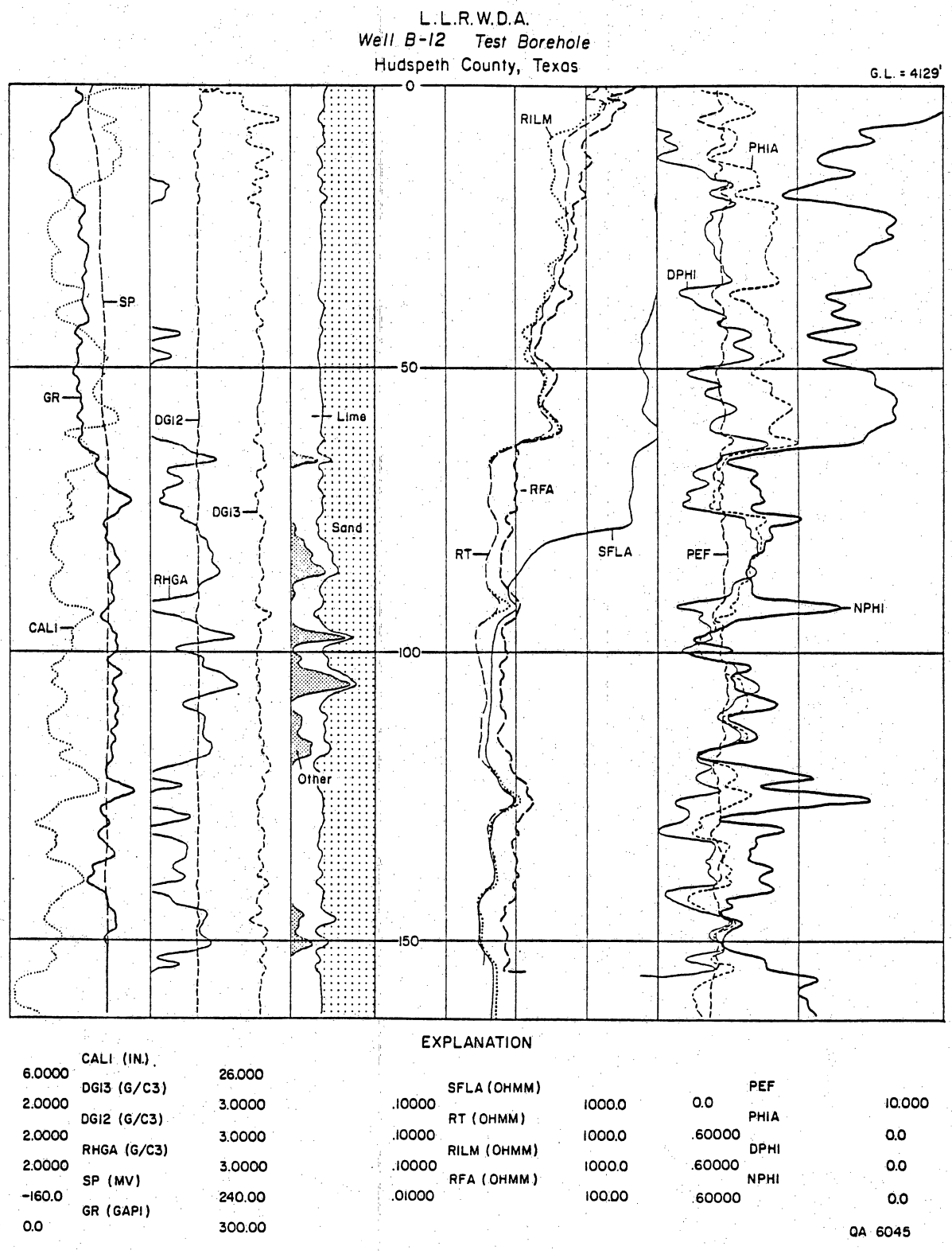

Figure 44. Composite geophysical log for borehole 12. Location of the borehole is shown in figure 23.

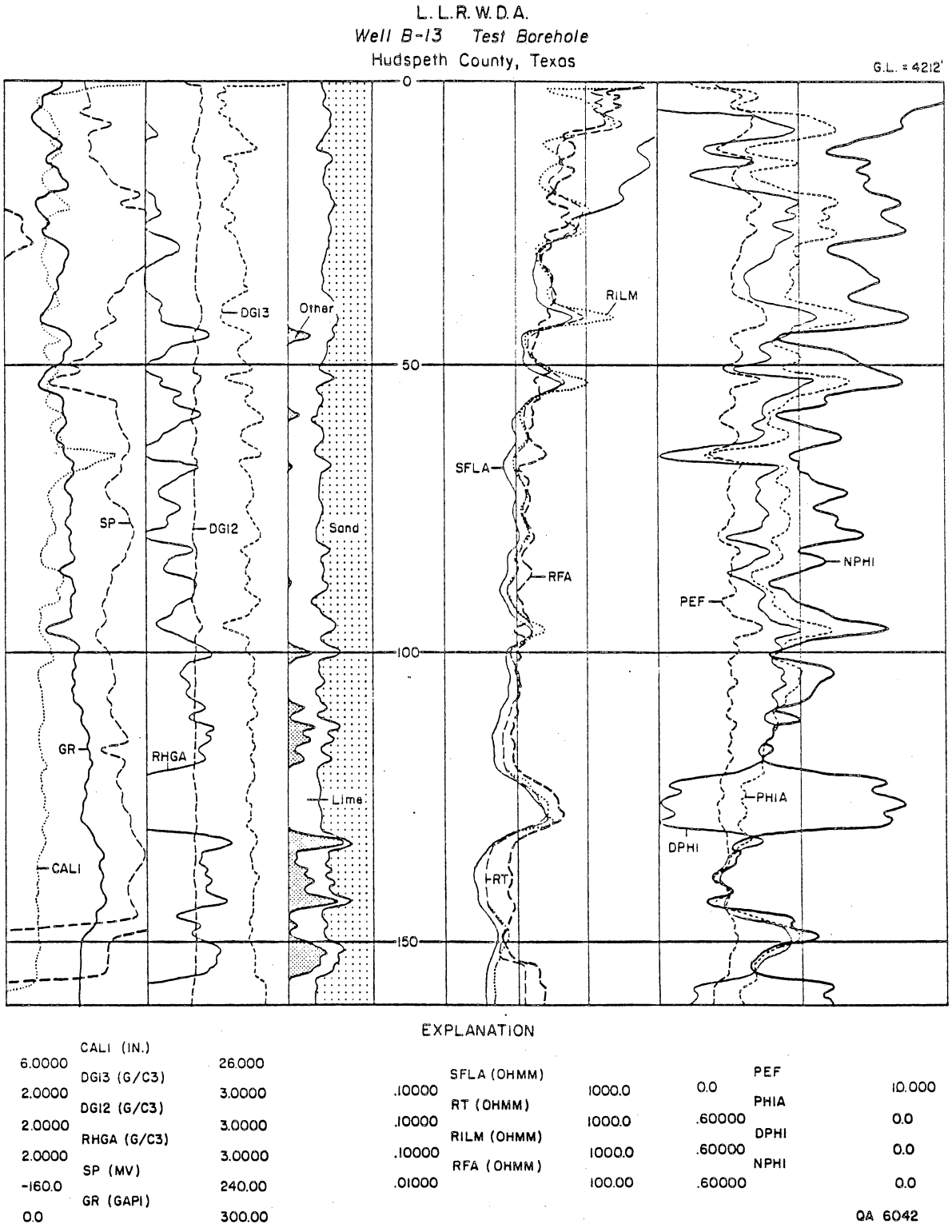

Figure 45. Composite geophysical log for borehole 13. Location of the borehole is shown in figure 23.

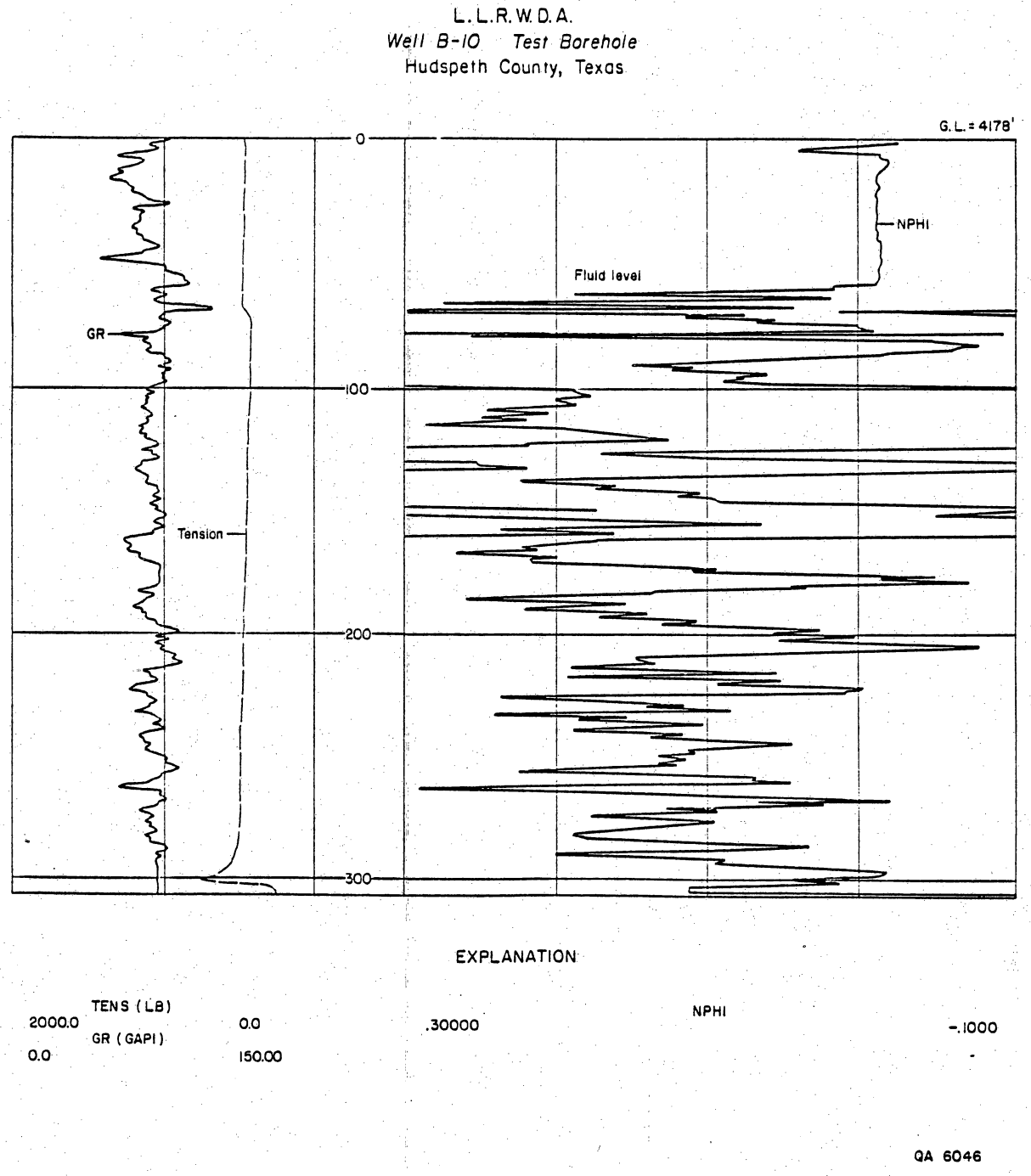

Figure 46. Composite geophysical log for borehole 10. Location of the borehole is shown in figure 23.

useful in lithologic determination and may also be used to quantify shale or clay content of the formation.

One method used to determine percent clay or shale content of an individual unit or to establish base lines over a specified interval involves the following equation (Schlumberger, 1974):

$$I_{GR} = \frac{GR_{log} - GR_{min}}{GR_{max} - GR_{min}}$$

where I_{GR} = gamma-ray index

GR_{log} = gamma-ray reading of formation

GR_{min} = gamma-ray minimum

GR_{max} = gamma-ray maximum

Using this method to determine percent-clay lines for individual logs, the following data was compiled:

% Clay	B-7	B-11	B-12	B-13
0-25%	59'-39%	28'-19%	65'-43%	91'-61%
26-50%	44'-29%	69'-46%	59'-39%	34'-23%
51-75%	30'-20%	34'-23%	22'-15%	15'-10%
76-100%	17'-11%	19'-13%	4'- 3%	10'- 7%

The LDT has recently become a very important tool in identifying single and multiple lithologies within a borehole. One component of the LDT is a photoelectric curve (P_e). This curve may be very useful in determining the mineralogy of the matrix, based on the apparent photoelectric absorption cross section of a mineral. P_e values are recorded in barns per atom (one barn = $10^{-27}cm^2$). In this case, the P_e proved valuable in recording the presence of bolson gravels because of the gravel's calcite content. Basic divisions used in this case were (1) clean sands--1.4-1.8, (2) sandy clays to clays--1.8-2.8, and (3) calcite gravels composed of Cretaceous

limestones from the Finley, Cox, and Bluff Mesa formations--2.8-5.1 (based on Gardner and Dumanoir, 1980).

	B-7	B-11	B-12	B-13
Clean sands	2'	0'	4'	0'
Sandy clays to clays	119'	121'	146'	119'
Calcareous gravels	29'	31'	0'*	31'
Base of upper gravels	53'	56'	64'*	54'
Total footage-sandy silt to silty clay	82'	47'	144'	35'

*Although log response does not record the presence of limestone gravels in B-12 as in other boreholes, its presence was confirmed during coring operations. The absence of a calcite response may result from an increase in clay content that masks the calcite or may be a result of significant borehole invasion by drilling fluids as recorded by resistivity logs.

Porosity Determination

The LDT may also serve as a porosity tool when combined with the CNL, another porosity device. Accurate porosity analysis for both consolidated and unconsolidated sediments is possible when both tools are used. Using Schlumberger porosity chart CP-5 (Schlumberger, 1984) appropriate corrections can be made to determine real porosity. In this case, true porosity is 1-2 porosity units greater than the computer-derived average porosity (labeled PHIA). The following data is compiled from LDT-CNL crossplots for the four open boreholes:

	B-7	B-11	B-12	B-13
Maximum porosity	54%	45%	54%	50%
Depth of maximum porosity	32'	142'	142'	115'
Minimum porosity	21%	16%	30%	19%
Depth of minimum porosity	5'	14'	63'	41'
Total footage < 36% porosity	51'	84'	18'	98'
Total footage > 48% porosity	6'	0'	15'	2'
Total footage 36-48% porosity	93'	66'	117'	50'

Formation Resistivity

Resistivity logs are typically used to delineate water- versus hydrocarbon-bearing intervals. They may also be used to locate permeable zones and as an aid in stratigraphic or structural correlations. As was the case with SP logs in the area, the absence of formation water restricts possible quantification of true formation water resistivity values. Qualitative observations can be made, however, with regard to the location of more permeable intervals and also to the detection of potential perched aquifers.

The Dual Induction Focused log (DIL) is a standard resistivity tool composed of a deep-reading induction device (ILd), a medium-reading induction device (ILm), and a shallow-reading spherically focused device (SFL). Differences in resistivity values between ILd and SFL curves may be used to differentiate between true resistivity and drilling fluid resistivity. At the Fort Hancock S-34 area, the only water present in the unsaturated zone is the irreducible water content trapped and coating the sand- to clay-sized grains. Since permeabilities also were found to be low for these intervals based on in situ and laboratory testing, minimal borehole invasion by the drilling fluids occurred. This results in a situation where all three logging tools are reading similar if not identical conditions for the unsaturated sediments.

Variations in resistivity values may be used qualitatively to indicate higher versus lower water contents and permeability values. Two sequences in B-7 illustrate this situation. The gravel section from 0-50 ft records higher resistivity values than do the predominantly clay sections from 50-80 ft and 120-150 ft. This is also true of the sand from 80-116 ft. This indicates a higher content of irreducible water within the larger grained deposits. Higher permeability sections are best illustrated where some separation between ILd and SFL is recorded as is the case in B-7 from 0-22 ft. The ILd in this example is measuring resistivity at a borehole depth of 64 inches while the SFL records conditions 16 inches deep. The separation that occurs in B-7 from 0-22 ft indicates that drilling fluids have invaded the borehole at least 16 inches but less than 64 inches because of the fluid resistivity contrast.

Appendix 11. B-14 water well summary.

On April 4, 1986, drilling of B-14 at the Fort Hancock Site S-34 was initiated. This additional water well became necessary after the cement packer in B-10 (the first water well) failed during cementing operations. Total depth of B-14 is 530 ft*, with a static water level of 478 ft (*all depths reported in this appendix were measured below land surface). Final drilling operations on this well were completed on April 16, and all sampling and testing was completed on April 23. Three goals were set for this well, two of which were fulfilled: determination of the static water level at the site and sampling of standard chemistry and isotopes. The results of chemical and isotopic analysis are in appendix 4. This section is to document (1) drilling and completion activities, (2) recommendations for possible completion of this well, (3) and lithologies encountered.

April 4--Locate and rig up for drilling B-14. This location is 213 ft east-northeast of B-10. Begin drilling at 10:45 a.m. with fresh-water gel-based mud system. Drill to 135 ft with 7 7/8-inch tri-cone rock bit. Drill to 180 ft with 7 7/8-inch drag bit.

April 5--Drill to 393 ft. At this point cuttings indicate presence of limestone, rate of penetration slowed because of increased hardness of formation; suction-pit water level dropped 2 inches because of presence of a lost circulation zone. Based on local information, the first sign of lost circulation is usually indicative of both porosity and water-bearing strata. At this point, conditioned hole and pulled pipe in preparation to run casing. Ran 4-inch steel casing to T.D. (total depth) of 393 ft. Successfully cemented casing from T.D. to surface.

April 6--Run 3 1/2-inch tri-cone bit in hole and staged out drilling mud with air in 100-ft increments. Had circulation problems while drilling with compressed

air due to small size differential between drill bit and drill pipe (1/4-inch clearance). Drilled out from bottom of casing to 399 ft.

April 7--Run new 4-inch drag bit into hole in attempt to increase clearance differential. Drilling with circulation problem continues however. Ran split spoon to T.D. in attempt to determine lithology that may be partly responsible for circulation problem. Sample recovered was moderately compacted and cemented, tan to brown, medium grain sand with occasional small limestone gravels. Sample was only slightly damp, a result of uphole drilling fluids and not formational water. Due to circulation problems, only 18 inch of new hole drilled.

April 8--Wait on air compressor repairs. Due to circulation problem have switched to drilling with a foam system. Lithology determination while drilling with foam difficult. In attempt to accurately determine depth of water strata from 400-500 ft, drilling was stopped after each 10-ft interval, cuttings were circulated bottoms-up, then foam was cut off and dry air circulated for 20 minutes. After air was circulated, returns checked for presence of moisture content. No moisture was detected while drilling from 400-480 ft. After drilling from 480-490 ft and following above procedure, definite presence of moisture was detected at a constant rate. Drilled to 500 ft as temporary T.D. so that water levels could be monitored.

April 9--Trip pipe into hole to T.D. to determine amount of fill and to condition borehole for water-level measurements. Two ft of borehole caving into bottom of open hole was recorded. Water level was measured at 478 ft below land surface. Attempts to bail well unsuccessful because of insufficient bailing line on rig to reach water level.

April 14--Measured water level to confirm that previous measurement was static. Water level static at 478 ft below land surface. In attempt to condition borehole made 9 runs with 2 1/2 inch diameter, 20 ft bailer. Recovered approximately 3 gallons of drilling fluid and formation water with each run. After last trip into hole remeasured water level at 478 ft below land surface.

April 16--In order to increase depth of water in borehole for pump test, well was deepened to 530 ft T.D. This depth was approaching maximum depth capacity of drilling rig. Final conditioning before pump test involved slugging hole with foam and then circulating dry air for 30 minutes. This process was repeated three times. After final circulation, returns were observed still to have high moisture content.

April 18--Difficulty anticipated for successful pump test because of extremely small clearance between submersible pump (3 3/4 inch O.D.) and open borehole (4 inch O.D.). Tight hole conditions were confirmed as maximum depth of free clearance because the pump was 489 ft below land surface, allowing only 11 ft of water coverage over the pump at the start of the test.

Pump test started with empty return pipe and no check valve to restrict backflow of water into formation during a pump shutdown. During first 4 minutes of pump test water-level drawdown was measured, then water level began to rise, indicating pump failure. Attempts to correct pump failure unsuccessful and pump test was temporarily abandoned so that pump could be pulled from well and inspected. Results of inspection indicated that turbine intakes on pump had been completely packed off with loose sand, a result of borehole wall caving. Two possible remedies to this situation were to install check valve in pump at the return pipe connection and to fill return pipe with formation water obtained during bailing. Reasoning for this solution was that initial surge of pump at start of test

with no restriction in return pipe resulted in large amounts of sand caving into open hole and subsequently into pump intakes.

April 23--In addition to measures listed above that were taken to enhance the pump test, the submersible pump was also wrapped with Dupont filter fiber to reduce sand intake. Depth for which pump was set to start test was again 489 ft below land surface. Measures taken to correct pump test #1 results proved partly successful, as returns at the surface were monitored and collected from the start of the test. Restriction to flow, however, was still apparent, as returns were measured at only .26 gpm. The low yield was insufficient to drawdown water level, as rates of recharge exceeded rates of production.

Obtaining a clean water sample from the pump test for chemistry and isotope analysis also was a high priority and so the pump test was continued. After approximately 68 minutes, discharge at the surface dropped to a trace. At this point the pump was raised 5 ft to 484 ft below land surface in an attempt to increase borehole clearance and to continue to clear up formation water for sampling. This increased production to approximately .8 gpm. Although it was clear that rate of return could be increased by opening control valve at the surface, at this point only 4 ft of water covered the pump intakes and caution had to be used to maintain water levels above the intake level. In order to determine quality of formation water, temperature, salinity, and conductivity were constantly monitored using a battery powered conductivity meter. After 139 minutes of pumping, temperature, salinity and conductivity had stabilized at $17^{o}C$, 1.7%, and 2550 micromhos, respectively. At this point, formation water was then collected and sampled for cations, anions, ^{13}C, ^{14}C, ^{18}O, ^{2}H, ^{34}S, and

tritium. Production began to decrease at 159 minutes and totally stopped at 167 minutes.

It was determined that with current bottom-hole conditions, a successful drawdown pump test was improbable due to low clearance differential, and further modifications would have to be employed before further attempts could be made. Two possible solutions were considered.

One possible solution would be to reenter the well with an underreaming drill bit and increase the diameter of the open hole from 393 ft to a T.D. of 530 ft. This would greatly reduce pump intake restriction and allow pump positioning at a deeper depth for greater drawdown potential. The greatest risk in this operation occurs after underreaming has been completed and reamer blades are closed for removal. If the blades do not close because of mechanical problems there would be no alternative to economically salvage the well.

Another possibility with greater risks would be to attempt a cement squeeze job over the entire open hole from 393 ft to the top of water-bearing strata at 480 ft. This might be attempted by (1) filling the borehole with sand from 530 ft to 480 ft, (2) placing a 2-4 ft bentonite plug on top of sand, (3) fill rest of open hole from 476 to 393 ft with a wet cement slurry to allow for formation penetration, (4) and, after allowing adequate time for cement to cure, drill back to T.D. with 4-inch bit. If all of the steps were successful, then a cement liner would restrict any possible sand caving into submersible pump intakes during testing and production. However, this method would involve signficantly greater risks than the first method discussed.

The current design of B-14 is as follows:

-4 inch steel casing from -393 ft to +2 ft.

-open borehole from -393 ft to -530 ft.

-3-ft square cement pad at surface with locking well cap.

Although drilling conditions were not conducive for accurate lithology determination, some conclusions can be made as to the general sequences encountered.

*0-6 ft--tan silty sand

*7-33 ft--limestone gravels and silts

*34-44 ft--silt to silty clay

*45-50 ft--limestone gravels, sands, and silts

*51-100 ft--silt to silty clay

*100-125 ft--unconsolidated fine sand, some silt

*125-345 ft--predominantly clay with minor amounts of silt, occasional thin lenses with higher silt and sand content

*345-392 ft--silty clay with well-cemented lenses of sand and occasional limestone gravels

*392-393 ft--hard, apparently well-cemented limestone gravel; encountered partial loss of circulation in this interval

*393-480 ft--interbedded layers of silty clays, loose uncompacted fine-grained sands, and limestone gravels

*480-530 ft--lithology determination complicated while drilling with foam; two different scenarios are reasonable. The most reasonable conclusion is that, based on rates of penetration and returns, Cretaceous rocks were encountered at 480 ft of either the Finley or Bluff Mesa formations. The returns during this interval were predominantly black limestones. Another possible conclusion is that this interval was simply a well-cemented basal bolson gravel.

Future testing in this area should definitely include continuous coring in at least one borehole from 150 ft to 650-700 ft so that stratigraphic and hydrologic questions raised by inadequate sample returns can be answered.

Appendix 12. Hydraulic conductivity measurements in the unsaturated zone of the bolson fill.

The hydraulic conductivity of two sequences of gravels and clays-and-sand in the bolson fill were measured in the site area. Procedure and interpretations follow the determination of hydraulic conductivity in soil above water table (Boersma, 1965). This method is known as the shallow well - pump-in method, the piezometer method, or the dry-auger-hole method. According to this method, an auger hole is dug, and then water is supplied to the hole. The water in the hole is maintained at a constant level. The rate of water input is determined until a steady state is obtained. The hydraulic conductivity is calculated from the following equation:

$$K = \frac{\left[\ln\left(\frac{h}{r} + \sqrt{\left(\frac{h}{r}\right)^2 - 1}\right) - 1\right] Q}{2\pi h^2}$$

where K is the hydraulic conductivity (cm/hr), h is the depth of water maintained in the hole as measured from the bottom of the hole (cm), r is the radius of the hole (cm), and Q is the rate at which water is flowing into the soil (cc/hr). Two different lithologies within the bolson fill were tested: The gravels that cover the finer materials from land surface to a depth of 9 to 15 m (30 to 50 ft), and the clays, silts, and fine sands that underlie the gravels to a depth of 148 m (485 ft) below land surface (B-1 and B-8 respectively, fig. 23a). Each of the boreholes was filled with coarse sand to prevent caving in the sides of the holes. The gravel interval was cased when testing the finer materials--sequences of sand and clays.

Results of the test are presented in the following table:

Tested lithology	Depth of the borehole (cm)	Length of the tested interval (cm)	Radius of the borehole (cm)	Final rate of flow into the borehole (cc/hr)	Hydraulic conductivity (cm/hr)
gravel	1,311	1,311	11.43	64,000	0.026
clays and silty sand	4,628	3,165	4.37	4,440	0.013

The hydraulic conductivity of the gravels was calculated to be 7.56 ft/yr (2.3 m/yr) and that of the clays and sands is 3.8 ft/yr (1.15 m/yr).

Appendix 13. Estimate of annual recharge in Hudspeth site based on chloride analyses of soil cores.

The annual recharge into the gravels overlying the bolson fill at the Hudspeth site was estimated based on soil cores that were analyzed for their chloride concentrations. Procedures and interpretation followed a method that was suggested by Allison and Hughes (1978). When rainwater containing chloride percolates into a soil subject to water loss by transpiration, it is expected that at a steady-state, chloride concentrations in soil water will increase monotonically through the root zone. Beneath the bottom of the root zone the chloride concentrations should be constant with depth. Assuming that the only source for chloride in the soil is rainfall, then the annual recharge can be calculated using the equation:

$$R = \frac{Cl_p}{Cl_s} \times P$$

where R is the annual recharge, Cl_p is the chloride concentration in the local rainfall, Cl_s is the the chloride concentration in the soil profile below the root zone where it is constant with depth, and P is the annual amount of precipitation.

Five holes were augered in the gravels that overlie the bolson fill at the Hudspeth site area to depths of 30 to 50 ft (9 to 15 m) below land surface (LLWA 1 to LLWA 5 in figs. 23 and 24). Core samples were taken in each borehole at depths of 1, 3, 5, 7, 10, 15, 20, 25, 30, 40, and 50 ft (0.3, 1, 1.5, 2.1, 3, 4.6, 6.1, 7.6, 9.1, 12.2, and 15.2 m). No drilling fluids were used while augering. All samples were weighed at the site and immediately sealed in airtight containers. Water content was determined gravimetrically using about 20 g of

sample. The soil samples were weighed again in the lab, oven-dried at 105°C for 24 hr, and then were weighed again to determine the water content. Chloride concentration was determined on the oven-dried samples used for the determination of water content. These were stirred with 50 ml of distilled water for more than 2 days. Aliquots of the filtrate were titrated potentiometrically to obtain chloride concentration. Water content and assumed bulk density of 1.5 g/cm^3 were used for calculating the concentration of chloride in the soil solution. They are reported as the concentration in the soil water solution (mg/l). Variations in lithology, water contents, and chloride concentrations along each borehole are presented in figure 29. Annual rainfall amount was assumed to be 8 inches (20.3 cm). Because information about chloride concentration in rain water at Hudspeth County was not available, we decided to calculate a range of recharge estimates based on measurements of chloride in rainfall at San Angelo (3.71 mg/l) and Amarillo (0.6 mg/l) (Lodge and others, 1969). Chloride concentration used to calculate recharge estimate in each borehole was the mean value of all chloride measurements starting at the salinity peak, down to the bottom of the hole (fig. 29). The following values of annual recharge were calculated for each borehole:

Borehole no.	Cl concentration used (mg/l)	Calculated recharge (inch/yr) assuming Cl_p=3.71 mg/l	Calculated recharge (inch/yr) assuming Cl_p=0.6 mg/l
1	561	0.053	0.009
2	3259	0.009	0.002
3	1875	0.016	0.003
4	8989	0.0033	0.0005
5	2283	0.013	0.002

The mean value of annual recharge into the gravel cover of the bolson fill, based on results from five boreholes, ranges from 0.003 to 0.02 inch/yr (0.07 to 0.5 mm/yr) which is less than 1% of the annual rainfall. Similar values, 0.007 to 0.05 inch/yr (0.18 to 1.25 mm/yr), were reported for the Southern High Plains in New Mexico (Stone, 1984).